

**Design of Stiffened Plates Using
Soft Computing Techniques**

**PhD Thesis
in
Civil Engineering
University of Gaziantep**

**Supervisor
Prof. Dr. Mustafa ÖZAKÇA
Co-Supervisor
Assoc. Prof. Dr. Abdülkadir ÇEVİK**

**by
Mehmet Tolga GÖĞÜŞ
February 2010**

T.C.
UNIVERSITY OF GAZIANTEP
GRADUATE SCHOOL OF
NATURAL & APPLIED SCIENCES
CIVIL ENGINEERING DEPARTMENT

Name of the thesis: Design of Stiffened Plates Using Soft Computing Techniques
Name of the student: Mehmet Tolga GÖĞÜŞ
Exam date:01.02.2010

Approval of the Graduate School of Natural and Applied Sciences

Prof. Dr. Ramazan KOÇ
Director

I certify that this thesis satisfies all the requirements as a thesis for the degree of Doctor of Philosophy.

Assoc. Prof. Dr. Mustafa GÜNAL
Head of Department

This is to certify that we have read this thesis and that in our opinion it is fully adequate, in scope and quality, as a thesis for the degree of Master of Science/Doctor of Philosophy.

Assoc. Prof. Dr. Abdülkadir ÇEVİK
Co-Supervisor

Prof. Dr Mustafa ÖZAKÇA
Supervisor

Examining Committee Members

Prof. Dr. İbrahim H. GÜZELBEY(Chairman)

Prof. Dr. Mustafa ÖZAKÇA

Assoc. Prof. Dr. Hüseyin R. YERLİ

Assist. Prof. Dr. Mustafa ŞAHMARAN

Assist. Prof. Dr. Nildem TAYŞI

ABSTRACT

Design of Stiffened Plates Using Soft Computing Techniques

GÖĞÜŞ, Mehmet Tolga

PhD. in Civil Eng.

Supervisor: Prof. Dr. Mustafa ÖZAKÇA

Co-supervisor: Assoc. Prof. Dr. Abdülkadir ÇEVİK

February 2010, 131 pages

This thesis deals with development of reliable, accurate and efficient soft computing tools for the analysis and design of structures. The efficiency of soft computing techniques in structural design such as, particular algorithms based on genetic algorithm, neural network, gene expression programming and large-scale continuous or discrete structural design problems are studied. The algorithms are studied both in deterministic and reliability based structural design problems. To increase the computational efficiency as well as the robustness of the design procedure, an effort is put forth. Structural optimization process requires the efficient integration of computer assisted geometry modeling, automated mesh generation, structural analysis and soft computing applications. The use of soft computing techniques is motivated from the time-consuming repeated finite strip analysis required during the optimization process. A trained soft computing technique is used to perform deterministic constraints check in the case of reliability based design. The suitability of the soft computing techniques predictions will be investigated in a number of structural design problems in order to demonstrate the computational advantages of the proposed methodologies.

Principally, it is desired that this thesis will provide stable bases for further investigation, leading to a more intensive use of structural optimization algorithms with soft computing techniques to solve practical problems. Because of the broad diversity of structures encountered in practice, it becomes clear that this thesis is concentrated on buckling and free vibration analyses of stiffened plates.

All soft computing models used in this study are presented in explicit form neural network and gene expression programming models. The most accurate results are obtained by neural network model rather than gene expression programming. Neural networks are treated as black box in general. It should be noted that explicit formulation of neural network models is of significant importance as it will serve for important advantages in the analysis and design of structures. This thesis aims to open the black box and to present the neural network models in its explicit form. An alternative algorithm for the selection of optimum neural network architecture that automatically selects the best architecture is proposed. By using finite strip method large testing and training sets are constructed and high generalization capabilities of the models are obtained.

Key Words: finite strip method, stiffened plates, buckling, free vibration, structural optimization, soft computing

ÖZET

Esnek Hesaplama Teknikleri Kullanarak Takviyeli Plakların Tasarımı

GÖĞÜŞ, Mehmet Tolga
Doktora Tezi, İnş Müh. Bölümü
Tez Yöneticisi: Prof. Dr Mustafa ÖZAKÇA
Yardımcı Tez Yöneticisi: Doç. Dr. Abdülkadir ÇEVİK
Şubat 2010, 131 sayfa

Bu tez, analiz ve yapı tasarımı için, doğru, güvenilir ve verimli esnek hesaplama araçlarının geliştirilmesiyle ilgilidir. Esnek hesaplama teknikleri olarak özellikle genetik algoritma, yapay sinir ağları, gen ifadesi programlama yöntemleri ile büyük ölçekli, sürekli veya ayrık yapısal tasarım problemlerinin verimliliği çalışılmıştır. Bu algoritmalar, hem rastsal olmayan hem de güvenilirliğe dayalı yapısal tasarım problemlerine uygulanmıştır. Ayrıca, tasarım sürecinin hesaplama verimliliğinin yanında sağlamlığı da artırılmaya çalışılmıştır. Yapısal optimizasyon süreci, bilgisayar destekli ağ geometri modelleme, otomatik ağ üretimi, analizi ve esnek hesaplama uygulamalarını içermektedir. Bu çalışmada esnek hesaplama yöntemlerinin yoğunlaştığı kısım, optimizasyon sürecinde zaman alıcı ve sürekli tekrarlanan sonlu şeritler analizleridir. Eğitilmiş bir esnek hesaplama tekniği rastsal olmayan kısıtlayıcı kontrollerinde kullanılabilir. Esnek hesaplama tekniklerinin kestirimlerinin uygunluğu ve önerilen algoritmaların hesaplama avantajları bazı yapısal tasarım problemleri üzerinde incelenecektir.

Özellikle, ilerleyen araştırmalar için sağlam bir taban oluşturmak amacıyla, uygulamaya yönelik yapısal optimizasyon algoritmaları ile esnek hesaplama yöntemlerinin birlikte kullanımının artırılması öne çıkarılması hedeflenmiştir. Uygulamada kullanılan yapı tiplerinin geniş çeşitliliğe sahiptir, fakat bu tezde sadece takviyeli plakların burkulma ve serbest titreşim analizleri üzerine yoğunlaşmıştır.

Bu çalışmada kullanılan yapay sinir ağları ve gen ifade programlama modelleri açık formda sunulmuştur. Yapay sinir ağları ile elde edilen modeller, gen ifade programlama yöntemi modellerine göre daha hassas sonuçlar vermiştir. Yapay sinir ağları genel olarak kapalı kutu olarak değerlendirilmektedir. Yapay sinir ağlarının açık formda verilmesi yapı analiz ve tasarımında kullanılabilmesi için önem arz etmektedir. Bu tez de kapalı halde verilen yapay sinir ağları modellerini açık biçimde sunmayı amaçlamaktadır. Optimum yapay sinir ağı mimarisinin seçimi için alternatif bir algoritma önerilmiştir. Sonlu şeritler yöntemiyle geniş test ve eğitim setleri elde türetilip, yüksek genelleme yeteneğine sahip modeller elde edilmiştir.

Anahtar Kelimeler: sonlu şeritler metodu, takviyeli plak, burkulma, serbest titreşim, yapısal optimizasyon, esnek hesaplama

ACKNOWLEDGMENTS

I would like to express my sincere thanks to my supervisor, Prof. Dr. Mustafa Özakça, for giving his time, support, guidance, advice and generous supervision. His active interest in my work and the discussions with him created and inspired working environment. My thanks also go to my co-supervisor, Assoc. Prof. Dr. Abdülkadir Çevik for his helpful discussions.

Many thanks to my colleague Assist. Prof. Dr Nildem Tayşı, for her friendship, help useful technical discussions, her support, encouragement and reading early versions of my thesis during the last turn of this research

I would also like to thank my dear friends Res. Asst. Talha Ekmekyapar and Mr. M. Ali Arslan for helping me with various aspects of conducting research and their support and encouragement during the preparation of this research.

Part of this research is supported by TUBITAK (The Scientific and Technical Research Council of Turkey) Grant No: 107M648. I would like to express my deeply grateful to TUBITAK for supporting this thesis study.

I would like to express my appreciation to the Civil Engineering Department academic personnel and to the departmental secretaries.

TABLE OF CONTENTS

	page
TABLE OF CONTENTS	vi
LIST OF FIGURES	ix
LIST OF TABLES	xiii
LIST OF SYMBOLS	xiv
Chapter 1: INTRODUCTION.....	1
1.1 General Introduction	1
1.2 Thesis Objectives	2
1.3 Structure Type Considered in This Thesis	3
1.4 Soft Computing Techniques Considered in This Thesis.....	3
1.5 Software Developed in This Thesis	4
1.6 Layout of Thesis.....	4
Chapter 2: LITERATURE SURVEY	6
2.1 Introduction	6
2.2 Finite Strip Analysis.....	6
2.2.1 Stiffened Panel Analysis with Finite Strip Method	6
2.3 Structural Optimization with Mathematical Programming.....	9
2.4 Soft Computing Techniques in Structural Mechanics	10
2.4.1. Neural Computing.....	10
2.4.2. Evolutionary Computing.....	11
2.4.3. Fuzzy Systems.....	12
Chapter 3: STRUCTURAL ANALYSIS	14
3.1 Introduction	14
3.2 Structural Theories	14
3.3 Buckling Analysis	15
3.3.1 Strain Energy.....	16
3.3.2 Potential Energy of the Applied Inplane Stresses	20
3.3.3 Finite Strip Idealization.....	21
3.3.4 Stiffness Matrix.....	24

3.3.5 Geometric Stiffness Matrix	25
3.3.6 Branched Strips	27
3.4 Free Vibration Analysis of Structures.....	28
3.5 Examples	31
3.5.1 Buckling Analysis of Stiffened Panels.....	31
3.5.2 Free Vibration Analysis of Stiffened Panels.....	33
 Chapter 4: OPTIMIZATION OF STIFFENED PLATES	 35
4.1 Introduction	35
4.2 Optimization Process	36
4.2.1 Parameter Definition	36
4.2.2 Design Constraints	37
4.2.3 Material Properties, Loading and Boundary Conditions	38
4.3 Optimum Design of Stiffened Plates.....	38
4.3.1 Straight Stiffened Plate	40
4.3.2 Straight Stiffened Plate with Substiffeners	44
4.3.3 Straight Stiffened Plate with Substiffeners and Pads under Stiffeners	48
4.3.4 L Shaped Stiffened Plates	54
4.4 Discussions of All Stiffened Plates	58
 Chapter 5: SOFT COMPUTING TECHNIQUES AND OPTIMIZATION	 61
5.1 Introduction	61
5.2 Soft Computing Techniques.....	63
5.2.1 Neural Computing.....	63
5.2.2 Neural Networks	63
5.2.3 Components of Neural Networks.....	64
5.2.4 Backpropagation Algorithm.....	67
5.3 Fuzzy Logic.....	69
5.3.1 Neuro–Fuzzy Systems.....	71
5.3.2 Solving a Simple Problem with ANFIS	71
5.4. Evolutionary Computing.....	73
5.4.1. Genetic Programming	74
5.4.2. Gene Expression Programming	75
5.4.3 Implementation of GEP	78

Chapter 6: BUCKLING AND FREE VIBRATION SENSITIVITY ANALYSIS AND SOFT COMPUTING APPLICATIONS.....	81
6.1 Introduction.....	81
6.2 Problem Definition of Stiffened Panels	81
6.3 Sensitivity Analysis of FS Buckling Results (Main effect plots)	83
6.4 Numerical Applications of Soft Computing Techniques for Buckling Analysis	85
6.4.1 Performance and Reliability of GEP Model	85
6.4.2 Performance and Reliability of Neural Network Model.....	89
6.5 Free Vibration Sensitivity Analysis of FS Results (Main effect plots).....	93
6.6 Free Vibration Numerical Applications of Soft Computing Techniques.....	95
6.6.1 Performance and Reliability of GEP Model	96
6.6.2 Performance and Reliability of Neural Network Model.....	99
 Chapter 7: CONCLUSION	 103
7.1 Summary of Achievements	103
7.2 General Conclusions	103
7.2.1 Structural analysis	104
7.2.2 Structural shape optimization.....	104
7.2.3 Soft computing.....	105
Suggestion for Further Work	107
 REFERENCES.....	 108
 APPENDIX A: INTERACTION PLOT FOR BUCKLING ANALYSIS OF STIFFENED PANELS	 116
A.1 Introduction	116
 APPENDIX B: CONTOUR PLOT FOR FREE VIBRATION ANALYSIS OF STIFFENED PANELS	 124
B.1 Introduction	124
 CURRICULUM VITAE.....	 132

LIST OF FIGURES

	page
Figure 3.1 Definition of Mindlin–Reissner FSs	17
Figure 3.2 Isotropic stiffened panels from the NASA set [71]	32
Figure 3.3 Details of repeating elements in isotropic stiffened panels in mm (a) Panel I and II $h = 34.34$ mm for Panel I and $h = 50.04$ mm for Panel II and (b) Panel III	32
Figure 3.4 Dimensions and geometry of a stiffened panel.....	34
Figure 4.1 Plate variable parameters (design variables)	36
Figure 4.2 A sample three dimensional aspect of stiffened plate (Straight stiffener with five stiffeners).....	37
Figure 4.3 Loading and boundary conditions.....	38
Figure 4.4 Straight stiffened plate	40
Figure 4.5 Initial and optimum shapes of straight stiffened panels size optimization (a), (b) and (c) three, four and five stiffeners respectively	42
Figure 4.6 Initial and optimum shapes of straight stiffened panels after shape (type one) optimization (a), (b) and (c) three, four and five stiffeners respectively	43
Figure 4.7 Comparison of size and shape optimizations (type one)	44
Figure 4.8 Straight stiffened plate with substiffeners	44
Figure 4.9 Initial and optimum Shapes of straight stiffened plate with sub–stiffeners after size optimization (a), (b) and (c) three, four and five stiffeners respectively	46
Figure 4.10 Initial and optimum shapes of straight stiffened plate with sub–stiffeners after shape optimization (type one) (a), (b) and (c) three, four and five stiffeners respectively	47
Figure 4.11 Comparison of size and shape optimizations (type one)	48
Figure 4.12 Straight stiffened plate with substiffeners and pads under stiffeners	48
Figure4.13 Initial and optimum shapes of straight stiffened plate with substiffeners and pads under stiffeners after size optimization. (a), (b) and (c) three, four and five stiffeners respectively.....	50
Figure4.14 Initial and optimum shapes of straight stiffened plate with substiffeners and pads under stiffeners after shape optimization (type one) (a), (b) and (c) three, four and five stiffeners respectively	51

Figure 4.15 Initial and optimum shapes of straight stiffened plate with substiffeners and pads under stiffeners after shape optimization (type two) (a), (b) and (c) three, four and five stiffeners respectively	53
Figure 4.16 Comparison of size, shape one (type one) and shape optimizations (type two)	53
Figure 4.17 L shaped plate geometry	54
Figure 4.19 Initial and optimum shapes of L shaped stiffened plates after shape optimization (type one) (a), (b) and (c) three, four and five stiffeners respectively	56
Figure 4.20 Initial and optimum shapes of L shaped stiffened plates after shape optimization (type two) (a), (b) and (c) three, four and five stiffeners respectively	57
Figure 4.21 Comparison of size, shape (type one) and shape optimizations (type two)	58
Figure 4.22 Comparison of maximum loads of plate types	59
Figure 5.1 SC techniques.	62
Figure 5.2 Basic component of NNs [87] (a) Biological neuron (b) Artificial neuron	64
Figure 5.3 Basic elements of an artificial neuron.....	65
Figure 5.4 Common types of activation functions; (a) Threshold activation function (b) Piecewise-linear function (c) Sigmoid function (d) Hyperbolic tangent function. [87].....	66
Figure 5.5 Classification of NNs.....	67
Figure 5.6 Weight correction representation of back propagation NNs.	68
Figure 5.7 Back-propagation algorithm.....	68
Figure 5.8 Input data membership values [94].....	70
Figure 5.9 The Sugeno fuzzy model [78].....	71
Figure 5.10 Initial membership functions	72
Figure 5.11 Final membership functions.	73
Figure 5.12 Fuzzy inference diagrams	73
Figure 5.13 General scheme of evolutionary computing.	74
Figure 5.14 GP flowchart [98].	77
Figure 5.15 Expression tree representation [98].	78
Figure 5.16 Expression tree representation for perfect solution [98].....	80
Figure 6.1 Typical section of stiffened panel	82
Figure 6.2 Isotropic panels loading for buckling	82
Figure 6.3 Main effect plots of FS for buckling.....	83

Figure 6.4 Main effect plots of FS for case $n_{blade}=2$ for buckling	83
Figure 6.5 Main effect plots of FS for case $n_{blade}=3$ for buckling	84
Figure 6.6 Main effect plots of FS for case $n_{blade}=4$ for buckling	84
Figure 6.7 Main effect plots of FS for case $n_{blade}=5$ for buckling	85
Figure 6.8 Expression tree for proposed GEP model for buckling analyses	87
Figure 6.9 GEP Model solutions versus FS solutions and correlations for test set...	88
Figure 6.10 GEP Model solutions versus FS solutions and correlations for train set	88
Figure 6.11 GEP Model solutions versus FS solutions and correlations for total set	89
Figure 6.12 Proposed NN architecture for buckling analysis	90
Figure 6.13 NN Model solutions versus FS solutions and correlations for test set. .	91
Figure 6.14 NN Model solutions versus FS solutions and correlations for train set	91
Figure 6.15 NN Model solutions versus FS solutions and correlations for total set.	92
Figure 6.16 Main effect plots of FS.	93
Figure 6.17 Main effect plots of FS for case $n_{blade}=2$	94
Figure 6.18 Main effect plots of FS for case $n_{blade}=3$	94
Figure 6.19 Main effect plots of FS for case $n_{blade}=4$	95
Figure 6.20 Main effect plots of FS for case $n_{blade}=5$	95
Figure 6.21 Expression tree for proposed GEP model.....	98
Figure 6.22 GEP Model solutions versus FS solutions and correlations for test set.	98
Figure 6.23 GEP Model solutions versus FS solutions and correlations for train set	99
Figure 6.24 GEP Model solutions versus FS solutions and correlations for total set	99
Figure 6.25 Proposed NN architecture for free vibration analysis.....	100
Figure 6.26 NN Model solutions versus FS solutions and correlations for test set	101
Figure 6.27 NN Model solutions versus FS solutions and correlations for train set	101
Figure 6.28 NN Model solutions versus FS solutions and correlations for total set	102
Figure A.1. Interaction plot for FS for t_1/b versus t_2/b	116
Figure A.2. Interaction plot for FS for t_2/b versus s_2/b	117
Figure A.3. Interaction plot for FS for t_1/b versus s_2/b	117
Figure A.4. Interaction plot for FS for t_2/b versus s_1/b	118
Figure A.5 Interaction plot for FS for t_1/b versus s_1/b	118
Figure A.6. Interaction plot for FS for s_2/b versus s_1/b	119
Figure A.7. Interaction plot for FS for t_2/b versus l/b	119
Figure A.8. Interaction plot for FS for t_1/b versus l/b	120
Figure A.9. Interaction plot for FS for l/b versus s_2/b	120

Figure A.10. Interaction plot for FS for l/b versus s_1/b	121
Figure A.11. Interaction plot for FS for t_2/b versus n_{blade}	121
Figure A.12. Interaction plot for FS for t_1/b versus n_{blade}	122
Figure A.13. Interaction plot for FS for n_{blade} versus s_2/b	122
Figure A.14. Interaction plot for FS for s_1/b versus n_{blade}	123
Figure A.15. Interaction plot for FS for l/b versus n_{blade}	123
Figure B.1. Contour plot for FS for t_1/b versus t_2/b	124
Figure B.2. Contour plot for FS for t_2/b versus s_2/b	125
Figure B.3. Contour plot for FS for t_1/b versus s_2/b	125
Figure B.4. Contour plot for FS for t_2/b versus s_1/b	126
Figure B.5. Contour plot for FS for t_1/b versus s_1/b	126
Figure B.6. Contour plot for FS for s_2/b versus s_1/b	127
Figure B.7. Contour plot for FS for t_2/b versus l/b	127
Figure B.8. Contour plot for FS for t_1/b versus l/b	128
Figure B.9. Contour plot for FS for l/b versus s_2/b	128
Figure B.10. Contour plot for FS for l/b versus s_1/b	129
Figure B.11. Contour plot for FS for t_2/b versus n_{blade}	129
Figure B.12. Contour plot for FS for t_1/b versus n_{blade}	130
Figure B.13. Contour plot for FS for n_{blade} versus s_2/b	130
Figure B.14. Contour plot for FS for s_1/b versus n_{blade}	131
Figure B.15. Contour plot for FS for l/b versus n_{blade}	131

LIST OF TABLES

	page
Table 4.1 Common constraints.....	37
Table 4.2 Design constraints of all stiffened plates.....	40
Table 4.3 Size optimization of straight stiffened plate.....	41
Table 4.4 Shape optimization (type one) of Straight stiffened plate.....	43
Table 4.5 Size optimization of stiffened plate with stiffener	45
Table 4.6 Shape optimization (type one) of stiffened plate with stiffener	47
Table 4.7 Size optimization of straight stiffened plate with substiffeners and pads under stiffeners	49
Table 4.8 Shape optimization (type one) of straight stiffened plate with substiffeners and pads under stiffeners with six design variables.....	51
Table 4.9 Shape optimization (type two) of straight stiffened plate with substiffeners and pads under stiffeners with seven design variables	52
Figure4.15 Initial and optimum shapes of straight stiffened plate with substiffeners and pads under stiffeners after shape optimization (type two) (a), (b) and (c) three, four and five stiffeners respectively.	53
Table 4.10 Size optimization of L shaped stiffened plates.....	55
Figure4.18 Initial and optimum shapes of L shaped stiffened plates after size optimization (a), (b) and (c) three, four and five stiffeners respectively.....	55
Table 4.11 Shape optimization (type one) of L shaped stiffened plates	56
Table 4.12 Shape optimization (type two) of L shaped stiffened plates with five design variables.....	57
Figure 4.20 Initial and optimum shapes of L shaped stiffened plates after shape optimization (type two) (a), (b) and (c) three, four and five stiffeners respectively	57
Table 6.1 The range of variables used in the database	82
Table 6.2 Parameters of GEP model	86
Table 6.3 Comparison of test, training and total sets GEP.....	87
Table 6.4 Comparison of test, training and total sets for NN for buckling analyses.	90
Table 6.5 Parameters of GEP model	97
Table 6.6 Comparison of test, training and total sets GEP.....	97
Table 6.7 Statistical parameters of test, training and total sets for NN for free vibration analysis	100

LIST OF SYMBOLS

Abbreviations

FS	Finite Strip
FEM	Finite Element Method
DOF	Degrees Of Freedom
DV	Design Variable
GA	Genetic Algorithm
GP	Genetic Programming
GEP	Gene Expression Programming
NN	Neural Network
SC	Soft Computing
SE	Strain Energy
SSE	Sum of Squared Error
SO	Shape Optimization
SSO	Structural Shape Optimization
SQP	Sequential Quadratic Programming

Scalars

A	Cross-sectional area
b	length of strip
$C(0), C(1), C(2)$	order of continuity
C_p, S_p	cosine and sine function
d	displacement
D_m, D_b, D_s	membrane, bending and shear rigidities
E	Young's modulus
G	Shear modulus
I	total virtual work

Scalars (continued)

I^e	total work from strip (or element) e
J	Jacobian
(m, n)	mode and half-sine wave
N_i	shape function associated with node i
R	radius of curvature
t_i	thickness at node i
$U^{(e)}$	element strain energy
u, v, w	global displacement parameters
u^p, v^p, w^p	displacement amplitudes of p^{th} harmonic
u_ℓ, v_ℓ, w_ℓ	displacement components in ℓ , y and n -direction
ℓ	length
V_g	potential energy of shell volume of V
x, y, z	global cartesian coordinates
x_i, y_i, z_i	typical cartesian coordinates of node i

Vectors

\mathbf{d}	vector of unknown displacements
$\bar{\mathbf{d}}$	displacement vector in local direction
$\bar{\mathbf{d}}_p$	p^{th} mode shape
\mathbf{d}^0	global displacement vector
\mathbf{d}_i^e	displacement vector (eigenvector) associated with element e and node i
$\hat{\mathbf{d}}_p$	p th vibration mode (eigenvector)
$\bar{\mathbf{d}}_i$	displacement vector (eigenvector) at node i

Matrices

\mathbf{B}	strain–displacement matrix
\mathbf{B}_{mi}^e	membrane strain–displacement matrix for element e and node i

Matrices (continued)

\mathbf{B}_{bi}^e	bending strain–displacement matrix for element e and node i
\mathbf{B}_{si}^e	shear strain–displacement matrix for element e and node i
\mathbf{B}_{mi}	membrane strain–displacement matrix for node i
\mathbf{B}_{bi}	bending strain–displacement matrix for node i
\mathbf{B}_{si}	shear strain–displacement matrix for node i
$\bar{\mathbf{B}}_{mi}, \bar{\mathbf{B}}_{bi}, \bar{\mathbf{B}}_{si}$	transformed strain–displacement matrices
\mathbf{B}_{pi}	in–plane strain displacement matrix
\mathbf{D}	matrix of rigidities
$\mathbf{D}_m, \mathbf{D}_b, \mathbf{D}_s$	matrices of membrane, bending and shear rigidities
$\mathbf{D}_p, \mathbf{D}_s$	in–plane and transverse elasticity matrix
\mathbf{I}_3	the 3×3 identity matrix
\mathbf{J}	Jacobian matrix
\mathbf{K}^e	element stiffness matrix
\mathbf{K}_{ij}^e	stiffness matrix associated with element e and nodes i and j
\mathbf{K}	symmetric, banded stiffness matrix
\mathbf{K}_{mij}^e	membrane stiffness matrix for element e and nodes i and j
\mathbf{K}_{bij}^e	bending stiffness matrix for element e and nodes i and j
\mathbf{K}_{sij}^e	shear stiffness matrix for element e and nodes i and j
\mathbf{M}	global mass matrix
\mathbf{M}_{ij}^e	mass matrix associated with element e and nodes i and j
\mathbf{T}	transformation matrix

Greek Symbols

α	angle between local and global axes,
ε	axial strains
$\varepsilon_m, \varepsilon_b, \varepsilon_s$	membrane, bending and transverse shear strains

Greek Symbols (continued)

$\boldsymbol{\varepsilon}_m, \boldsymbol{\varepsilon}_b, \boldsymbol{\varepsilon}_s$	membrane, bending and transverse shear strain vectors
$\varepsilon_\ell, \varepsilon_y$	strain in ℓ direction and longitudinal strain
$\varepsilon_y, \varepsilon_z$	bending strain in y and z axes
δ	stiffness proportional damping coefficient
$\gamma_{\ell y}, \gamma_{yn}$	shear strain
$\gamma_{xx}, \gamma_{xy}, \gamma_{xz}$	shear strain in x, y and z axes
κ	shear modification factor
κ_ℓ	curvature in the ℓ -direction
κ_y	longitudinal curvature
$\kappa_{\ell y}$	twisting curvature
$\theta_x, \theta_y, \theta_z$	rotational degrees of freedom about x, y and z axes
ν	Poisson's ratio
ω_n	fundamental frequency
ξ	isoparametric element natural (curvilinear) coordinates
σ	stress component
Π	total potential energy
$\boldsymbol{\sigma}_m, \boldsymbol{\sigma}_b, \boldsymbol{\sigma}_s$	membrane, bending and shear stress resultant vectors
ρ	mass density
$\partial/\partial\ell$	partial differential of ℓ

CHAPTER 1

INTRODUCTION

1.1 General Introduction

This thesis deals with the implementation of reliable, accurate and efficient Soft Computing (SC) tools for the analysis and design of structures. The SC techniques in structural design with particular algorithms based on genetic algorithm, Neural Network (NN), Gene Expression Programming (GEP) depends on the accuracy of continuous or discrete structural design model. The use of SC techniques is motivated by the time-consuming repeated Finite Element (FE) or Finite Strip (FS) analysis required during analysis, design and optimization process.

Nowadays, computers are essential instruments for engineering science activities. It has been to suit very simplified to forecast the behavior and functioning of complex structures with the development of computer supported applications. In these applications, it is significant to understand the behavior of a system. Over the last decade, SC techniques came along as an effective instrument that could be an alternative technique for time consuming or expensive computing in such engineering problems. Moreover, SC techniques can effectively consider with the problems with nonlinear and noisy data which are often encountered in engineering problems. SC tools have the learning and generalization ability from examples and experience to discover solutions to problems. This learning can be achieved even if the input data is highly nonlinear or noisy which is often typical of the engineering design process. SC techniques have become popular tools for various engineering problems due to their outstanding features.

Because of severe economic constraints and stringent deadlines coupled with the enormous growth in computer speed and power, engineers are resorting to numerical methods for the analysis and design of structures. Among the various numerical methods, the FE method and its variance, such as the FS method, have become firmly established as engineering tools for the linear elastic analysis of plate and shell structures.

The predominant advantage of the FE method lies in its ability to analyze complex structures with varying thickness, difficult boundary conditions and arbitrary loading. However, from the engineering point of view, the use of the FE method for structural analysis has drastically increased the computational time cannot be affordable.

The introduction of the FS method, which in its most usual form makes use of a combination of the FE method and Fourier series, has provided a very useful and economical analysis tool for this class of prismatic structures.

1.2 Thesis Objectives

The essential objective of the thesis is to develop reliable and efficient computational tools for free vibration and buckling analysis and optimization of structures, particularly, stiffened plates. Structural optimization process of the type considered in this work requires the efficient integration of computer assisted geometry modeling, automated mesh generation, structural analysis and SC applications. The specific objectives of this thesis can be summarized as follows:

- to present a general formulation for variable thickness, isoparametric, Mindlin–Reissner, finite strips/finite elements for buckling and free vibration analysis of plates and shells, the accuracy and relative performance of formulation are compared with other numerical solutions.
- to improve and demonstrate the use of a reliable and competitive procedure for finding the optimum solutions with continuous design variables based on sequential quadratic programming,

- to develop SC models with NNs, GEP and genetic algorithms, and demonstrate their reliability and generalization capability of proposed models,

During the course of research work, a series of studies is assure to provide evidence of the effectiveness of the presented models, comparing numerical predictions with analytical or experimental results whenever possible.

Principally, it is desired that this thesis will provide stable bases for further investigation, leading to a more intensive use of structural optimization algorithms to solve practical problems.

1.3 Structure Type Considered in This Thesis

Because of the broad diversity of structures encountered in practice, it becomes clear that a thesis considering with analysis and structural optimization should concentrate on selected topics. For this reason, structures considered in this thesis are composed longitudinally stiffeners with plates usually called stiffened panel for convenience. Stiffened panels find wide applications heavily loaded thin wall and types of weight critical structures, because of their simplicity in fabrication and excellent strength to weight ratio. In such structures stiffened panels are basic strength members. These structures are generally subjected combined loadings, but primarily load component is axially compression. In this situation, determinations of critical buckling load of stiffened panels are required for structural design and safety assessment.

1.4 Soft Computing Techniques Considered in This Thesis

In this thesis, mathematical programming and genetic algorithm is adopted for the optimization process. Here, it is important to note that genetic algorithm requires no sensitivity analysis in the search method. The search method depends solely on the objective function information and mimics the ‘survival of the fittest’ process found in nature. Most mathematical programming algorithms assume that the design variables are continuous, but in many practical problems, the design variables are

discrete. This is what makes genetic algorithms as useful as they accept both discrete and continuous design variables.

1.5 Software Developed in This Thesis

In this study, reliable, effective and robust computer programs and SC models are prepared to attend structural engineers in designing structurally efficient forms and allow appreciable insight into the structural behavior. Five main computer programs have been developed and verified for analysis and optimization:

- BUCKFS deals with the buckling FS analysis and shape optimization of shells. This program is modified in Fortran90 using double precision and based on Özakça and co workers program [1].
- VIBFS deals with the free vibration analysis and shape optimization of shells. This program is modified in Fortran90 using double precision based on Özakça and co workers program [1].
- SCGEN deals with SC generation of datasets for models. It is written in FORTRAN90. It is an interface of BUCKFS and VIBFS programs to NNBEST and GeneXpro which is produced by Gepsoft.
- NNBEST deals with determination of best NN architecture by trial and error approach and genetic algorithms. This program is written on MATLAB computing environment.
- SCOPT deals with optimization of SC models by mathematical programming and genetic algorithms. This program is also written on MATLAB computing environment.

1.6 Layout of Thesis

This thesis consists of seven chapters. The contents of each chapter are now briefly described:

- A literature survey for SC techniques and their structural applications and FS analysis and optimization of structures are summarized in Chapter 2
- Chapter 3 covers presentation of basic FS analysis formulation of shells and also it is verified.

- Chapter 4 includes buckling load optimization with mathematical programming algorithm and its application of stiffened panels considered in TUBİTAK (107M648) Project [2].
- Chapter 5 gives a detailed review of important aspects of the SC techniques.
- Chapter 6 presents SC modelling of stiffened panels.
- Chapter 7 provides the conclusions of the present work and discusses the scope for further work.

CHAPTER 2

LITERATURE SURVEY

2.1 Introduction

Computer based structural analysis and SC technologies have now passed more than three decades from their birthday. Over these last three decades, structural analysis and SC applications have been continually developed and improved so that these techniques have matured to become useful design tools. We now provide a brief and selective review of the literature on FS analysis and SC applications.

2.2 Finite Strip Analysis

The FS method, mentioned first in 1968 by Cheung [3], is an effective and specific form of the FE technique. The FS method possesses the capability of solving structural analysis problems that have prismatic form and simple boundary conditions. FS forms fewer equations to be solved than FE. As an effect of this simplification, FS method is faster and powerful then FE method for specific structures. Two main types of strips are successfully developed: the semi analytical (or classical FSs) [4–23] and the spline FSs [24–25].

2.2.1 Stiffened Panel Analysis with Finite Strip Method

The structural design involves, for economic reasons, the selection of the minimum amount of material necessary to ensure the required resistance and stiffness to a structure assuming that an adequate safety parameter is guaranteed. For economics designs, in many branches of engineering, panels are used. The panels are often

attached with suitable stiffened structural form to enhance the specific strength/stiffness to weight ratio of the structure attached with suitable stiffened structural form to enhance the specific strength/stiffness to weight ratio of the structure. These structures experience in-plane forces in many situations. In the use of thin walled, as in panels, it must be kept in mind that thin elements may prove unstable under the action of forces in their own planes, and fail by buckling sideways [26–30].

Dawe and co-workers [4–11] used FS method which, based on the use of both classical thin plate theory and shear deformation plate theory, to determine the buckling stresses, the geometrically nonlinear response and natural frequencies of vibration of prismatic plate. Benson and Hinton [12] presented a comprehensive study including static, free vibration and stability analyses of thick and thin rectangular and curved plates using quadratic strips. Hinton and co-workers [13–15] used linear, quadratic and cubic FS based on Mindlin–Reissner assumptions for the free vibration and static analysis of curved and variable thickness, prismatic structures straight or curved planform. Later Hinton et. al. [16,17] have been dealt with buckling analysis of prismatic folded plate structures supported on diaphragms at two opposite edges. Özakça et al. [18] have been deal with buckling optimization of variable thickness prismatic folded plates and stiffened panels. Xie and Ibrahim [19] employed a method of FS to establish the equations of equilibrium for the rib-stiffened plates under axial compressive load. They also study on buckling mode localization in rib-stiffened plates with randomly misplaced stiffeners. Bui [20] presented an investigation of the buckling behaviour of thin-walled sections subjected to general loading conditions by FS method. The existing results are only for sections subjected to a uniform loading, namely: uniform compression, uniform bending and uniform distributed loads, which are applied at the shear centre. For a general loading condition, he proposed the realizing linear analysis first to give longitudinal stresses. Bradford and Azhari [21] presented a FS method of analysis which enables the elastic local buckling of plates and plate structures with different boundary conditions along the loaded ends to be studied.

Lillico et al. [22] present post-buckling analysis of isotropic stiffened panels loaded in compression. They repeated analysis different number of stiffener numbers with

new stiffener model which was following Shanley–type approach. Riks [23] applied FS method for determination of buckling load of stiffened panels in wing box structures.

Kwon and Hancock [24] presented analysis of buckling behavior of thin walled member using spline FS method. Azhari et al. [25] presented local buckling coefficients of plate structures by using bubble functions with spline FS method with different boundary conditions. Guo and Lindner [26] presented elastic and plastic interaction buckling of interaction imperfect longitudinally stiffened panels under compression.

Another crucial phenomenon at thin walled members is free vibration analysis. Vibration analysis is needed so as to ensure structural safety and durability under dynamic loading circumstances.

Liew et al. [31] presented a survey on vibration of shell panels which covers a large literature on the subject. Xie and Chen [32] presented paper on vibration mode localization of rib–stiffened plates with randomly misplaced stiffeners in one direction. Kantorovich's method and FS method are applied to set up the transfer matrices of stiffened plates, respectively. Obtained results from Kantorovich's method and FS method are indicated excellent agreement.

Yuan and Dawe [33] developed a B–spline strip method for the determination of natural vibration frequencies and buckling stresses of rectangular sandwich panels which are stiffened L, hat and blade type stiffeners. Stiffened plates may have various shapes, boundary conditions, loadings and also possessing various dispositions of stiffeners.

Sheikh and Mukhopadhyay [34] extended general spline FS method has been extended in their paper to the analysis of stiffened plates having arbitrary shape. The main contribution of the formulation lied in the treatment of stiffeners. It has been shown that the stiffener can be placed anywhere within the plate strip which introduces a considerable amount of flexibility in the analysis. As available in the literature, have been analysed by the proposed approach. Sheikh and Mukhopadhyay

[35] applied spline FS method for linear and nonlinear transient vibration analysis of plates and stiffened plates in another study. The stiffener has been elegantly modelled so that it may lie anywhere within the plate strip. Generalized formulation is implemented so that plates are having any shape and stiffeners having any orientation and eccentricity can be analyzed.

2.3 Structural Optimization with Mathematical Programming

Structural shape optimization process based on the FE/FS method has been applied for four decades with some success in the design of structures and structural members such as mathematical programming, genetic algorithms and NNs etc. Detailed information of these optimization algorithms presented many textbooks [36–38].

A lot of techniques and algorithms have been improved for optimum design of structural systems. Most of the techniques consider with continuous design variables and use mathematical programming techniques. Most popular mathematical optimization techniques are sequential linear programming [37,39], Sequential Quadratic Programming (SQP) [37] and method of moving asymptotes [40].

Genetic algorithm is a fairly new optimization technique based on the Darwinian survival of the fittest theory. The method has been proposed first by John Holland in 1975 [41] at the University of Michigan. Genetic algorithm is an evolutionary computing approach which is an alternative to traditional optimization methods. In most practical design problems, the design variables are discrete. Genetic algorithms are most appropriate for complex non-linear models where location of the global optimum is a difficult task.

Shape optimization of structures modeled using two dimensional representations was first investigated by Zienkiewicz and Campbell [39]. Since then much work has been reported.

Murphy et al. [42] presented an investigation of the potential of introducing local skin sub-stiffening to effectively tailor local skin buckling and panel collapse

performance. This study work undertaken has been enabled the development of simple design guidelines for sub-stiffening and potential analysis and optimization techniques for the combined panel configuration and local sub-stiffener design. Özakça et al. [43] investigated buckling performance of panels with substiffening or local tailoring of the skin thickness using linear variable thickness FS analysis. Design rules for substiffened panels were derived based on optimization of panels with SQP. Kim and Kim [44] proposed an accurate and realistic post buckling model for a stiffened composite panel and studied optimization module. In order to predict the realistic behavior in the post buckling region, cohesive elements were introduced to the analysis model to account for skin-stiffener debonding

Bedair and Troitsky [45] investigated the fundamental frequency characteristics of eccentrically and concentrically simply supported stiffened supported plates. They presented influence of the plate/stiffener geometric parameters on the fundamental frequency of the structure with various concentric and eccentric stiffening configurations and optimum solutions which are obtained with sequential quadratic programming.

2.4 Soft Computing Techniques in Structural Mechanics

SC attracts inspiration from nature. Neural computing attempts mimic the human brain, evolutionary computing founded on basis of theory Darwinian evolution and fuzzy computing is heavily motivated by the highly inexact nature of human speech and uncertain situations. SC is the combination of methodologies that were studied to model and enable solutions to real life problems, which are not modeled, or too difficult to model, mathematically or have highly expensive solution cost.

2.4.1. Neural Computing

The application of NNs in structural engineering has been gaining support in the recent years. The NN models adopted for structural mechanics may have different architectures and may possess different patterns of connectivity. NNs have been used as computational tools in various areas of structural mechanics, amongst them, optimization, analysis and design. The range of applications of back propagation

NNs in computational structural mechanics may include design, optimization, identification, mesh generation and analysis [46]. NNs have been widely used as an alternative tool for both civil and mechanical engineering disciplines during the last decade and have been applied to almost every type of problem in the field of engineering mechanics [46–49]. Several other researchers have applied NNs, mostly back–propagation algorithms, in structural engineering and mechanics and related engineering problems [50–54]. A detailed literature review on application of NNs in structural analysis and design can be found in Lu [55]. Some of stiffened panel literature summarized as follows;

Bisagni and Lanzi [56] dealt with post–buckling optimization procedure for the design of composite stiffened panels subjected to compression loads. They developed an optimization procedure is based on a global approximation strategy, where the structure response is given by a system of NNs trained by means of FE analyses, and on genetic algorithms. Lanzi and Giavotto [57] implemented an optimization methodology for the design of stiffened composite shells by considering post–buckling constraint which is based on genetic algorithms and global approximation techniques. Three different kind of global approximation techniques are proposed and compared which are NNs, radial basis functions and kriging approximation. Global approximations are used to contain the high computational efforts required to predict the post–buckling behavior of each configuration analyzed throughout the optimization process.

2.4.2. Evolutionary Computing

Evolutionary computation is emerging as a new engineering computational paradigm, which may significantly change the present structural design practice. An extensive review of evolutionary computation is reviewed in the field of structural design presented by Kicinger et al. [58]. Some of stiffened panel literature summarized as follows;

Iuspa and Ruocco [59] investigated topological optimal design of isotropic /orthotropic thin structures performed via genetic algorithms. Examples involving structural weight minimization under compressive load or buckling load

maximization are presented. In particular, a semi-analytical FS formulation for the determination of eigenvalues and eigenvectors adopted and mesh-independent solver, involving a reduced number of degrees of freedom implemented and interfaced with a genetic optimizer in order to reduce computational efforts requested by the optimization task. Wang [60] et al. presented an optimal design of laminated composite stiffened panels of symmetric and balanced layup with different number of T-shape stiffeners. The stiffened panels are simply supported and subjected to uniform biaxial compressive load. In the optimization for the maximum buckling load without weight penalty, the panel skin and the stiffened laminate stacking sequence, thickness and the height of the stiffeners are chosen as design variables. The optimization is carried out by applying an ant colony algorithm is a kind of evolutionary computing with the ply contiguous constraint taken into account.

2.4.3. Fuzzy Systems

Fuzzy logic is first presented in 1965 by Zadeh [61]. The transition from the Aristotelian logic to the fuzzy logic was accepted by the researcher with hesitation. The power of modeling the uncertainty through fuzzy logic appealed numerous investigators that contributed to the basis of several fuzzy logic concepts relative to engineering design [62].

Noor et al. [63] presented a study is made of the variability in the nonlinear response of three stiffened composite panels associated with variations in their geometric and material parameters. The three panels have a cylindrical skin with either four or five T-shaped stiffeners. The major parameters taken to fuzzy parameters and a fuzzy set analysis are used to determine the range of variation of the response associated with pre-selected variations in the major parameters. Ji et al. [64] described a hybrid mode/Fourier transform approach for estimating the vibration response of a beam-stiffened plate system. Provided the plate receiver is flexible enough so that its vibration tends to exhibit non-resonant behavior in the frequency range of interest. Close agreement observed with fuzzy structure theory. Ji et al. [65] another research study, described mode-based approach for the mid-frequency vibration analysis of a complex structure built-up from a long-wavelength source and a short-wavelength receiver. The source and the receiver respectively have low and high modal densities

and modal overlaps. Each substructure is described in terms of its uncoupled, free–interface natural modes. The interface forces and displacements are decomposed in terms of a set of interface basis functions. They were found that these approaches yield the same results in the ‘fuzzy’ limit.

As a results of the broad literature survey, the following consequences are found. Buckling and vibration analysis of stiffened panels and types of stiffeners are widely considered with different with solution methods by so many researchers. FS method is most powerful and effective method analysis of stiffened panels is observed from literature. A diversity of SC methods is in existence and the combination of methodologies that were studied to model and enable solutions to stiffened panels. Although NNs are widely employed in structural engineering applications, the particular subject of NN application buckling and vibration analysis of stiffened panels needs further contributions. One of the major tasks in NN studies is apparently the finding of the optimal NN architecture which is based on trial and error processes. There is no well established study in the fields of structural analysis by NNs handling the automatic selection of the optimum NN architecture. This will economize much more time and simplify NN applications to a great extent.

CHAPTER 3

STRUCTURAL ANALYSIS

3.1 Introduction

Although the subject of buckling and free vibration analysis and optimization had been discussed frequently over recent years, this chapter was included to illustrate the validity of analysis program, which is utilized in optimization and SC programs. In this chapter, buckling and free vibration FS methods are presented and before any optimization and SC techniques are implemented, each analysis program was examined against known benchmark solutions, to confirm integrity of the analyses.

3.2 Structural Theories

Many engineering structures have constant geometrical properties along a particular direction. Such prismatic structures are very common in plate and shell problems where the transverse cross-section of the structure often remain constant in the longitudinal direction. If the material properties of the structures are also constant in the same direction, the buckling analysis can be simplified by the combined use of FEs and Fourier expansions to model the transverse and longitudinal behavior respectively.

Thin shell theories neglect transverse shear and rotary inertia effects and consequently may yield incorrect results, especially for higher values of the ratio of the thickness-to-minimum radius of curvature and also for higher modes. For example, in plate analysis, the buckling loads are overestimated for all buckling modes in shear-weak situations and for the higher buckling modes in shear-stiff

cases. In such circumstances, the effects of shear deformation and rotatory inertia should be taken into account.

Mindlin–Reissner shell theory allows for transverse shear deformation effects and thus offers an attractive alternative to classical Kirchhoff–Love thin shell theory. The main assumptions are that:

- displacements are small compared to the shell thickness,
- stress normal to the mid–surface is negligible,
- normals to the mid–surface before deformation remain straight but not necessarily normal to the mid–surface after deformation [66].

It is well known that displacement–based Mindlin–Reissner FSs require only $C(0)$ continuity of the displacements and independent normal rotations between adjacent elements. This provides an important advantage over FS based on classical Kirchhoff–Love thin shell theory where $C(1)$ continuity is strictly required. Thus, Mindlin–Reissner shell elements are simpler to formulate and they have the added advantage of being able to model shear–weak and shear–stiff shells. However, several difficulties can be encountered when Mindlin–Reissner shell elements are used in thin or shear–stiff situations. The success of the Mindlin–Reissner formulation presented here for both thick and thin shell analysis lays in the use of reduced integration techniques for the numerical computation of stiffness matrix. This simply implies that the shear terms contributing to the stiffness matrix are numerically integrated with a lower order Gaussian quadrature than that needed for their exact computation, whereas the rest of the stiffness matrix is exactly calculated [66]. Care has been taken to avoid mechanism or spurious zero–energy modes.

In this section the Mindlin–Reissner FS formulation for prismatic plates and shells in right planform will be derived in detail.

3.3 Buckling Analysis

The property of thinness of a shell structure has a consequence that is pointed out in [67,68]. The membrane stiffness is generally several orders of magnitude greater than the bending stiffness. A thin shell can absorb a great deal of membrane strain energy

without deforming too much [13]. It must deform much more in order to absorb an equivalent amount of bending strain energy. If the shell is loaded in such a way that most of its strain energy is in the form of membrane compression, and if there is a way that this store up membrane energy can be converted into bending energy, the shell may fail rather dramatically in a process called buckling as it exchanges its membrane energy to bending energy. Very large deflections are generally required to convert a given amount of membrane energy into bending energy. The way in which buckling occurs depends on how the shell is loaded and on its geometrical and material properties.

3.3.1 Strain Energy

Consider the buckling of the Mindlin–Reissner shell strip shown in Figure 3.1. Translations in the ℓ , y and n directions are represented by the displacement components u_ℓ , v_ℓ and w_ℓ . The displacement components u_ℓ and w_ℓ may be written in terms of global displacements u and w in the x and z directions as

$$\begin{aligned} u_\ell &= u \cos \alpha + w \sin \alpha \\ w_\ell &= -u \sin \alpha + w \cos \alpha \end{aligned} \quad (3.1)$$

where α is the angle between the x and ℓ axes; see Figure 3.1. The radius of curvature R may be obtained from the expression

$$\frac{d\alpha}{d\ell} = -\frac{1}{R} \quad (3.2)$$

Note that the displacement components v_ℓ and v coincide.

The strain energy for a typical curved Mindlin–Reissner strip e of length b shown in Figure 3.1 is given in terms of the global displacements u, v, w and the rotations ϕ and ψ of the mid-surface normal in the ℓn and yn planes respectively by the expressions (3.1)

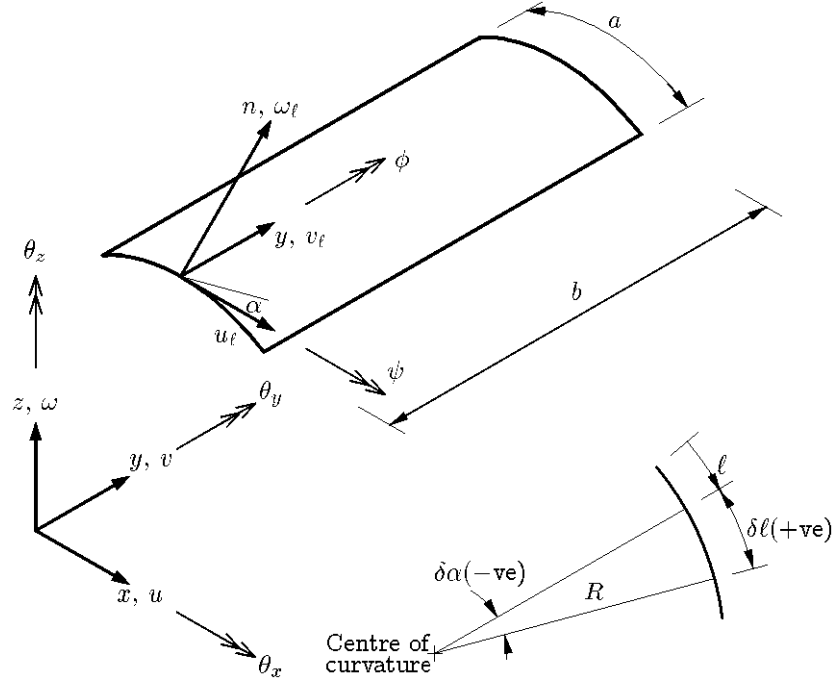


Figure 3.1 Definition of Mindlin–Reissner FSs

$$U^e = \frac{1}{2} \int_0^b \int_{\ell^e} \left(\mathbf{D}_m^T \boldsymbol{\varepsilon}_m + \boldsymbol{\varepsilon}_b^T \mathbf{D}_b \boldsymbol{\varepsilon}_b + \boldsymbol{\varepsilon}_s^T \mathbf{D}_s \boldsymbol{\varepsilon}_s \right) d\ell dy \quad (3.3)$$

where the inplane strains $\boldsymbol{\varepsilon}_m$ are given by

$$\boldsymbol{\varepsilon}_m = [\varepsilon_\ell, \varepsilon_y, \gamma_{\ell y}]^T \quad (3.4)$$

in which the strain in the ℓ –direction may be expressed in terms of the local

displacements as

$$\varepsilon_\ell = \frac{\partial u_\ell}{\partial \ell} + \frac{w_\ell}{R} \quad (3.5)$$

or in terms of the global displacements as

$$\varepsilon_\ell = \frac{\partial u}{\partial \ell} \cos \alpha + \frac{\partial w}{\partial \ell} \sin \alpha \quad (3.6)$$

The longitudinal strain is expressed as

$$\varepsilon_y = \frac{\partial v}{\partial y} \quad (3.7)$$

and the shear strain is written in the form

$$\gamma_{\ell y} = \frac{\partial u_\ell}{\partial y} + \frac{\partial v}{\partial \ell} \quad (3.8)$$

or

$$\gamma_{\ell y} = \frac{\partial u}{\partial y} \cos \alpha + \frac{\partial w}{\partial y} \sin \alpha + \frac{\partial v}{\partial \ell} \quad (3.9)$$

The bending strains or curvatures $\boldsymbol{\varepsilon}_b$ are given by

$$\boldsymbol{\varepsilon}_b = [\kappa_\ell, \kappa_y, \kappa_{\ell y}]^T \quad (3.10)$$

where the curvature in the ℓ -direction is

$$\kappa_\ell = -\frac{\partial \phi}{\partial \ell} \quad (3.11)$$

The longitudinal curvature is given as

$$\kappa_y = -\frac{\partial \psi}{\partial y} \quad (3.12)$$

and the twisting curvature has the form

$$\kappa_{\ell y} = -\left(\frac{\partial \phi}{\partial y} + \frac{\partial \psi}{\partial \ell} \right) + \frac{\partial u_\ell}{\partial y} \frac{1}{R} \quad (3.13)$$

or

$$\kappa_{\ell y} = -\left(\frac{\partial\phi}{\partial y} + \frac{\partial\psi}{\partial\ell}\right) - \left(\frac{\partial u}{\partial y} \cos\alpha + \frac{\partial w}{\partial y} \sin\alpha\right) \frac{d\alpha}{d\ell} \quad (3.14)$$

The transverse shear strains $\boldsymbol{\varepsilon}_s$ are given by

$$\boldsymbol{\varepsilon}_s = [\gamma_{\ell n}, \gamma_{yn}]^T \quad (3.15)$$

in which the transverse shear strain in the ℓn plane is

$$\gamma_{\ell n} = \frac{\partial w_\ell}{\partial\ell} - \phi - \frac{u_\ell}{R} \quad (3.16)$$

or

$$\gamma_{\ell n} = -\frac{\partial u}{\partial\ell} \sin\alpha + \frac{\partial w}{\partial\ell} \cos\alpha - \phi. \quad (3.17)$$

The longitudinal transverse shear in the yn plane is

$$\gamma_{yn} = \frac{\partial w_\ell}{\partial y} - \psi \quad (3.18)$$

or

$$\gamma_{yn} = -\frac{\partial u}{\partial y} \sin\alpha + \frac{\partial w}{\partial y} \cos\alpha - \psi. \quad (3.19)$$

For an isotropic material of elastic modulus E , Poisson's ratio ν and thickness t , the matrix of membrane rigidities has the form

$$\mathbf{D}_m = \frac{Et}{(1-\nu^2)} \begin{bmatrix} 1 & \nu & 0 \\ \nu & 1 & 0 \\ 0 & 0 & (1-\nu)/2 \end{bmatrix} \quad (3.20)$$

the matrix of flexural rigidities may be expressed as

$$\mathbf{D}_b = \frac{Et^3}{12(1-\nu^2)} \begin{bmatrix} 1 & \nu & 0 \\ \nu & 1 & 0 \\ 0 & 0 & (1-\nu)/2 \end{bmatrix} \quad (3.21)$$

and the matrix of shear rigidities is given as

$$\mathbf{D}_s = \frac{\kappa^2 Et}{2(1+\nu)} \begin{bmatrix} 1 & 0 \\ 0 & 1 \end{bmatrix} \quad (3.22)$$

where κ^2 is the shear modification factor and is usually taken as 5/6 for an isotropic material.

3.3.2 Potential Energy of the Applied Inplane Stresses

Buckling occurs when a structure converts inplane strain energy into strain energy of bending with no change in externally applied load. A critical condition, at which buckling impends, exist when it is possible that the deformation state may change slightly in a way that makes the loss in inplane strain energy numerically equal to the gain in bending strain energy. In a thin-walled structure such as a shell, inplane stiffness is typically orders of magnitude greater than bending stiffness. Accordingly, small inplane deformations can store a large amount of strain energy, but comparatively large lateral deflections and cross-section rotations are needed to absorb this energy in bending deformations.

The potential energy of the applied inplane stresses σ_ℓ^0 , σ_y^0 and $\tau_{\ell y}^0$ arises from the action of the applied stresses on the corresponding second order strains ε_ℓ^{nl} , ε_y^{nl} , $\gamma_{\ell y}^{nl}$ are taken from Dawe and Peshkam [9]. The potential energy of the shell of volume V is

$$V_g = \int_V \left(\sigma_\ell^0 \varepsilon_\ell^{nl} + \sigma_y^0 \varepsilon_y^{nl} + \tau_{\ell y}^0 \gamma_{\ell y}^{nl} \right) dV \quad (3.23)$$

integrating through the thickness, this becomes

$$\begin{aligned}
V_g = \frac{1}{2} t \iint_A & \left\{ \sigma_\ell^0 \left[\left(\frac{\partial u}{\partial \ell} \right)^2 + \left(\frac{\partial v}{\partial \ell} \right)^2 + \left(\frac{\partial w}{\partial \ell} \right)^2 \right] + \sigma_y^0 \left[\left(\frac{\partial u}{\partial y} \right)^2 + \left(\frac{\partial v}{\partial y} \right)^2 + \left(\frac{\partial w}{\partial y} \right)^2 \right] \right. \\
& + 2\tau_{\ell y}^0 \left[\frac{\partial u}{\partial \ell} \frac{\partial u}{\partial y} + \frac{\partial v}{\partial \ell} \frac{\partial v}{\partial y} + \frac{\partial w}{\partial \ell} \frac{\partial w}{\partial y} \right] \\
& + \frac{t^2}{12} \left\{ \sigma_\ell^0 \left[\left(\frac{\partial \phi}{\partial \ell} \right)^2 + \left(\frac{\partial \psi}{\partial \ell} \right)^2 \right] + \sigma_y^0 \left[\left(\frac{\partial \phi}{\partial y} \right)^2 + \left(\frac{\partial \psi}{\partial y} \right)^2 \right] \right. \\
& \left. \left. + 2\tau_{\ell y}^0 \left[\frac{\partial \phi}{\partial \ell} \frac{\partial \phi}{\partial y} + \frac{\partial \psi}{\partial \ell} \frac{\partial \psi}{\partial y} \right] \right\} d\ell dy \quad (3.24)
\end{aligned}$$

In equation (3.24), the terms involving the first derivative of w , ϕ and ψ represent the out of plane destabilizing influence of the prescribed stresses. The remaining terms, which are dependent upon first derivatives of u and v , are in plane destabilizing influences. The prescribed inplane shear stress $\tau_{\ell y}$ is rarely applied to structures, and is not considered in the present study.

$$\begin{aligned}
V_g^e = \frac{1}{2} \int_0^b \int_{\ell^e} & \left\{ t \left\{ \sigma_\ell^0 \left[\left(\frac{\partial u}{\partial \ell} \right)^2 + \left(\frac{\partial v}{\partial \ell} \right)^2 + \left(\frac{\partial w}{\partial \ell} \right)^2 \right] + \sigma_y^0 \left[\left(\frac{\partial u}{\partial y} \right)^2 + \left(\frac{\partial v}{\partial y} \right)^2 + \left(\frac{\partial w}{\partial y} \right)^2 \right] \right\} \right. \\
& \left. + \frac{t^3}{12} \left\{ \sigma_\ell^0 \left[\left(\frac{\partial \phi}{\partial \ell} \right)^2 + \left(\frac{\partial \psi}{\partial \ell} \right)^2 \right] + \sigma_y^0 \left[\left(\frac{\partial \phi}{\partial y} \right)^2 + \left(\frac{\partial \psi}{\partial y} \right)^2 \right] \right\} \right\} d\ell dy \quad (3.25)
\end{aligned}$$

3.3.3 Finite Strip Idealization

Using n -noded, $C(0)$ strips, the global displacements and rotations may be interpolated within each strip in terms of truncated Fourier series along direction y , in which both the material and geometrical properties of the plate are taken to be constant, i.e.

$$\begin{aligned}
u(\ell, y) &= \sum_{p=p_1}^{p_2} u^p(\ell) S_p; & v(\ell, y) &= \sum_{p=p_1}^{p_2} v^p(\ell) C_p \\
w(\ell, y) &= \sum_{p=p_1}^{p_2} w^p(\ell) S_p; & \phi(\ell, y) &= \sum_{p=p_1}^{p_2} \phi^p(\ell) S_p \\
\psi(\ell, y) &= \sum_{p=p_1}^{p_2} \psi^p(\ell) C_p \quad (3.26)
\end{aligned}$$

where $C_p = \cos(p\pi y/b)$ and $S_p = \sin(p\pi y/b)$, u^p, v^p, w^p, ϕ^p and ψ^p are displacement and rotation amplitudes for the p^{th} harmonic term. This corresponds to a single diaphragm support at the ends of the structure at $y=0$ and $y=b$, so that $v = w = \phi = 0$. As shown later, this will lead to an uncoupling of each harmonic term which in turn leads to an economic solution. Note that the strip displacement and rotation fields are generally expressed as a summation of a set of contributions from a lower limit p_1 to an upper limit p_2 . In the present work as there is no coupling between the harmonics p_1 and p_2 coincide. For many cases taking $p_1 = p_2 = 1$ provides the lowest buckling mode; however, in some cases p_1 and p_2 may be associated with a higher mode.

The next step is to discretise the displacement and rotation amplitudes (which are functions of the ℓ – coordinate only) using an n – noded FE representation so that within a strip e the amplitudes can be written as

$$\begin{aligned} u^p(\ell) &= \sum_{i=1}^n N_i u_i^p; & v^p(\ell) &= \sum_{i=1}^n N_i v_i^p; & w^p(\ell) &= \sum_{i=1}^n N_i w_i^p \\ \phi^p(\ell) &= \sum_{i=1}^n N_i \phi_i^p; & \psi^p(\ell) &= \sum_{i=1}^n N_i \psi_i^p \end{aligned} \quad (3.27)$$

where u^p, v^p, w^p, ϕ^p and ψ^p are typical nodal degrees of freedom associated with node i and harmonic p .

Thus, the process is equivalent to dividing the structure into longitudinal elements (or strips) so that each strip has a certain number of nodes associated with its transverse direction. The displacement field is defined longitudinally by the Fourier expansion of (3.26) and transversely by the FE discretisation of (3.27). Substituting (3.27) into (3.26) it is possible to write

$$\mathbf{u} = \sum_{p=p_1}^{p_2} \sum_{i=1}^n \mathbf{N}_i^p \mathbf{d}_i^p \quad (3.28)$$

where

$$\mathbf{u} = [v, w, \phi, \psi]^T$$

$$\mathbf{d}_i^p = [u_i^p, v_i^p, w_i^p, \phi_i^p, \psi_i^p]^T$$

and

$$\mathbf{N}_i^p = \begin{bmatrix} N_i S_p & 0 & 0 & 0 & 0 \\ 0 & N_i C_p & 0 & 0 & 0 \\ 0 & 0 & N_i S_p & 0 & 0 \\ 0 & 0 & 0 & N_i S_p & 0 \\ 0 & 0 & 0 & 0 & N_i C_p \end{bmatrix} \quad (3.29)$$

$N_i(\xi)$ is the shape function associated with node i [1]. These elements are essentially isoparametric so that

$$x = \sum_{i=1}^n N_i x_i; \quad y = \sum_{i=1}^n N_i y_i; \quad t = \sum_{i=1}^n N_i t_i \quad (3.30)$$

where x_i and y_i are typical coordinates of node i and t_i is the thickness at node i .

Note also that the Jacobian

$$J = \frac{d\ell}{d\xi} = \left[\left(\frac{dx}{d\xi} \right)^2 + \left(\frac{dy}{d\xi} \right)^2 \right]^{1/2}; \quad d\ell = J d\xi \quad (3.31)$$

where

$$\frac{dx}{d\xi} = \sum_{i=1}^n \frac{dN_i}{d\xi} x_i; \quad \frac{dy}{d\xi} = \sum_{i=1}^n \frac{dN_i}{d\xi} y_i \quad (3.32)$$

Also, it is possible to write that

$$\sin \alpha = \frac{dy}{d\xi} \frac{1}{J}; \quad \cos \alpha = \frac{dx}{d\xi} \frac{1}{J} \quad (3.33)$$

and

$$\frac{dN_i}{d\ell} = \frac{dN_i}{d\xi} \frac{1}{J} \quad (3.34).$$

3.3.4 Stiffness Matrix

We can now evaluate the stiffness matrix \mathbf{K}^e associated with the strain energy of the Mindlin–Reissner strip. The membrane strains $\boldsymbol{\varepsilon}_m$ may then be expressed as

$$\boldsymbol{\varepsilon}_m = \sum_{p=p_1}^{p_2} \sum_{i=1}^n \mathbf{B}_{mi}^p \mathbf{d}_i^p \quad (3.35)$$

where if we set $\bar{p} = p\pi/b$

$$\mathbf{B}_{mi}^p = \begin{bmatrix} (dN_i/d\ell)S_p \cos \alpha & 0 & (dN_i/d\ell)S_p \sin \alpha & 0 & 0 \\ 0 & -\bar{p}N_i S_p & 0 & 0 & 0 \\ \bar{p}N_i C_p \cos \alpha & (dN_i/d\ell)C_p & \bar{p}N_i C_p \sin \alpha & 0 & 0 \end{bmatrix}$$

The flexural strains or curvatures $\boldsymbol{\varepsilon}_b$ can be written as

$$\boldsymbol{\varepsilon}_b = \sum_{p=p_1}^{p_2} \sum_{i=1}^n \mathbf{B}_{bi}^p \mathbf{d}_i^p \quad (3.36)$$

where

$$\mathbf{B}_{bi}^p = \begin{bmatrix} 0 & 0 & 0 & -(dN_i/d\ell)S_p & 0 \\ 0 & 0 & 0 & 0 & \bar{p}N_i S_p \\ \bar{p}N_i C_p \cos \alpha & 0 & \bar{p}N_i C_p \sin \alpha & -\bar{p}N_i C_p & (dN_i/d\ell)C_p \end{bmatrix}$$

The transverse shear strains $\boldsymbol{\varepsilon}_s$ are approximated as

$$\boldsymbol{\varepsilon}_s = \sum_{p=p_1}^{p_2} \sum_{i=1}^n \mathbf{B}_{si}^p \mathbf{d}_i^p \quad (3.37)$$

where

$$\mathbf{B}_{si}^p = \begin{bmatrix} -(dN_i/d\ell)S_p \sin \alpha & 0 & (dN_i/d\ell)S_p \cos \alpha & -N_i S_p & 0 \\ -\bar{p}N_i C_p \sin \alpha & 0 & \bar{p}N_i C_p \cos \alpha & 0 & -N_i C_p \end{bmatrix}$$

The strain energy may then be expressed as

$$U^e = \frac{1}{2} \sum_{p=p_1, q=q_1}^{p_2} \sum_{i=1}^n \sum_{j=1}^n \mathbf{d}_i^p [\mathbf{K}_{ij}^e]^{pq} \mathbf{d}_j^q \quad (3.38)$$

where the typical submatrix of the stiffness \mathbf{K}^e of strip e linking nodes i and j and harmonics p and q has the form

$$[\mathbf{K}_{ij}^e]^{pq} = \int_0^b \int_{-1}^{+1} \left(\mathbf{B}_{mj}^p \right)^T \mathbf{D}_m \mathbf{B}_{mj}^q + [\mathbf{B}_{bj}^p]^T \mathbf{D}_b \mathbf{B}_{bj}^q + [\mathbf{B}_{sj}^p]^T \mathbf{D}_s \mathbf{B}_{sj}^q \Big) J d\xi dy \quad (3.39)$$

3.3.5 Geometric Stiffness Matrix

We can now evaluate the geometric stiffness matrix \mathbf{K}_σ^e associated with the potential energy V^e of the applied inplane stresses σ_ℓ^0 and σ_y^0 which can be expressed as

$$V^e = \frac{1}{2} \sum_{p=p_1, q=q_1}^{p_2} \sum_{i=1}^n \sum_{j=1}^n \mathbf{d}_i^p [\mathbf{K}_{\sigma ij}^e]^{pq} \mathbf{d}_j^q \quad (3.40)$$

where a typical sub-matrix \mathbf{K}_σ^e of strip e linking nodes i and j , harmonics p and q has the form

$$\begin{aligned} [\mathbf{K}_{\sigma ij}^e]^{pq} = & \int_0^b \int_{-1}^{+1} \left(t[\mathbf{S}_{ui}^p]^T \mathbf{H} \mathbf{S}_{uj}^q + t[\mathbf{S}_{vi}^p]^T \mathbf{H} \mathbf{S}_{vj}^q + t[\mathbf{S}_{wi}^p]^T \mathbf{H} \mathbf{S}_{wj}^q \right. \\ & \left. + \left(\frac{t^3}{12} [\mathbf{Q}_i^p]^T \mathbf{H} \mathbf{Q}_j^q + \frac{t^3}{12} [\mathbf{R}_i^p]^T \mathbf{H} \mathbf{R}_j^q \right) \right) J d\xi dy \end{aligned} \quad (3.41)$$

in which

$$\begin{aligned} \mathbf{S}_{ui}^p &= \begin{bmatrix} (dN_i/d\ell)S_p & 0 & 0 & 0 & 0 \\ N_i(p\pi/b)C_p & 0 & 0 & 0 & 0 \end{bmatrix}, \\ \mathbf{S}_{vi}^p &= \begin{bmatrix} 0 & (dN_i/d\ell)C_p & 0 & 0 & 0 \\ 0 & -N_i(p\pi/b)S_p & 0 & 0 & 0 \end{bmatrix}, \\ \mathbf{S}_{wi}^p &= \begin{bmatrix} 0 & 0 & (dN_i/d\ell)S_p & 0 & 0 \\ 0 & 0 & N_i(p\pi/b)C_p & 0 & 0 \end{bmatrix}, \\ \mathbf{Q}_i^p &= \begin{bmatrix} 0 & 0 & 0 & (dN_i/d\ell)S_p & 0 \\ 0 & 0 & 0 & 0 & -N_i(p\pi/b)S_p \end{bmatrix}, \end{aligned}$$

$$\mathbf{R}_i^p = \begin{bmatrix} 0 & 0 & 0 & 0 & (dN_i/d\ell)C_p \\ 0 & 0 & 0 & N_i(p\pi/b)C_p & 0 \end{bmatrix},$$

and

$$\mathbf{H} = \begin{bmatrix} \sigma_\ell^0 & 0 \\ 0 & \sigma_y^0 \end{bmatrix}.$$

Matrix \mathbf{K}_σ^e is defined by an element's geometry, displacement field, and state of stress. Thus, \mathbf{K}_σ^e is independent of elastic properties. However, by introducing the stress–strain relation, \mathbf{K}_σ^e can alternatively be written in terms of elastic properties and strains or deformations.

If the structure geometry is well modeled, then such a formulation yields an upper bound to the magnitude of the true buckling load. The ‘true’ buckling load is the linear bifurcation load of the structure in its reference configuration; it is not necessarily the collapse load of the actual structure. The FS formulation given in this section yields the ‘true’ buckling load.

Note that, $[\mathbf{K}_{ij}^e]^{pq}$ and $[\mathbf{K}_{\sigma ij}^e]^{pq} = 0$ if $p \neq q$ because of the orthogonality conditions

$$\begin{aligned} \int_0^b \sin(p\pi y/b) \sin(q\pi y/b) dy &= b/2 && \text{if } p = q \\ \int_0^b \sin(p\pi y/b) \sin(q\pi y/b) dy &= 0 && \text{if } p \neq q \\ \int_0^b \cos(p\pi y/b) \cos(q\pi y/b) dy &= b/2 && \text{if } p = q \\ \int_0^b \cos(p\pi y/b) \cos(q\pi y/b) dy &= 0 && \text{if } p \neq q \end{aligned} \quad (3.42)$$

To avoid locking behavior, reduced integration may be adopted, i.e. 1–, 2–, 3–point Gauss–Legendre quadrature is used for the 2–, 3– and 4–noded strips respectively. Note also that since the rigidities $\mathbf{D}_m, \mathbf{D}_b$ and \mathbf{D}_s all depend on t and since t is interpolated within each strip e from the nodal values t_i , strips of variable thickness in the transverse direction may be easily accommodated in the present formulation.

Nothing the orthogonality relation (3.42), on assembly of the contributions to the total potential energy $U + V$ from all of the strips and subsequent minimization with respect to the nodal values the following eigenvalue expression is obtained for each harmonic p

$$[\mathbf{K}^{pp} + \lambda^p \mathbf{K}_\sigma^{pp}] \bar{\mathbf{d}}^p = 0 \quad (3.43)$$

where λ^p is the load factor by which the inplane stress σ_ℓ^0 and σ_y^0 are multiplied to produce instability and $\bar{\mathbf{d}}^p$ is the associated buckling mode. In the present studies the eigenvalues are evaluated using the subspace iteration algorithm [70].

3.3.6 Branched Strips

In the case of plates the strips all lie in the same plane, which coincides with the strip middle surface, whereas for branched structures the strips meet at different angles. Thus, to assemble the complete stiffness matrix for branched shell structures, displacements at joints must be expressed in a common and uniquely defined coordinate system. The translational degrees of freedom u , v and w are already expressed in the global x , y and z directions and therefore the associated stiffness terms do not require any further transformation. However, rotation degrees of freedom ψ_i are related to the local axis ℓ and therefore the associated stiffness terms must be transformed accordingly. Thus it is possible to write that

$$\mathbf{d}_i^p = \mathbf{T} \bar{\mathbf{d}}_i^p \quad (3.44)$$

where

$$\bar{\mathbf{d}}_i^p = [u_i^p, v_i^p, w_i^p, \theta_{xi}^p, \theta_{yi}^p, \theta_{zi}^p]^T \quad (3.45)$$

is the displacement vector at node i of strip where $\theta_{xi}^p, \theta_{yi}^p$ and θ_{zi}^p are the rotations about the x , y and z axes and $\phi_i = \theta_{yi}$. The matrix \mathbf{T} can now be defined as

$$\mathbf{T} = \begin{bmatrix} 1 & 0 & 0 & 0 & 0 & 0 \\ 0 & 1 & 0 & 0 & 0 & 0 \\ 0 & 0 & 1 & 0 & 0 & 0 \\ 0 & 0 & 0 & 0 & 1 & 0 \\ 0 & 0 & 0 & \cos \alpha & 0 & \sin \alpha \end{bmatrix} \quad (3.46)$$

The membrane strain displacement matrices are then modified to

$$\bar{\mathbf{B}}_{mi} = \mathbf{B}_{mi} \mathbf{T} \quad (3.47)$$

with similar expressions for $\bar{\mathbf{B}}_{bi}$, $\bar{\mathbf{B}}_{si}$, $\bar{\mathbf{Q}}_i$ and $\bar{\mathbf{R}}_i$. The stiffness and geometric stiffness matrices can be written as

$$[\mathbf{K}_{ij}^e]^{pp} = \int_0^b \int_{-1}^1 \left(\bar{\mathbf{B}}_{mi}^p \right)^T \mathbf{D}_m \bar{\mathbf{B}}_{mj}^p + \left(\bar{\mathbf{B}}_{bi}^p \right)^T \mathbf{D}_b \bar{\mathbf{B}}_{bj}^p + \left(\bar{\mathbf{B}}_{si}^p \right)^T \mathbf{D}_s \bar{\mathbf{B}}_{sj}^p \right) J d\xi dy \quad (3.48)$$

and

$$[\mathbf{K}_{\sigma ij}^e]^{pp} = \int_0^b \int_{-1}^1 \left(t [\mathbf{S}_{ui}^p]^T \mathbf{H} \mathbf{S}_{uj}^p + t [\mathbf{S}_{vi}^p]^T \mathbf{H} \mathbf{S}_{vj}^p + t [\mathbf{S}_{wi}^p]^T \mathbf{H} \mathbf{S}_{wi}^p \right) \left(\frac{t^3}{12} [\bar{\mathbf{Q}}_i^p]^T \mathbf{H} \bar{\mathbf{Q}}_j^p + \frac{t^3}{12} [\bar{\mathbf{R}}_i^p]^T \mathbf{H} \bar{\mathbf{R}}_j^p \right) J d\xi dy \quad (3.49).$$

3.4 Free Vibration Analysis of Structures

The predictions of the dynamic characteristics of structure are of considerable practical importance in the design. These structures often have constant geometrical properties along a particular direction. Such prismatic structures are very common in plate and shell problems where the transverse cross-section of the structure often remain constant in the longitudinal direction. The analysis of such structures in static and dynamic situations is most efficiently carried out using semi-analytical semi-numerical methods such as the FS method which combines the use of Fourier expansions and one dimensional FE to model the longitudinal and transverse structural behavior respectively. The geometrical and material properties are uniform in a longitudinal direction.

In previous section, structural theories about Mindlin–Reissner FSs and derivation of stiffness matrices for FS analysis are discussed with all details. In order to prevent repetition, general energy integral equation and derivation of mass matrix only is given below. Consider the free vibration of the Mindlin-Reissner curved shell strip shown in Figure 3.1. In the absence of the external loads and damping effects, the virtual work (or more precisely the virtual power) for a typical curved Mindlin-Reissner strip e of length b is given in terms of the global displacements u , v , w and the rotations ϕ and ψ of the midsurface normal in the ℓn and yn planes respectively by the expression.

$$I_e = \int_0^b \int_{e'} (\delta \boldsymbol{\varepsilon}_m^T \mathbf{D}_m \boldsymbol{\varepsilon}_m + \delta \boldsymbol{\varepsilon}_b^T \mathbf{D}_b \boldsymbol{\varepsilon}_b + \delta \boldsymbol{\varepsilon}_s^T \mathbf{D}_s \boldsymbol{\varepsilon}_s + \delta \mathbf{u}^T \mathbf{P} \ddot{\mathbf{u}}) d\ell dy \quad (3.50)$$

where the strains $\boldsymbol{\varepsilon}_m$, $\boldsymbol{\varepsilon}_b$, and $\boldsymbol{\varepsilon}_s$, the matrices of elastic rigidities \mathbf{D}_m , \mathbf{D}_b , and \mathbf{D}_s and displacement components \mathbf{u} have the same meaning as for FSs in buckling analysis.

$$\mathbf{P} = \rho t \begin{bmatrix} 1 & 0 & 0 & 0 & 0 \\ 0 & 1 & 0 & 0 & 0 \\ 0 & 0 & t^2/12 & 0 & 0 \\ 0 & 0 & 0 & t^2/12 & 0 \\ 0 & 0 & 0 & 0 & t^2/12 \end{bmatrix} \quad (3.51)$$

where ρ is the mass density of the material – thus rotatory inertia effects are included. The vector $\ddot{\mathbf{u}}$ contains the accelerations of the displacement components u , v and w as well as the normal rotations ϕ and ψ – a superposed dot implies differentiation with respect to time.

Using n -noded, $C(0)$ strips, the global displacements and rotations may be interpolated within each strip. The next step is to discretize the displacement and rotations amplitudes using n -noded FE representation as given in previous section.

If we list the nodal displacements and accelerations in a vector \mathbf{d} and $\ddot{\mathbf{d}}$ respectively, then we discretize FS idealization into (3.1) for all the strips and assuming simple harmonic motion we obtain the expression

$$\delta \mathbf{d} \left[\mathbf{K} \mathbf{d} + \mathbf{M} \ddot{\mathbf{d}} \right] = \mathbf{0} \quad (3.52)$$

where \mathbf{K} and \mathbf{M} are the global stiffness and mass matrices respectively and contain submatrices contributed from each strip e linking nodes i and j and harmonics p and q . The stiffness matrix was given in buckling analysis section and can be used for free vibration, the mass submatrix has the form

$$[\mathbf{M}_{ij}^e]^{pq} = \int_0^b \int_{-1}^{+1} \{[\mathbf{N}_i^p]^T \mathbf{P} \mathbf{N}_j^q\} J d\xi dy \quad (3.54)$$

where typically

$$\mathbf{N}_i^p = N_i \begin{bmatrix} S_p & 0 & 0 & 0 & 0 \\ 0 & C_p & 0 & 0 & 0 \\ 0 & 0 & S_p & 0 & 0 \\ 0 & 0 & 0 & S_p & 0 \\ 0 & 0 & 0 & 0 & C_p \end{bmatrix} \quad (3.55)$$

$[\mathbf{K}_{ij}^e]^{pq}$ and $[\mathbf{M}_{ij}^e]^{pq} = \mathbf{0}$ if $p \neq q$ because of the orthogonality conditions. The matrix $[\mathbf{M}_{ij}^e]^{pp}$ is independent of the harmonic number p and therefore, the same matrix can be used for all the different harmonic equations as

$$[\mathbf{M}_{ij}^e]^{pp} = b/2 \int_{-1}^{+1} \{[\mathbf{N}_i]^T \mathbf{P} \mathbf{N}_j\} J d\xi \quad (3.56)$$

$\mathbf{N}_i = N_i \mathbf{I}_5$ in which \mathbf{I}_5 is the 5×5 identity matrix. Similar to buckling analysis, reduced integration is adopted to avoid locking behaviour.

Since (3.52) must be true for any set of virtual displacements $\delta \mathbf{d}^p$, (3.52) may be written in uncoupled form for each harmonic p as

$$\mathbf{K}^{pp} \mathbf{d}^p + \mathbf{M}^{pp} \ddot{\mathbf{d}}^p = \mathbf{0} \quad (3.57)$$

The general solution of (3.57) is written as

$$\mathbf{d}^p = \bar{\mathbf{d}}^p e^{i\omega_p t} \quad (3.58)$$

where $e^{i\omega_p t} = \cos(\omega_p t) + i \sin(\omega_p t)$ and ω_p and $\bar{\mathbf{d}}^p$ are p th natural frequency and vibration mode (eigenvector). Thus (3.52) may be rewritten in the standard eigenvalue form for each harmonic p as

$$(\mathbf{K}^{pp} - \omega_p^2 \mathbf{M}^{pp}) \bar{\mathbf{d}}^p = \mathbf{0} \quad (3.59)$$

In the present studies the eigenvalues are evaluated using the subspace iteration algorithm [70].

3.5 Examples

3.5.1 Buckling Analysis of Stiffened Panels

Problem definition: Isotropic stiffened panels analyzed under longitudinal compression by Stroud et. al [71] and Dawe and Peshkam [9] are will be examined. Stroud et al. [71] used FE method and Dawe and Peshkam [9] used a Mindlin–Reissner superstrip procedure involving a very fine mesh of cubic strips to analyze panels. In all cases, the boundary conditions at the ends of the structure simple diaphragm supports. In the analysis, reduced integration is used to evaluate the stiffness matrix and the shear correction factor is assumed $\kappa^2 = 0.8333$. The geometry of the squared shape with side length $a = 762 \text{ mm}$ and six repeating elements is shown in Figure 3.2 and Figure 3.3.

The following material properties are used: elastic modulus $E = 72.44 \text{ N/m}^2$ and Poisson's ratio $\nu = 0.32$. The panels subjected to pre-buckling load distribution for each plate flat in NASA examples when $N_y^0 = 175.13 \text{ kN/m}$ is shown in Table 3.1.

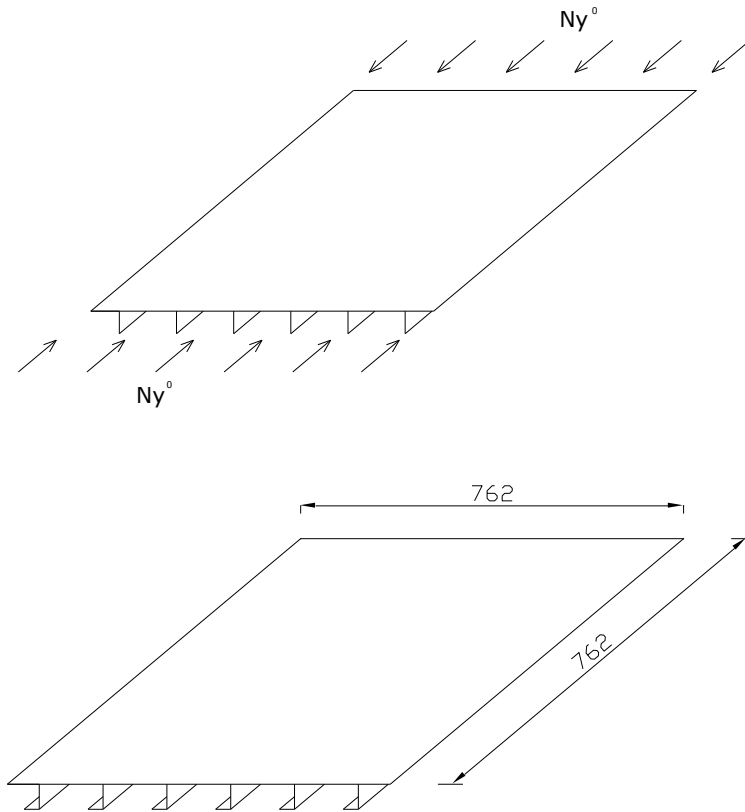


Figure 3.2 Isotropic stiffened panels from the NASA set [71]

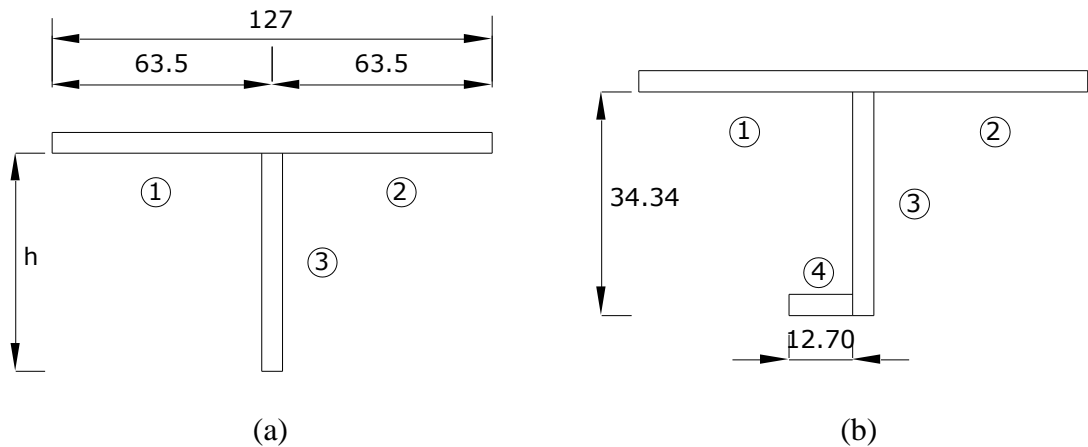


Figure 3.3 Details of repeating elements in isotropic stiffened panels in mm (a) Panel I and II $h = 34.34$ mm for Panel I and $h = 50.04$ mm for Panel II and (b) Panel III

Discussion of results: The subdivisions chosen for blade stiffened panel are indicated in Figure 3.3. Table 3.2 shows the results for the various subdivisions and strip types for Panel-I. A close agreement is observed between the FE and the superstrip solutions. In Panel-II a mesh of 73 cubic strips is used and the resulting buckling

factor of 0.29499 compares well with the values of 0.2965 and 0.2944 obtained using the FE and superstrip solutions respectively. The lowest buckling load is obtained with $p_1 = p_2 = 7$. This agrees with the shape of the buckling modes obtained using the FE and superstrip solutions. In Panel–III a mesh of 84 cubic strips is used and results in a buckling factor of 1.34887 compares again with the values of 1.356 and 1.3454 obtained using the FE and superstrip solutions respectively. The panel buckles with seven longitudinal half sine waves. This is in agreement with FE and superstrip lowest buckling mode.

Table 3.1 Pre–buckling load distribution for each plate flat in NASA panels when $N_y = 175.13kN/m$

Panel type	Internal load distribution N_y^0 (kN /m)			
	Flat 1	Flat 2	Flat 3	Flat 4
I	145.57	101.90	147.57	
II	133.31	154.64	133.31	
III	139.46	139.46	96.29	96.29

Table 3.2 Buckling factors for blade–stiffened panel I

Number of nodes	Buckling factors		
	Linear strips	Quad. strips	Cubic strips
79	0.94331	0.97102	0.97083
109	0.95550	0.97098	0.97096
181	0.96590	0.97096	0.97096
217	0.96707	0.97095	0.97094
FE sol.[71]	0.9759	0.9759	0.9759
Superstrip[9]	0.9709	0.9709	0.9709

3.5.2 Free Vibration Analysis of Stiffened Panels

Problem definition: A structure in the configuration of a panel with four stiffeners is examined with Cheung and Cheung thin–strips [72]. The geometry and dimensions of the panel are shown in Figure 3.4. The boundary conditions at the ends of the

structure simple diaphragm supports and the other edges are free. In the analysis, reduced integration is used to evaluate the stiffness matrix and the shear correction factor is assumed $\kappa^2 = 0.8333$. Non dimensional frequency parameter $\lambda_{m,n}$ is used. In parameter, subscript m denotes mode number and n denotes harmonic number.

$$\lambda_{m,n} = \frac{\omega_{m,n} \ell}{\sqrt{E/\rho}} \quad (3.60)$$

where ℓ is the length of the panel and E is the modulus of elasticity and ρ is the material mass density. $\ell/\sqrt{E/\rho}$ is arranged to unity for simplification of results. Poisson's ratio ν is assumed to 0.33.

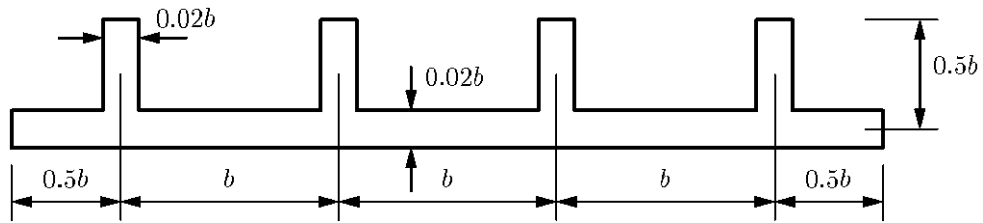


Figure 3.4 Dimensions and geometry of a stiffened panel

Discussion of results: FS analysis carried out by cubic elements with 143 d.o.f. Obtained $\lambda_{m,n}$ for present formulation and reference thin-strip formulation [72] tabulated in Table 3.3 result are presented for first harmonic number. Close agreement is observed.

Table 3.3 Natural frequency of stiffened panel

Mode number	Present	Thin-strip[72]
1	0.0287	0.0287
2	0.0292	0.0292
3	0.0368	0.0365
4	0.0369	0.0366
5	0.0396	0.0396
6	0.0634	0.0639

CHAPTER 4

OPTIMIZATION OF STIFFENED PLATES

4.1 Introduction

In structural engineering it is one of the first priorities to save weight, without loss of any strength in used structural elements against subjected loads. Stiffeners provide improvement to load carrying capacity of structures. The benefit of stiffening of a structure lies in achieving lightweight and robust design of the structure. For this purpose they have wide use in structural engineering domain. Specially stiffened plates are used in critical and sensitive structures such as in aircrafts, ship hulls and box girders in which safety and a perfect design is crucial. Buckling is the one of the most complex phenomenon that is inevitable for axially heavily loaded stiffened plate structures. For this purpose it is necessary to carry a deep interest and investigation about their responses under expected loads to design such structures safely.

The approach that uses the stiffeners to improve structural response is simple, but the practical stiffened plate design is a complex task. Therefore, a robust optimization algorithm is necessary to obtain maximum efficiency from stiffened plates. Various researches have been carried out to optimize the response of plates [73–76].

In this chapter, buckling optimization of the stiffened plates which have prismatic, rectangular main and sub stiffeners, pads and also L shaped stiffeners. In the first step, the baseline panel designs are done from which the initial values of parameters are developed. A complete description of the baseline design is outlined later in this

chapter. The buckling load carrying capacities of stiffened plates are maximized by optimizing the plate section dimensions under constant volume constraint. Buckling analysis is carried by using Fortran code which was developed by Özakça [1]. The buckling loads will be determined using cubic, $C(0)$ continuity Mindlin–Reissner FSs. The code uses SQP to carry out structural optimization process.

4.2 Optimization Process

4.2.1 Parameter Definition

Figure 4.1 below describes the cross section and geometric (design variables) parameters associated with the prismatic blade sub-stiffened panel.

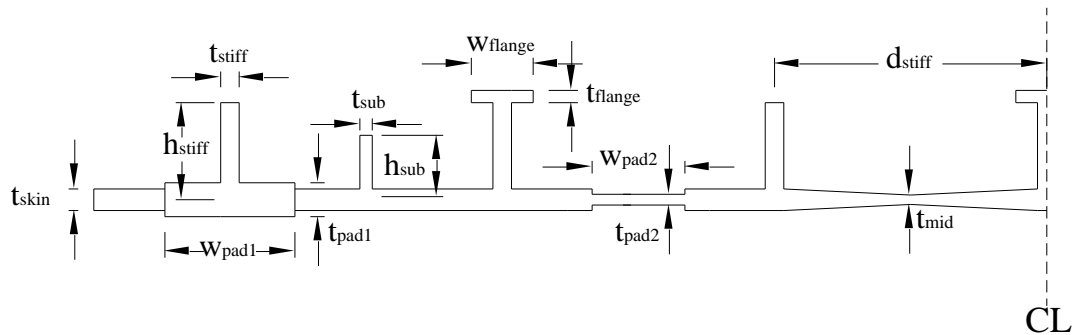


Figure 4.1 Plate variable parameters (design variables)

- t_{skin} Skin thickness
- h_{stiff} Primary stiffener height
- t_{stiff} Primary stiffener thickness
- W_{pad1} Width of pad under stiffeners
- t_{pad1} Thickness of pad under stiffeners
- h_{sub} Sub-stiffener height
- t_{sub} Sub-stiffener thickness
- W_{flange} Flange width
- t_{flange} Flange thickness
- W_{pad2} Width of pad between stiffeners

- t_{pad2} Thickness of pad between stiffeners
- t_{mid} Midspan thickness
- d_{stiff} Distance between stiffeners
- n_{stiff} Number of stiffeners

4.2.2 Design Constraints

There are a number of design constraints based on either the general design strategy or the manufacturing process as outlined below. All types of examined plates have the common fixed constraints as shown in Table 4.1. The common constraints are shown on a three dimensional aspect of five straight stiffened plate in Figure 4.2.

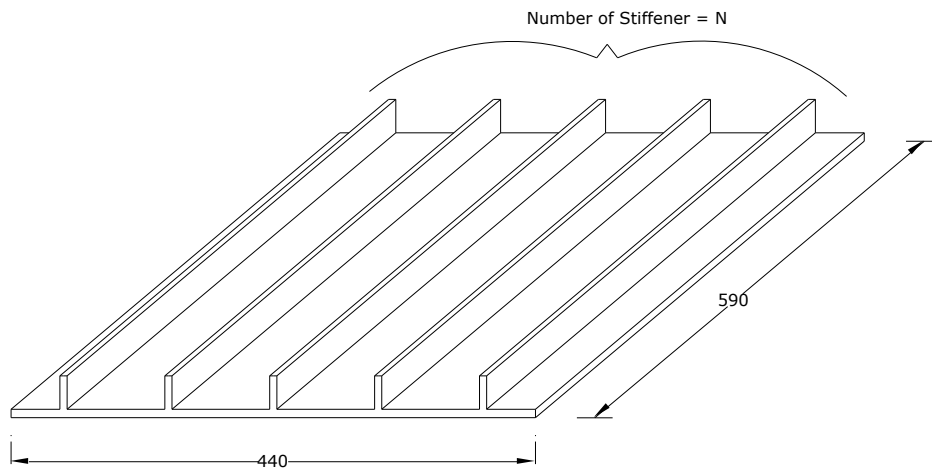


Figure 4.2 A sample three dimensional aspect of stiffened plate (Straight stiffener with five stiffeners)

Also design variables have constrains (minimum and maximum limits) that are expressed in relevant sections.

Table 4.1 Common constraints

Plate width	440 mm
Plate length	590 mm
Total plate volume	691480 mm ³

4.2.3 Material Properties, Loading and Boundary Conditions

In this study eigenvalue buckling analysis is considered. This analysis only requires elastic material properties. The panels are made of aluminum and the following material properties are used;

Modulus of elasticity (E): $73 \times 10^9 \text{ N/m}^2$

Poisson's ratio (ν): 0.33

The loading direction and boundary conditions are shown in Figure 4.3

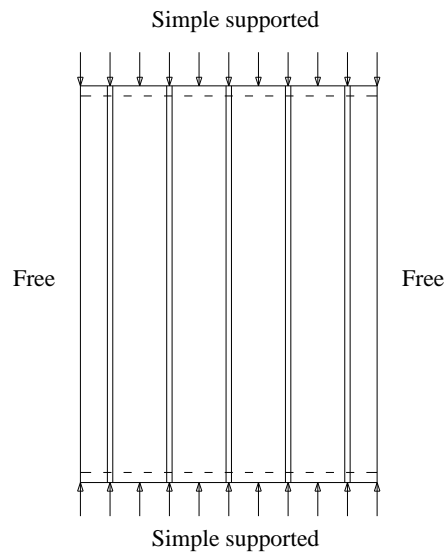


Figure 4.3 Loading and boundary conditions

The loaded sides of plate are simply supported and the other two sides are free. The plate is loaded in uniform compression in stiffeners direction.

4.3 Optimum Design of Stiffened Plates

It is desired that two consecutive linear eigenvalue optimizations are run. The first design is carried out for obtaining thickness of initial values of baseline plate by providing constant cross sectional area. Then second run will apply the design constraints associated with the manufacturing process and other issues. Full details of the DVs and constraints are outlined in the previous sections.

The baseline panel is the foundation for the sub-stiffened design. The panel cross section is constant along its length. The baseline panel cross section has a total area of 1172 mm² of skin material available for manipulation. The design has a number of sub-stiffeners running parallel to the primary stiffeners at 90 degrees to the loading plane.

In each plate type optimization processes are repeated for size, shape (type one and type two) optimizations;

- i) *Size optimization*: Optimization is carried out using only thickness design variables. These are thickness of plate skin (t_{skin}), thickness of stiffeners (t_{stiff}), thickness of substiffeners (t_{sub}), thickness of pad (t_{pad}) and thickness of flange (t_f). During this stage height of stiffeners (h_{stiff}) and height of substiffeners (h_{sub}) have constant values of 28.0mm and 14.0mm.
- ii) *Shape optimization (type one)*: Height of stiffeners (h_{stiff}) and height of substiffeners (h_{sub}) are included as design variable in this stage
- iii) *Shape optimization (type two)*: Finally width of pads (w_{pad}) and width of flanges (w_f) are included as design variable in this stage.

Design constraints of all optimizations are specified in Table 4.2.

Optimization is carried out for the following types of stiffened plates that are expressed below and plate types are shown on five stiffened plate template and given in each section.

- a) Straight stiffened plate
- b) Straight stiffened plate with sub-stiffeners
- c) Straight stiffened plate with substiffeners and pads under stiffeners
- d) L shaped stiffened plate

Optimization processes definition, results of optimizations and discussions are presented in each section.

Table 4.2 Design constraints of all stiffened plates

		Min (mm)	Max (mm)
Thickness of plate	t_{skin}	1.4	3.0
Thickness of stiffener	t_{stiff}	1.3	4.0
Height of stiffener	h_{stiff}	8.0	40.0
Thickness of substiffeners	t_{sub}	1.0	3.0
Height of substiffeners	h_{sub}	5.0	20.0
Thickness of pad	t_{pad1}	2.0	5.0
Width of pad	w_{pad1}	$d_{stiff}/10$	$d_{stiff}/2$
Thickness of flange	t_f	1.0	3.0
Width of flange	w_f	7.0	14.0

Effect of number of stiffeners is also observed. Number of stiffeners from two to eight is optimized. Optimizations are carried out for maximization of critical buckling load subject to constant volume constraint.

4.3.1 Straight Stiffened Plate

In this type, stiffened plates by using only main stiffeners are optimized. Figure 4.4 shows straight stiffened plate with five stiffeners.

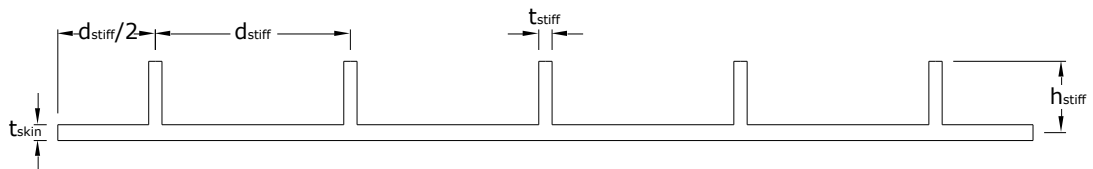


Figure 4.4 Straight stiffened plate

Two types of optimization are performed. These are size optimization with two design variables ($t_{skin}-t_{stiff}$) and shape optimization (type one) with three design variables ($t_{skin}-t_{stiff}-h_{stiff}$).

i) Size optimization: Thicknesses of plate and stiffeners are kept equal at the initial design. The height of stiffeners is constant and equal to 28.0 mm. The optimum values of design variables and critical buckling load are given in Table 4.3. The highest improvement is obtained for four stiffeners case and approximately equal to 10.3 %. The stiffened panel analyzed using cubic strips. In order to obtain more accurate results the large number of degrees of freedom is taken in all analysis. The highest critical buckling load is obtained in eight stiffeners case and equal to 219833 N. The improvement of critical buckling load for eight stiffeners is 664.0 % compared to two stiffeners case. Moreover, it is important to note that in optimum results skin thickness is thicker than stiffener thickness except eight stiffeners case and by the increasing of number of stiffeners skin thickness is going to be thinner and stiffener thickness is going to be thicker.

Initial and optimum shapes of stiffened panels with three, four and five stiffener are given in Figure 4.5. When the results are examined, plate thicknesses are higher than the stiffeners thicknesses. The thicknesses of plates are decreasing and the thicknesses of stiffeners are increasing while the number of stiffeners are increasing.

Table 4.3 Size optimization of straight stiffened plate

n_{stiff}	Optimum DVs values		Buckling loads		Imp (%)
	t_{skin}	t_{stiff}	P_i	P_{max}	
2	2.49	1.30	27392.7	28749.313	4.90
3	2.41	1.30	59731.7	64479.292	7.95
4	2.32	1.34	97565.0	107542.933	10.30
5	2.19	1.47	136548.5	148318.650	8.60
6	2.08	1.52	173160.7	183581.163	6.00
7	1.96	1.57	202204.3	206859.051	2.30
8	1.75	1.79	219819.9	219833.336	0.01

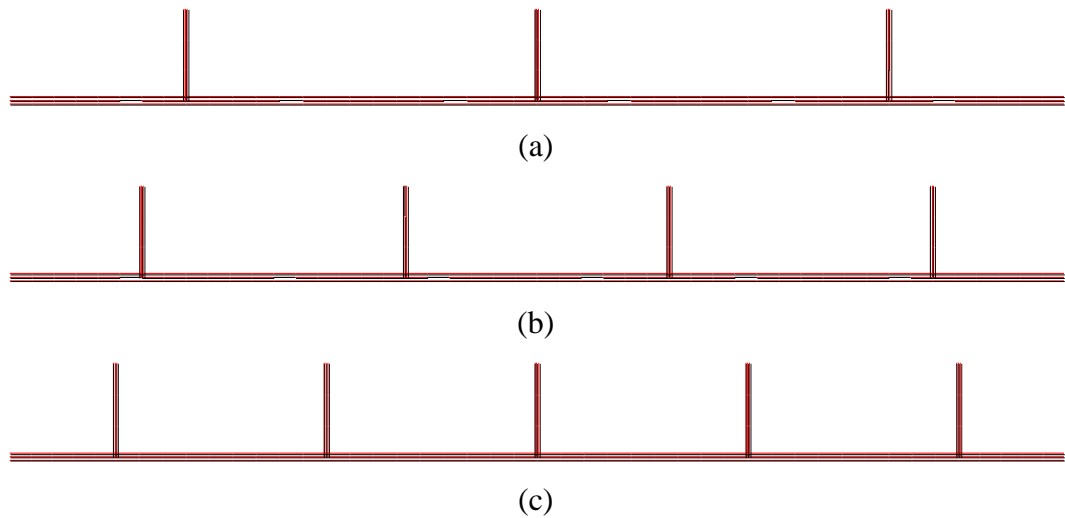


Figure 4.5 Initial and optimum shapes of straight stiffened panels size optimization (a), (b) and (c) three, four and five stiffeners respectively

ii) Shape optimization (type one): In addition of thickness of plate and stiffeners, the height of stiffeners is also considered as design variable (Note: During the optimization process, the height of stiffeners is equal to each other). The optimum values of design variables and critical buckling loads are presented in Table 4.4. The highest improvement, which is 41.4 %, obtained from eight stiffeners. When the number of stiffeners is increased critical buckling load is also increased similar to size optimization. The largest critical buckling load is again obtained from eight stiffeners case. The improvement is 926 % compared with two stiffeners case. Plate skin is thinner than stiffeners in optimum results and stiffener thicknesses reach upper limits.

Plate thicknesses have decreased according to stiffeners thicknesses and stiffeners thicknesses have reached to upper limits. In Figure 4.6, initial and optimum shapes of three, four and five stiffened panels are shown and compared with each other.

Table 4.4 Shape optimization (type one) of Straight stiffened plate

n_{stiff}	Optimum DVs values			Buckling loads		Imp (%)
	t_{skin}	t_{stiff}	h_{stiff}	P_i	P_{max}	
2	2.52	3.99	8.00	27392.7	30266.2	10.50
3	2.19	4.00	17.29	59731.7	66979.9	12.10
4	2.15	4.00	14.01	97565.0	114501.6	17.40
5	2.13	4.00	11.78	136548.5	171359.7	25.50
6	2.06	4.00	11.05	173160.7	237776.0	37.30
7	2.15	4.00	8.00	202204.2	283451.4	40.20
8	2.07	4.00	8.11	219819.9	310826.7	41.40

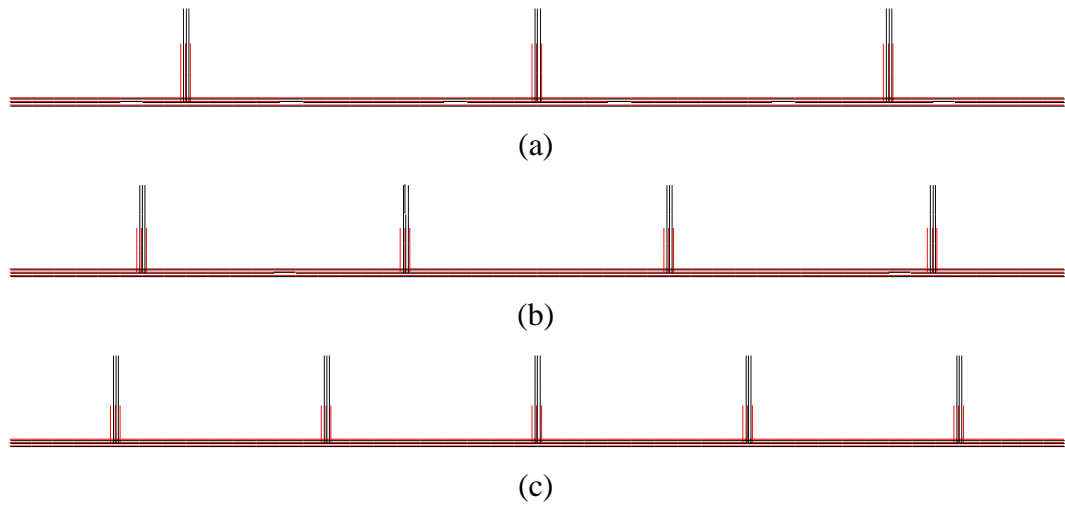


Figure 4.6 Initial and optimum shapes of straight stiffened panels after shape (type one) optimization (a), (b) and (c) three, four and five stiffeners respectively

Shape optimizations (type one) slightly gave better results compared to size optimizations as shown in Figure 4.7. For small number of stiffeners both optimizations give similar results. However when the number of stiffeners increase shape optimizations give better results. In shape optimization, stiffener thicknesses are going to be thicker than initial design values. The higher buckling loads in shape optimization type caused by the height of stiffeners. Shape optimization increases plate and stiffener thickness.

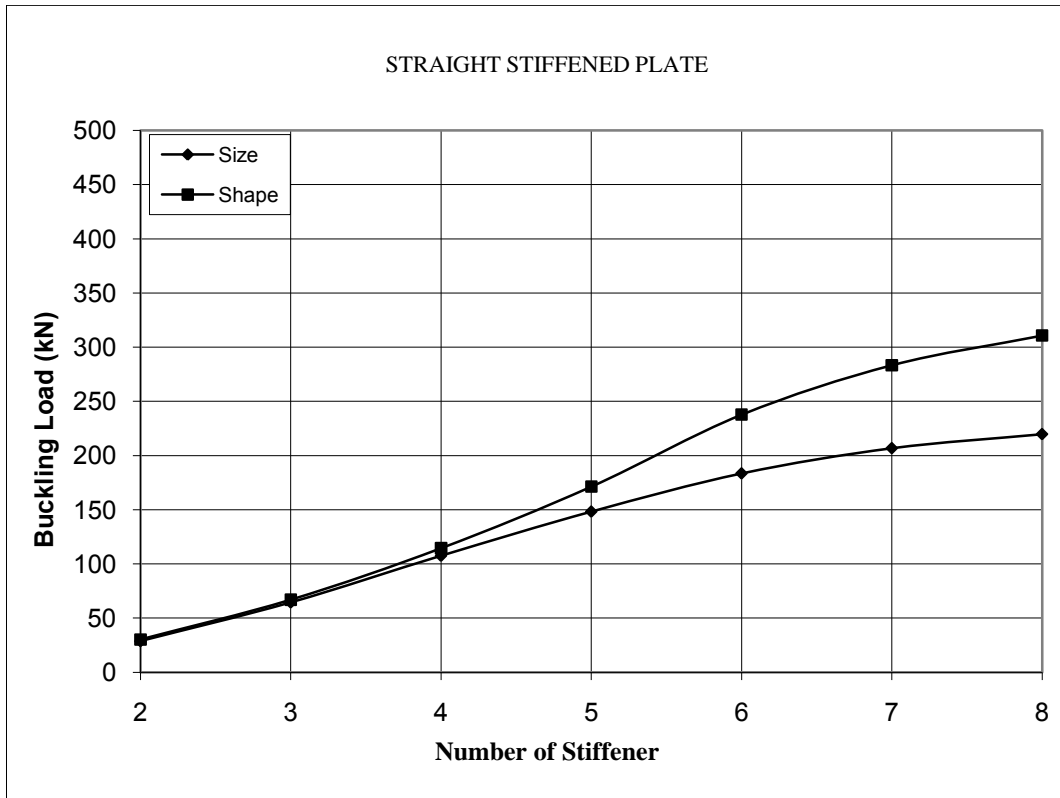


Figure 4.7 Comparison of size and shape optimizations (type one)

4.3.2 Straight Stiffened Plate with Substiffeners

Figure 4.8 shows straight stiffened plate with substiffeners. Substiffeners are attached between stiffeners, which divide the distance between stiffeners two equal parts.

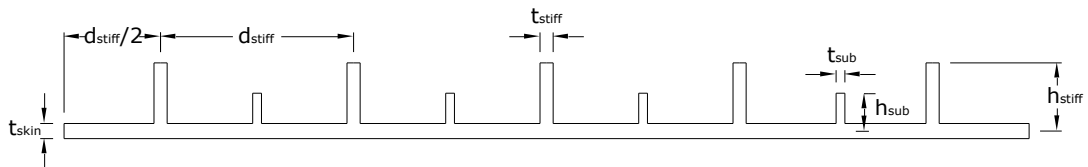


Figure 4.8 Straight stiffened plate with substiffeners

The effect of substiffeners between stiffeners to critical buckling load capacity is examined. Two types of optimization are performed. These are size optimization

with three design variables ($t_{skin}-t_{stiff}-t_{sub}$) and shape optimization (type one) with five design variables ($t_{skin}-t_{stiff}-t_{sub}-h_{stiff}-h_{sub}$).

i) Size optimization: Thickness of plate, stiffeners and substiffeners are kept equal in initial design. The height of stiffeners and height of substiffeners have constant values of 28.0 mm and 14.0 mm. The optimum values of design variables and critical buckling loads are given in Table 4.5. The highest improvement is obtained from five stiffeners case and it is approximately equal to 19.5 %. The highest critical buckling load is obtained from eight stiffeners case and equal to 218521 N. The improvement of critical buckling load is 537.0 % compared to two stiffeners case. Plate skin is thicker than stiffeners in optimum solutions and substiffeners thicknesses decreases to lower limit except two stiffeners case.

Table 4.5 Size optimization of stiffened plate with stiffener

n_{stiff}	Optimum DVs values			Buckling loads		Imp (%)
	t_{skin}	t_{stiff}	t_{sub}	P_i	P_{max}	
2	2.42	1.39	2.07	32807.4	33704.4	2.70
3	2.35	1.30	1.02	62291.5	71102.4	14.10
4	2.23	1.33	1.00	95546.9	113592.6	18.90
5	2.09	1.40	1.00	129335.9	154533.5	19.50
6	1.97	1.40	1.00	160361.9	188273.5	17.40
7	1.78	1.55	1.00	184862.8	205626.2	11.20
8	1.59	1.66	1.00	195678.6	218521.1	9.80

Initial and optimum shapes of stiffened panels with three, four and five stiffener are given in Figure 4.9. When the results are examined, plate thicknesses are larger than the stiffeners thicknesses, and the thickness of substiffeners are reached to lower limits.

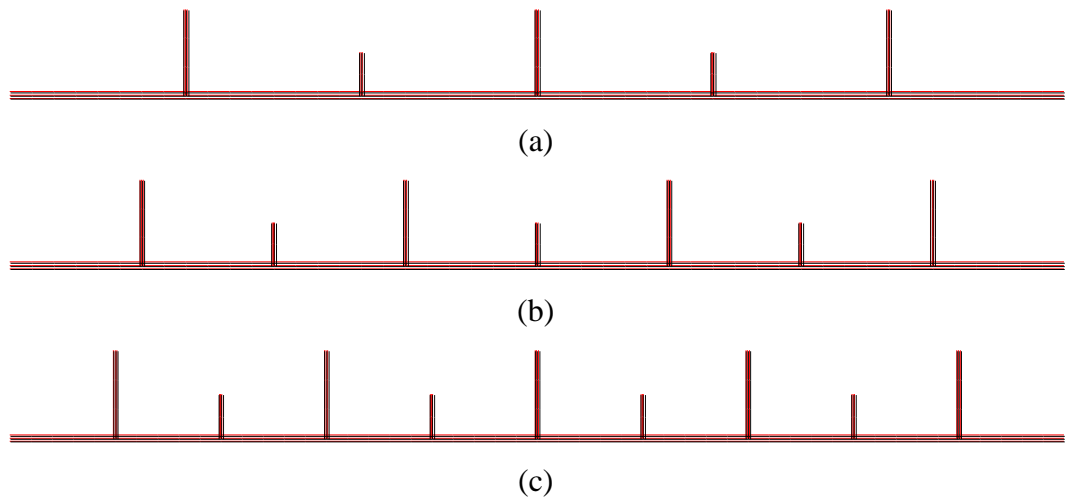


Figure 4.9 Initial and optimum Shapes of straight stiffened plate with sub-stiffeners after size optimization (a), (b) and (c) three, four and five stiffeners respectively

ii) Shape optimization (type one): In addition thicknesses of plate, stiffeners and substiffeners height of stiffeners and substiffeners are included in optimization process as design variables. The optimum values of design variables and critical buckling loads are presented in Table 4.6. The highest improvement is obtained from eight stiffeners case and it is approximately 67.7 %. Also the largest critical buckling load is obtained from eight stiffeners case. The improvement of critical buckling load is about 836.0 % compared to two stiffeners case and it has value of 328229 N.

By the increasing of number of stiffeners, stiffener's thicknesses reach upper limit. Height of stiffeners begins with a higher value and decrease near to lower limit by the increasing of number of stiffeners. Substiffeners' height decrease to lower limit in all plates.

When the initial and optimum shapes given in Figure 4.10 are examined, plate thicknesses are reached the upper limits while the number of stiffeners are increasing. Initially heights of stiffeners are at the top limit but while the numbers are increasing this heights are reaching bottom limits. And the all heights of substiffeners have reached to lower limits.

Table 4.6 Shape optimization (type one) of stiffened plate with stiffener

n_{stiff}	Optimum DVs values					Buckling loads		Imp (%)
	t_{skin}	t_{stiff}	t_{sub}	h_{stiff}	h_{sub}	P_i	P_{max}	
2	2.41	1.30	3.62	35.29	5.00	32807.4	35054.8	6.9
3	2.36	1.30	2.44	27.29	5.00	62291.5	72179.9	15.9
4	2.15	4.00	1.11	13.02	5.00	95546.9	115041.3	20.4
5	2.09	4.00	1.00	11.57	5.00	129335.9	169417.3	30.9
6	2.03	4.00	1.00	10.46	5.00	160361.9	230964.4	44.0
7	1.98	4.00	1.28	9.35	5.00	184862.8	286947.0	55.2
8	1.87	4.00	2.14	8.61	5.00	195678.6	328229.2	67.7

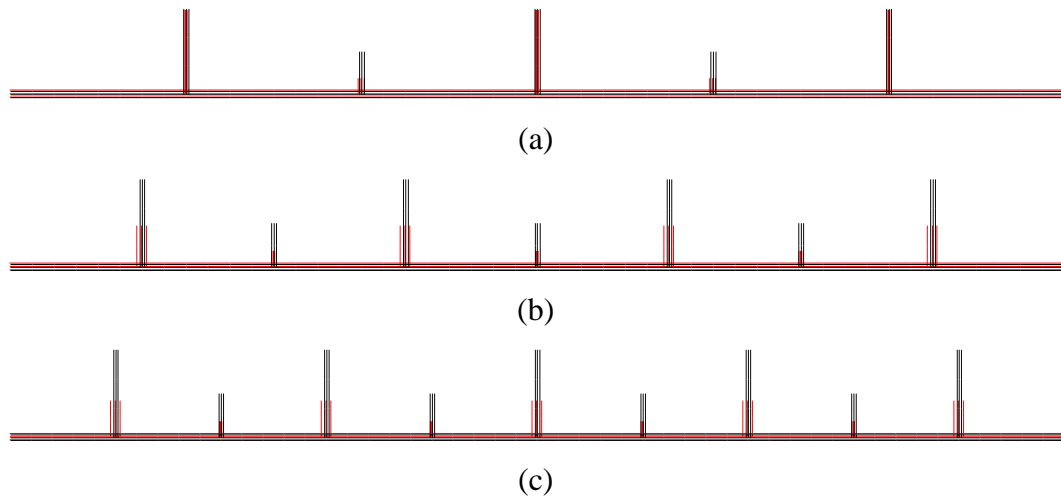


Figure 4.10 Initial and optimum shapes of straight stiffened plate with sub-stiffeners after shape optimization (type one) (a), (b) and (c) three, four and five stiffeners respectively

Shape optimizations (type one) obviously gave better results when compared size optimizations as shown Figure 4.11. Also for small number of stiffeners, both optimizations give similar results. However when the number of stiffeners increase shape optimizations give better results.

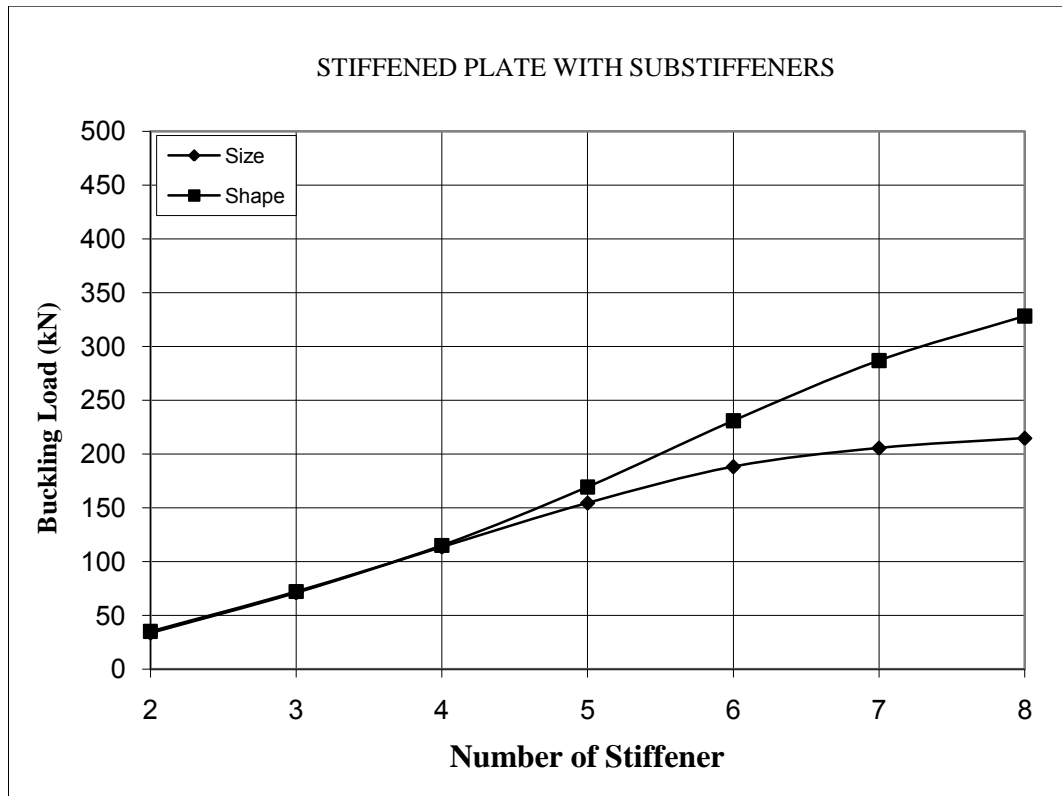


Figure 4.11 Comparison of size and shape optimizations (type one)

4.3.3 Straight Stiffened Plate with Substiffeners and Pads under Stiffeners

Substiffeners are added between stiffeners pad elements are also attached under stiffeners. Figure 4.12 shows straight stiffened plate with substiffeners and pads under stiffeners.

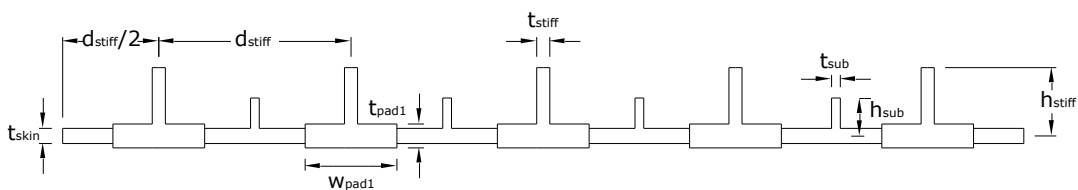


Figure 4.12 Straight stiffened plate with substiffeners and pads under stiffeners

The effect of substiffeners and pads are examined together in this type of plates. Three types of optimizations are performed. First one is size optimization with four design variables ($t_{skin} - t_{stiff} - t_{sub} - t_{pad1}$), second is shape optimization (type one) with

six design variables ($t_{skin}-t_{stiff}-t_{sub}-t_{pad1}-h_{stiff}-h_{sub}$) and the third one is shape optimization (type two) with seven design variables ($t_{skin}-t_{stiff}-t_{sub}-t_{pad1}-h_{stiff}-h_{sub}-w_{pad1}$). The effect of number of stiffeners also examined.

i) Size optimization: Thickness of plate and stiffeners are kept equal in initial design. Thickness of pads and thickness of substiffeners are kept 1.5 times and 0.75 times of thickness of plate. The height of stiffeners, height of substiffeners and width of pads are kept constant during this stage and they have values of 28.0mm, 14.0mm and $d_{stiff}/4$. The optimum values of design variables and critical buckling loads are given in Table 4.7. The highest improvement is obtained from four stiffeners case and the improvement is approximately 13.2 %. The highest critical buckling load is obtained from eight stiffeners case and equal to 237913 N. The improvement of this case is 500.0 % compared with two stiffeners case.

In optimum solutions, plate skin is thicker than stiffeners. Thickness of substiffeners reached to lower limits. Skin thickness is going to be thinner and stiffener thicknesses are going to be thicker by the increasing of number of stiffeners.

Table 4.7 Size optimization of straight stiffened plate with substiffeners and pads under stiffeners

n_{stiff}	Optimum DVs values				Buckling loads		Imp (%)
	t_{skin}	t_{stiff}	t_{sub}	t_{pad1}	P_i	P_{max}	
2	1.98	1.30	1.00	3.93	36316.4	39654.6	9.2
3	1.98	1.30	1.00	3.48	72736.7	81613.4	12.2
4	1.81	1.38	1.06	3.42	112890.9	127733.3	13.2
5	1.69	1.47	1.00	3.19	155308.9	172728.9	11.2
6	1.51	1.4	1.10	3.19	194556.6	208078.9	6.9
7	1.40	1.56	1.00	2.91	220346.4	233851.5	6.1
8	1.40	1.64	1.00	2.23	222514.5	237913.1	6.9

Initial and optimum shapes of stiffened panels with three, four and five stiffener are given in Figure 4.13. When the initial and optimum shapes given in Figure 4.13 are examined, in general plate thicknesses are larger than the stiffeners thicknesses, and the thickness of substiffeners are reached to lower limits. But while the numbers of stiffeners are increasing, the thicknesses of plates are decreasing and the thicknesses of stiffeners are increasing.

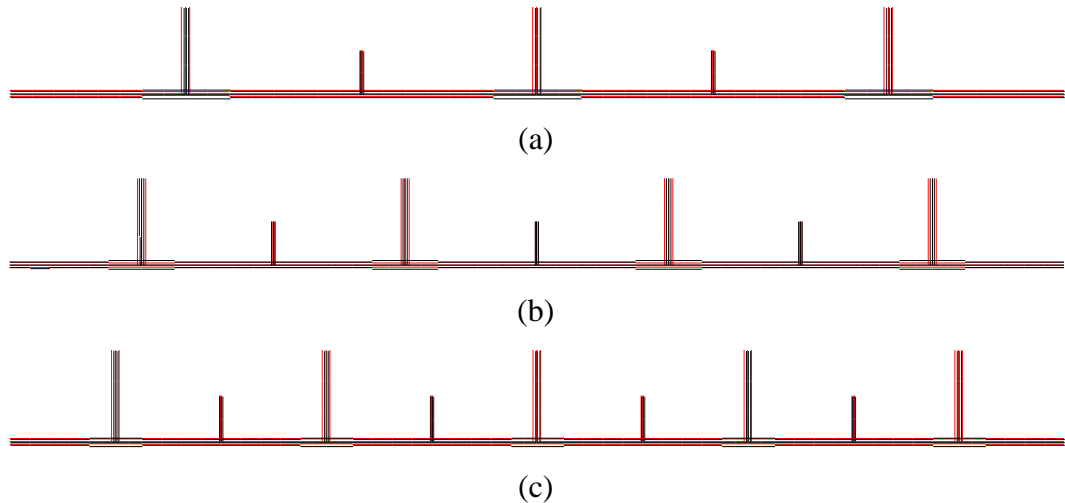


Figure4.13 Initial and optimum shapes of straight stiffened plate with substiffeners and pads under stiffeners after size optimization. (a), (b) and (c) three, four and five stiffeners respectively

ii) Shape optimization (type one): in addition to thicknesses of plate, stiffeners, substiffeners and pads height of stiffeners, width of substiffeners are included in optimization process as design variables. Still width of pads has constant values of $d_{stiff}/4$. The optimum values of design variables and critical buckling loads are presented in Table 4.8. The highest improvement is obtained from eight stiffeners case and it is approximately 97.5 %. Also the largest critical buckling load is obtained from eight stiffeners case. The improvement of critical buckling load is more than 1000.0 % compared to two stiffeners case and it has value of 439376 N.

When the initial and optimum shapes given in Figure 4.14 are examined, almost in all panels while the thicknesses of plates and stiffeners are decreasing stiffener heights are reached the lower limits and all heights of substiffeners have reached to lower limits.

Table 4.8 Shape optimization (type one) of straight stiffened plate with substiffeners and pads under stiffeners with six design variables

n_{stiff}	Optimum DVs values						Buckling loads		Imp (%)
	t_{skin}	t_{stiff}	t_{sub}	t_{pad1}	h_{stiff}	h_{sub}	P_i	P_{max}	
2	1.99	1.30	1.96	4.00	25.05	5.00	36316.4	39978.0	10.1
3	1.91	3.15	1.00	4.16	8.00	5.00	72736.7	82354.9	13.2
4	1.86	2.86	1.00	4.10	8.00	5.00	112890.9	136486.8	20.9
5	1.77	2.69	1.00	4.18	8.00	5.00	155308.9	201624.5	29.8
6	1.74	3.11	1.00	3.85	8.00	5.00	194556.6	274141.2	40.9
7	1.69	3.17	1.00	3.69	8.00	5.00	220346.4	352666.9	60.1
8	1.60	3.29	1.00	3.61	8.00	5.00	222514.5	439376.4	97.5

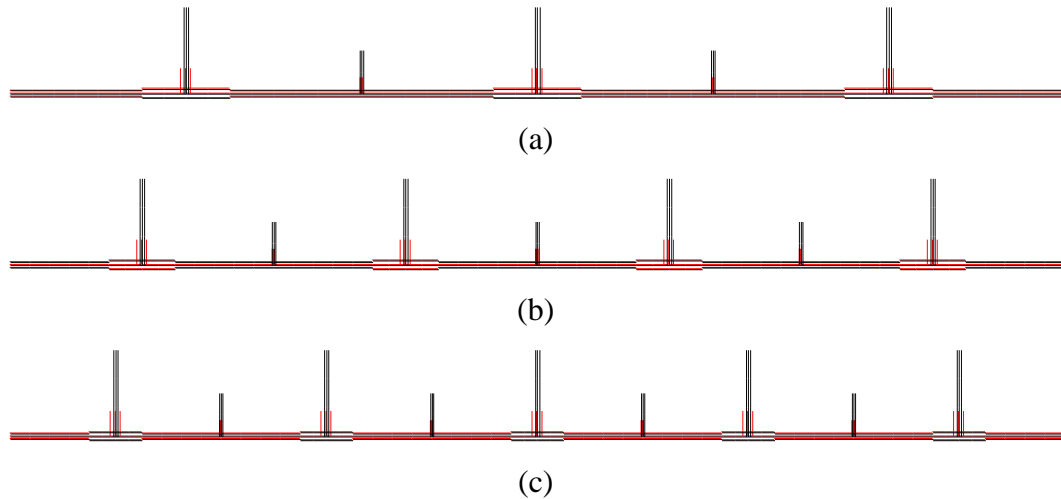


Figure 4.14 Initial and optimum shapes of straight stiffened plate with substiffeners and pads under stiffeners after shape optimization (type one) (a), (b) and (c) three, four and five stiffeners respectively

iii) Shape optimization (type two): In addition previous design variables width of pad included as a design variable. The optimum values of design variables and critical buckling loads are presented in Table 4.9. The highest improvement is obtained from eight stiffeners case and it is approximately 106.2 %. Largest critical buckling load also is obtained from eight stiffeners case and the plate has a critical buckling load of 458888 N. The improvement is 913.0 % compared with two stiffeners case.

In optimum solutions, skin is thinner than stiffeners. Skin thickness and pad thicknesses are going to be thinner and thicknesses of stiffeners are going to be thinner by the increasing of number of stiffeners. Height of stiffeners and substiffeners reach lower limits in all cases and width of pads reach upper limits except seven and eight stiffeners cases.

Table 4.9 Shape optimization (type two) of straight stiffened plate with substiffeners and pads under stiffeners with seven design variables

n_{stiff}	Optimum DVs values							Buckling loads		Imp (%)
	t_{skin}	t_{stiff}	t_{sub}	t_{pad1}	h_{stiff}	h_{sub}	w_{pad1}	P_i	P_{max}	
2	1.52	2.99	1.00	3.57	8.00	5.00	110.00	36316.4	45291.6	24.7
3	1.42	2.73	1.00	3.56	8.00	5.00	73.33	72736.7	95633.7	31.5
4	1.40	2.76	1.00	3.45	8.00	5.00	55.00	112890.9	160575.7	42.2
5	1.40	3.25	1.00	3.24	8.09	5.00	44.00	155308.9	233837.0	50.6
6	1.40	3.56	1.00	3.03	8.00	5.00	36.67	194556.6	311333.6	60.0
7	1.40	4.00	1.00	2.86	8.00	5.00	29.63	220346.4	389130.8	76.6
8	1.40	3.98	1.27	3.05	8.00	5.00	19.36	222514.5	458888.3	106.2

When the initial and optimum shapes given in Figure 4.15 are examined, plate thicknesses are larger than the stiffeners thicknesses. while the number of stiffeners are increasing, stiffener and pad thickness are decreasing . Initially heights of stiffeners are at the top limit but while the numbers are increasing this heights are reaching lower limits. And in all solutions, heights of main and sub stiffeners have reached to lower limits. But accept seven and eight stiffened plates, pad widths have reached to top limit.

Size optimizations and shape optimizations (type one) with six design variables gave similar results in small number of stiffeners as shown in Figure 4.16. But the shape optimization more stiffeners gave higher critical buckling loads. Shape optimization (type two)s with seven design variables gave higher results starting with small number of stiffeners.

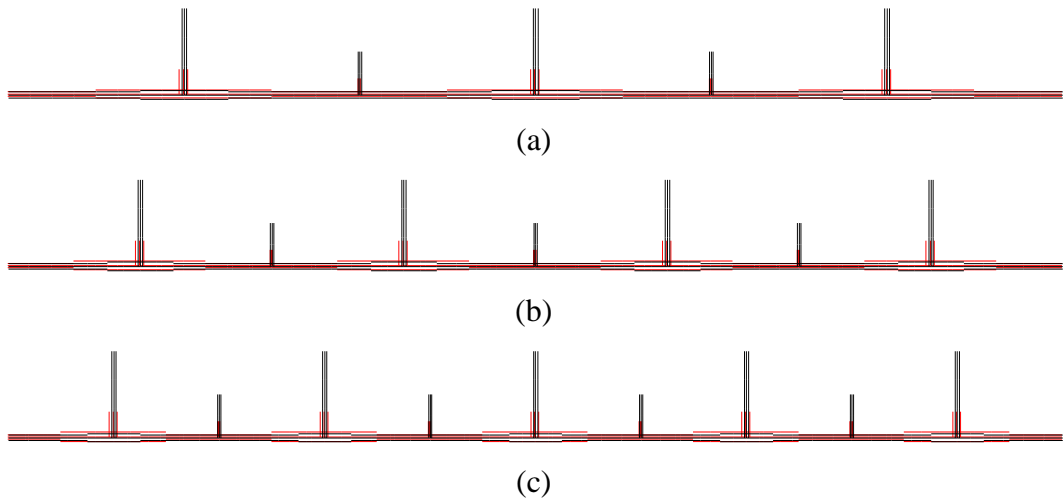


Figure 4.15 Initial and optimum shapes of straight stiffened plate with substiffeners and pads under stiffeners after shape optimization (type two) (a), (b) and (c) three, four and five stiffeners respectively.

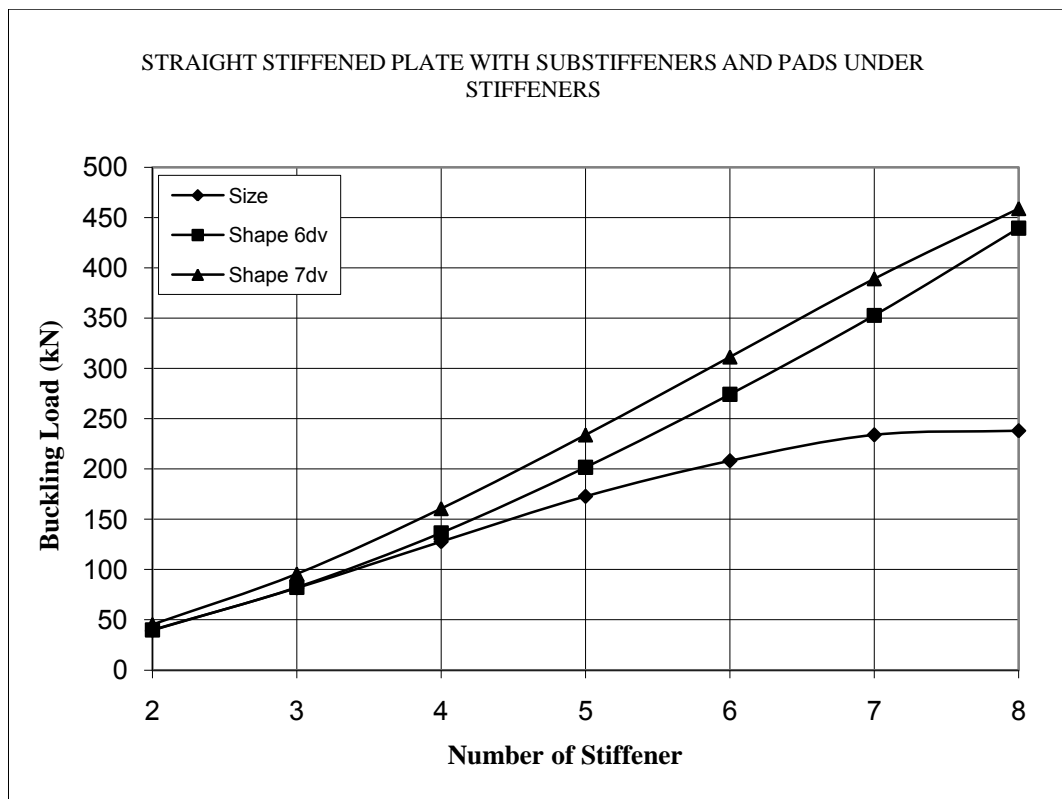


Figure 4.16 Comparison of size, shape one (type one) and shape optimizations (type two)

4.3.4 L Shaped Stiffened Plates

In this type, L shaped stiffeners are added to plate as shown in Figure 4.17 and optimized.

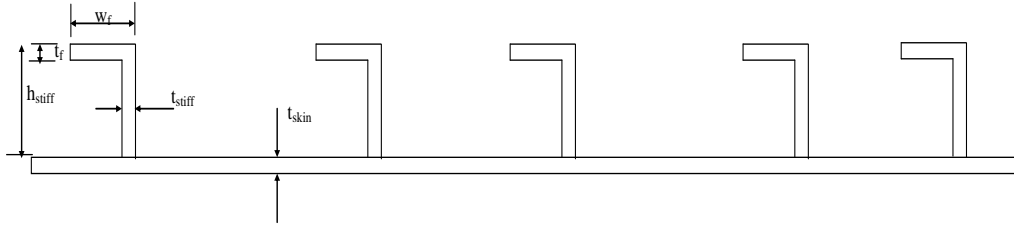


Figure 4.17 L shaped plate geometry

The effect of L shaped stiffeners is examined in this type of plates. Three types of optimizations are performed. First one is size optimization with three design variables ($t_{skin}-t_{stiff}-t_f$), second one is shape optimization (type one) with four design variables ($t_{skin}-t_{stiff}-t_f-h_{stiff}$) and the third one is shape optimization (type two) with five design variables ($t_{skin}-t_{stiff}-t_{sf}-h_{stiff}-w_f$).

i) Size optimization: Thickness of plate and stiffeners are kept equal in initial design. The heights of stiffeners are kept constant during this stage and 28.0mm. The optimum values of design variables and critical buckling loads are given in Table 4.10. The highest improvement is obtained from eight stiffeners case and the improvement is approximately 18.5 % and critical buckling load is equal to 295086 N. The improvement of this case is 794.0 % compared with two stiffeners case.

When the initial and optimum shapes given in Figure 4.18 are examined, thicknesses of plates and flanges have reached to lower limits in all plates except than 2 stiffener plates.

Table 4.10 Size optimization of L shaped stiffened plates

n_{stiff}	Optimum DVs values			Buckling loads		Imp (%)
	t_{skin}	t_{stiff}	t_f	P_i	P_{max}	
2	2.213	2.600	2.624	32100.981	32989.083	2.70
3	2.267	1.649	1.193	65638.740	67347.600	2.60
4	2.242	1.300	1.000	102714.971	110758.043	7.80
5	2.136	1.300	1.000	139652.630	157493.197	12.80
6	2.030	1.300	1.000	176997.204	205665.317	16.20
7	1.925	1.300	1.000	213703.296	252880.275	18.30
8	1.820	1.300	1.000	248934.079	295086.247	18.50

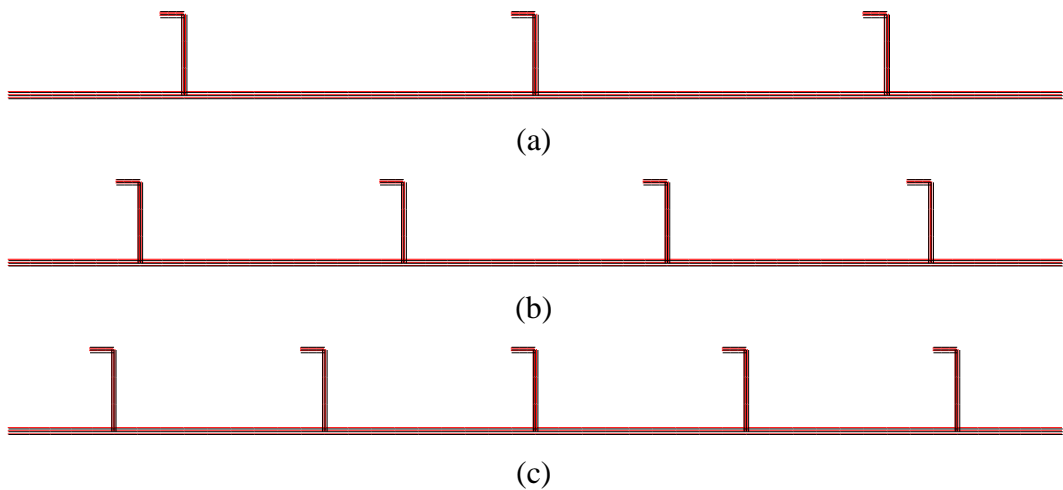


Figure 4.18 Initial and optimum shapes of L shaped stiffened plates after size optimization (a), (b) and (c) three, four and five stiffeners respectively.

ii) *Shape optimization (type one)*: In addition to thicknesses of plate and stiffeners, heights of stiffeners are included to optimization process as design variables. The optimum values of design variables and critical buckling loads are presented in Table 4.11. The highest improvement is obtained from eight stiffeners case and it is approximately 48.8 %. Also the largest critical buckling load is obtained from eight stiffeners case with 370472 N. The improvement of critical buckling load is about 1012.0 % compared to two stiffeners case.

Table 4.11 Shape optimization (type one) of L shaped stiffened plates

n_{stiff}	Optimum DVs values				Buckling loads		Imp (%)
	t_{skin}	t_{stiff}	t_f	h_{stiff}	P_i	P_{mak}	
2	2.207	2.823	2.942	25.144	32100.981	33293.108	3.70
3	2.231	2.530	2.274	16.097	65638.740	70785.486	7.80
4	2.222	2.727	2.089	10.156	102714.971	118418.901	15.30
5	2.165	2.382	1.626	11.585	139652.630	174021.341	24.60
6	2.114	3.792	1.000	8.000	176997.204	242355.804	36.90
7	1.989	2.989	1.760	8.307	213703.296	305449.188	42.90
8	1.860	3.428	1.675	8.004	248934.079	370472.023	48.80

When the initial and optimum shapes given in Figure 4.19 are examined, height of stiffeners are decreased in all cases.

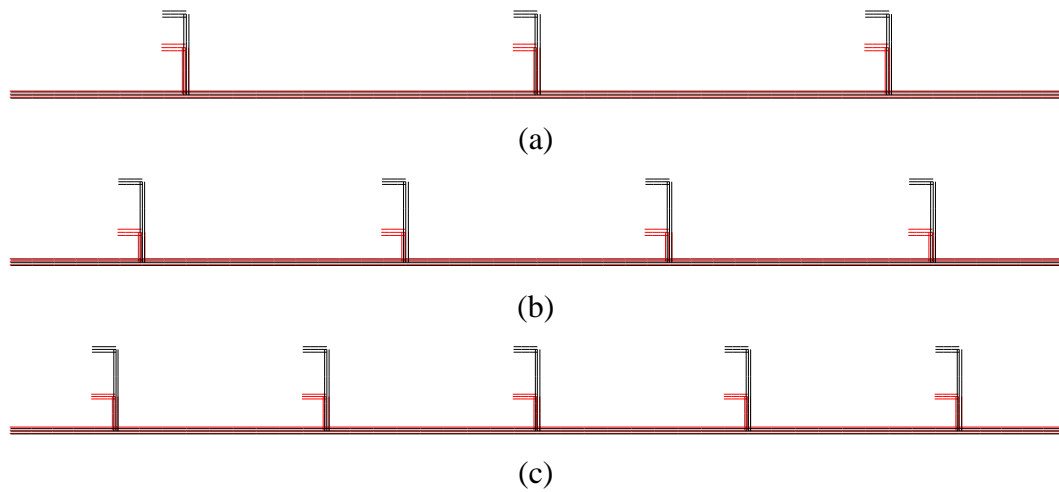


Figure 4.19 Initial and optimum shapes of L shaped stiffened plates after shape optimization (type one) (a), (b) and (c) three, four and five stiffeners respectively

Shape optimization (type two): In addition previous design variables width of flanges are included as design variable. The optimum values of design variables and critical buckling loads are presented in Table 4.12. The highest improvement is obtained from eight stiffeners case and it is approximately 57.1 %. Largest critical buckling load also is obtained from eight stiffeners case and the plate has a critical buckling

load of 391109 N. The improvement is 1076.0 % when compared with two stiffeners case.

Table 4.12 Shape optimization (type two) of L shaped stiffened plates with five design variables

n_{stiff}	Optimum DVs values					Buckling loads		Imp (%)
	t_{skin}	t_{stiff}	t_f	h_{stiff}	w_f	P_i	P_{mak}	
2	2.201	2.857	2.812	24.794	11.017	32100.981	33241.989	3.60
3	2.242	2.392	2.422	17.017	8.735	65638.740	70961.209	8.10
4	2.257	2.175	2.137	13.129	7.623	102714.971	119935.143	16.80
5	2.165	2.382	1.626	11.585	10.000	139652.630	174058.342	24.60
6	2.172	2.215	2.140	9.500	7.000	176997.204	246731.653	39.40
7	2.107	2.622	2.007	8.000	7.000	213703.296	319350.678	49.40
8	1.974	2.749	2.278	8.000	7.000	248934.079	391109.097	57.10

As shown in Figure 4.20 in optimum solutions, thicknesses of plates are larger than stiffeners thicknesses. Height of stiffeners have reached to lower limits in all cases

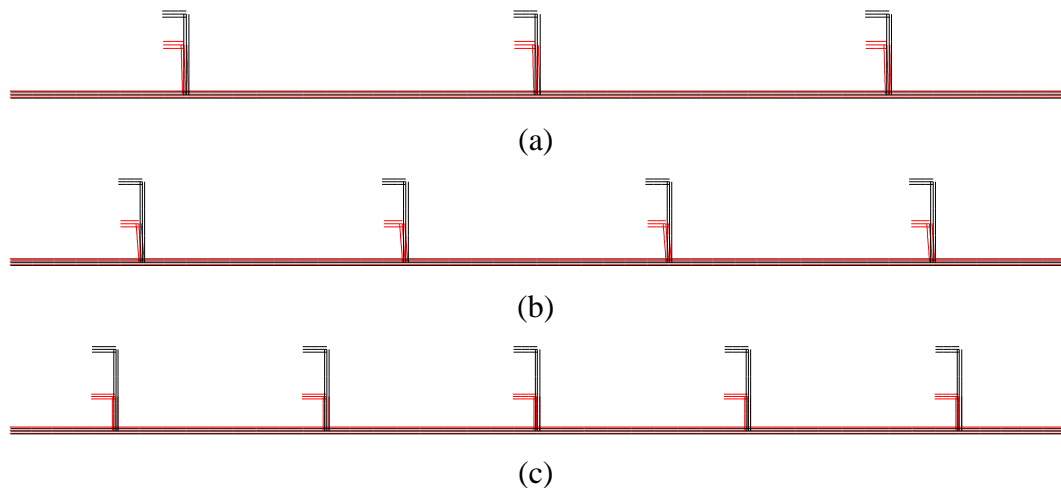


Figure 4.20 Initial and optimum shapes of L shaped stiffened plates after shape optimization (type two) (a), (b) and (c) three, four and five stiffeners respectively

Size and shape optimization (type one)s give similar results in small number of stiffeners as shown in Figure 4.21. But the shape optimization with higher number stiffeners gives higher critical buckling loads. Shape optimizations (type two) with seven design variables gave higher results even with less number of stiffeners.

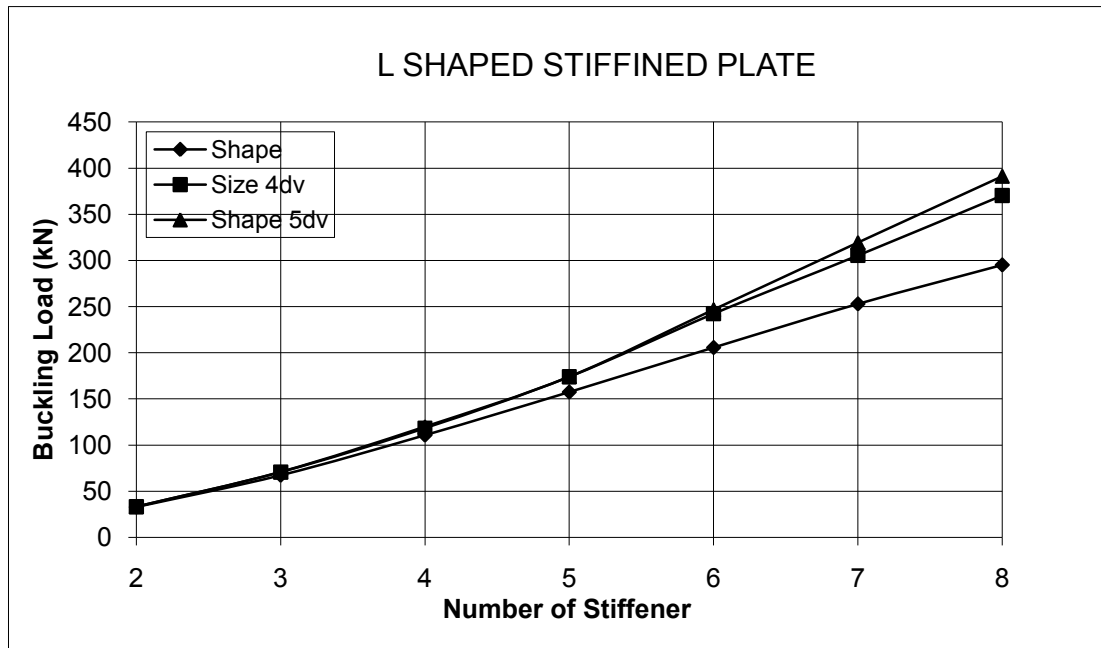


Figure 4.21 Comparison of size, shape (type one) and shape optimizations (type two)

4.4 Discussions of All Stiffened Plates

If the results are glanced, it is obviously seen that in all plate types the maximum buckling load is obtained from shape optimization (type two) of eight stiffeners case. Due to this result, it can be mentioned that lengths of elements are important for buckling fails as much as element thicknesses. Figure 4.22 shows obtained maximum buckling loads of investigated 4 stiffened plate types.

As seen from Figure 4.22, in optimized plates maximum critical buckling load is obtained from straight stiffened plate with substiffeners and pads under stiffeners.

The most crucial result that obtained from optimizations is the effect of the pad elements. From Figure 4.22 it is obviously seen that, plates with pads and without pads have remarkable difference of buckling loads. From this consequence, it is unquestionable that pad elements are the most effective ones against buckling.

Definitely, stiffeners are strengthening flat plate behavior in bending direction. Nevertheless, the joining points of stiffener elements and plate skin become weaker

because of stress concentration of corner points. By the increasing of applied inplane load, in that points stress concentration causes that points to rotate and buckling of stiffener elements take place. Pad elements prevent stress concentrations and shorten the buckling length of stiffener elements. Thus critical buckling of plate increases very sharply.

The obtained maximum load difference between straight and L shaped stiffened plates is also originated from the difference of effect of flanges and pads. In L shaped stiffened plates, flanges use somewhat volume from pads and plate skin. Therefore, the effective elements, against buckling failure become thinner. So the L shaped stiffened plates' maximum buckling load cannot reach the straights'.

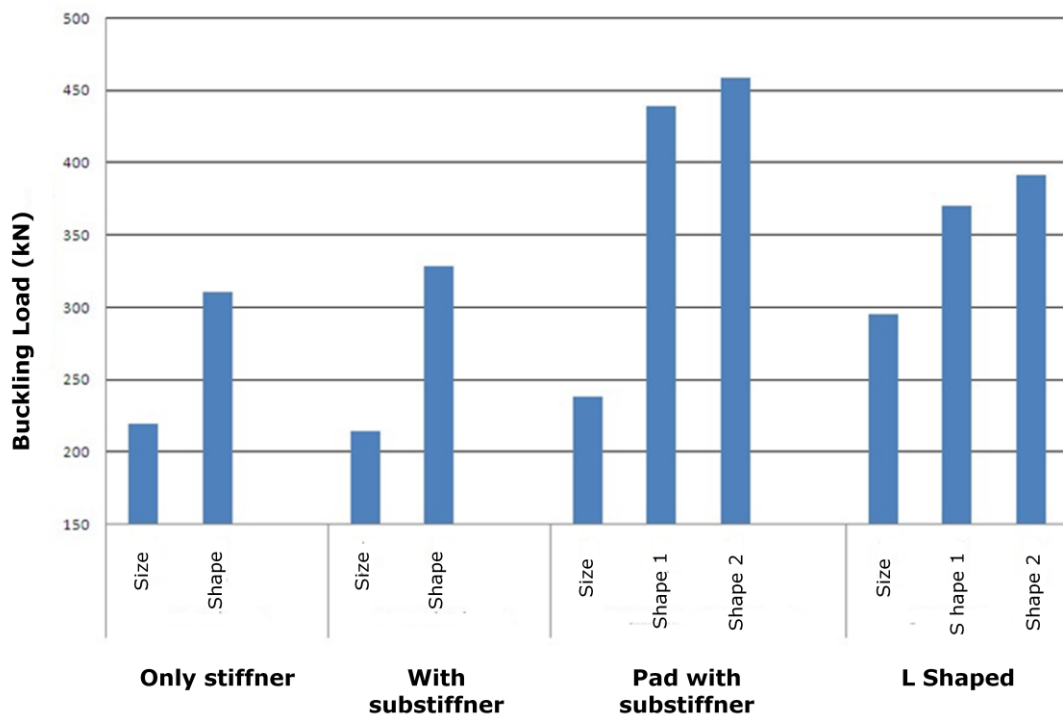


Figure 4.22 Comparison of maximum loads of plate types

Nevertheless, in plate types without pads, L shaped stiffened plates have larger critical buckling load values. This result emphasizes the effect of the flange elements. Flanges are lateral elements that are positioned top of the stiffeners. Therefore, flanges increase the moment of inertia of plate cross section in bending direction thus, critical buckling load of plate increases.

As discussed before the maximum loads are obtained from eight stiffeners case of each plate set. By the increasing of number of stiffeners, the distance between stiffeners (d_{stiff}) and the distance between stiffeners and plate sides ($d_{stiff}/2$), decrease at the same time. According to this process buckling length of plate skin regions, in other words unsupported length of plate skin decreases. Therefore, the stability of plate cross section increases remarkably and larger critical buckling loads could be gained.

It is necessary to mention about effect of substiffener elements finally. Plates with substiffeners have a little difference of buckling load when compared only straight stiffener case. Thus, it is understood that flange elements are more effective than substiffener elements so that substiffeners use volume from flanges and skin then critical buckling load decreases. In straight stiffened plate because of absence of flanges, substiffeners become effective and strengthen stability of plates slightly.

CHAPTER 5

SOFT COMPUTING TECHNIQUES AND OPTIMIZATION

5.1 Introduction

SC is entitled as generic term as techniques alike evolutionary algorithms, NNs, fuzzy logic, Genetic Programming (GP) and further bio–inspired methods. Zadeh [61], inventor of fuzzy logic and founding father of SC, specified SC as follows: “Soft computing differs from conventional or hard computing in that, unlike hard computing, it is tolerant of imprecision, uncertainty, partial truth and approximation. In effect, the role model for soft computing is the human mind. The guiding principle of soft computing is: exploit the tolerance for imprecision, uncertainty, partial truth and approximation to achieve tractability, low solution cost”.

At present a diversity of SC methods is in existence. SC is defined as a series of techniques covering a lot of areas that fall under several classes in computational intelligence. SC has three main branches. These are fuzzy systems, evolutionary computation, artificial neural computing, with the latter containing machine learning and probabilistic reasoning, rule based and wisdom based expert system, etc. as shown in Figure 5.1. All these techniques are kept under one umbrella stated as SC. SC is a partnership in which each of the partners contributes a distinct methodology for addressing problems in its domain. In this point of view, the main constituent methodologies in SC techniques are complementary rather than competitive. Furthermore, SC may be viewed as a foundation component for the emerging field of conceptual intelligence [77].

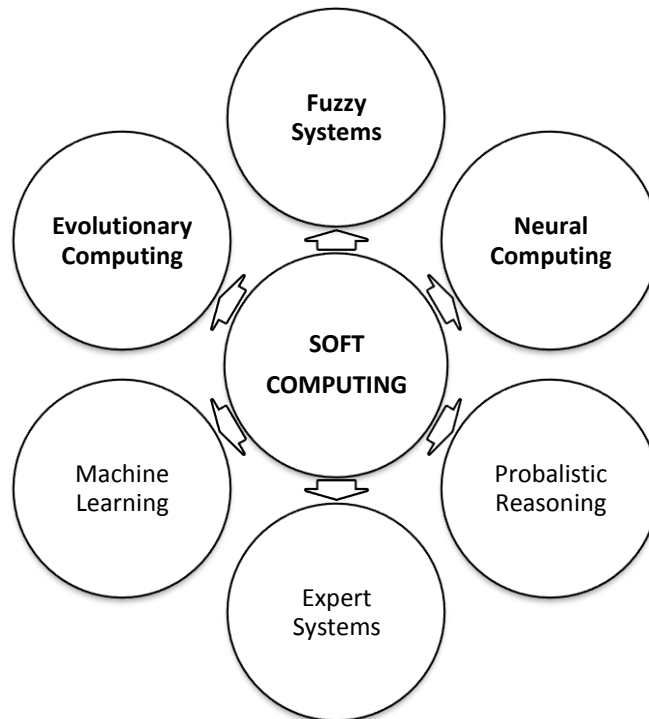


Figure 5.1 SC techniques.

The successful applications of SC and the rapid growth of the same suggest that the impact of SC will be felt increasingly. Currently, along with fuzzy logic, artificial NN and evolutionary algorithms are receiving intensive attention, in both academics and industry. Enormous research had already been done on SC techniques to identify a model and control of its different systems [77]. SC methodologies have been beneficial in numerous coverings. In contrast to analytical methods, SC methodologies are imitative awareness and knowledge in numerous significant values: they can determine from experience; they can generalize into fields where direct experience is absent; and, by parallel computer architectures, that simulate biological procedures. They may perform mapping from inputs to the outputs quicker than inherently series of analytical representations. The trade off, is a decrease in accuracy. If a tendency toward imprecision could embody tolerated, then it should be possible to extend the scope of the applications even to those problems where the analytical and mathematical representations are readily available. The motivation for such an extension is the expected decrease in computational load and consequent increase of computation speeds that permit more robust system [78].

5.2 Soft Computing Techniques

5.2.1 Neural Computing

Neural computing is one of the quickly growing fields of SC, attracting researcher from wide diversity of disciplines. The basic idea of neural computing is to capture the leading principles that underlay the brain's solution to engineering problems and utilize to the computers [79]. The main neural computing directions of development are to develop methods and algorithms for solving problems without following the way human being do so, but providing similar results, and to develop methods and systems for solving problems by modeling the human way of thinking or the way the brain works physically, for example, artificial NNs [80]. In computing statement, artificial NNs possess a particular set of features. They are not programmed; rather they are trained by being repeatedly shown large numbers of cases for the problem under consideration. As an effect of this, they can supply practical solutions in comparatively short timescales but only for certain cases of problem types, and then only when a good deal of handle is taken over the collection of the data, the pre-processing of this data and the design of the network [81]. Detailed treatment of artificial NNs summarized in the following section.

5.2.2 Neural Networks

NNs can be expressed as computer models that mimic the biological nervous system in general. There are many definitions of NNs in literature which can be summarized as follows:

A NN is a 'machine' that is designed to model the way in which the brain performs a particular task or function of interest, the network is usually implemented using electronic components or simulated in software on a digital computer [82].

Haykin [83] defines a NN as a massively parallel distributed processor that has a natural propensity for storing experiential knowledge and making it available for use. It resembles the brain in two respects, such as 'knowledge is acquired by the network through a learning process' and 'interneuron connection strengths known as synaptic weights are used to store the knowledge'.

However, according to Nigrin [84], a NN is a circuit composed of a very large number of simple processing elements that are neural based. Each element operates only on local information. Furthermore each element operates asynchronously; thus there is no overall system clock.

Another widely accepted definition of NNs is given by Zurada [85] as follows: Artificial neural systems, or NNs, are physical cellular systems which can acquire, store, and utilize experiential knowledge.

5.2.3 Components of Neural Networks

Basic component of NNs is artificial neurons shown in Figure 5.2. Figure 5.2a is a biological neuron and Figure 5.2b is a mathematical representation of artificial neuron. A biological neuron is consisting of four main elements: dendrites, synapses, axon and the cell body. The dendrites receive signals from other neurons. The axon of a single neuron serves to form synaptic connections with other neurons. The cell body of a neuron sums the incoming signals from dendrites. If input signals are sufficient to stimulate the neuron to its threshold level, the neuron sends an impulse to its axon. On the other hand, if the inputs do not reach the required level, no impulse will occur [86].

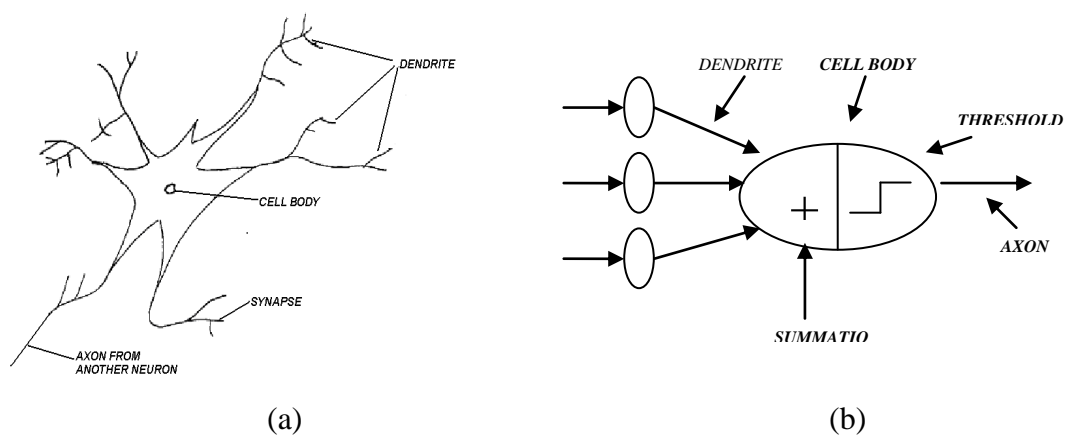


Figure 5.2 Basic component of NNs [87] (a)Biological neuron (b)Artificial neuron

The artificial neuron consists of three main components follows as weights, bias, and an activation function shown in Figure 5.3 [86]. Each neuron takes inputs

x_1, x_2, \dots, x_n , attached with a weight w_i which shows the connection strength for that input for each connection. Each input is then multiplied by the corresponding weight of the neuron connection. A bias b_i can be defined as a type of connection weight with a constant nonzero value added to the summation of inputs and corresponding weights u_i as follows,

$$u_i = \sum_{j=1}^H w_{ij} x_j + b_i \quad (5.1)$$

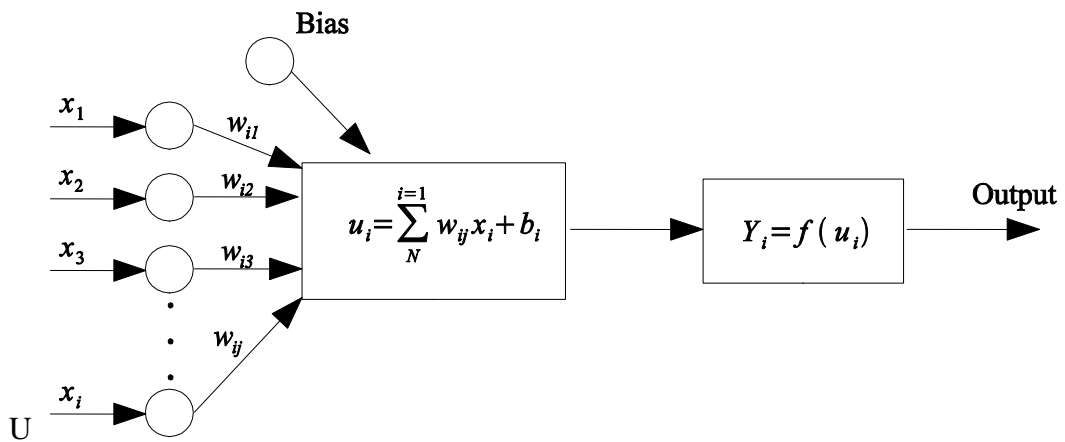


Figure 5.3 Basic elements of an artificial neuron.

The summation u_i is transformed using a scalar-to-scalar function called an "activation or transfer function", $F(u_i)$ yielding a value called the unit's "activation" as follows

$$Y_i = f(u_i) \quad (5.2)$$

The activation function is also referred to as a squashing function. Activation functions handle powerful relational operators of nonlinear of NNs. There are a numerous types of activation function and some common examples are shown in Figure 5.4 [88].

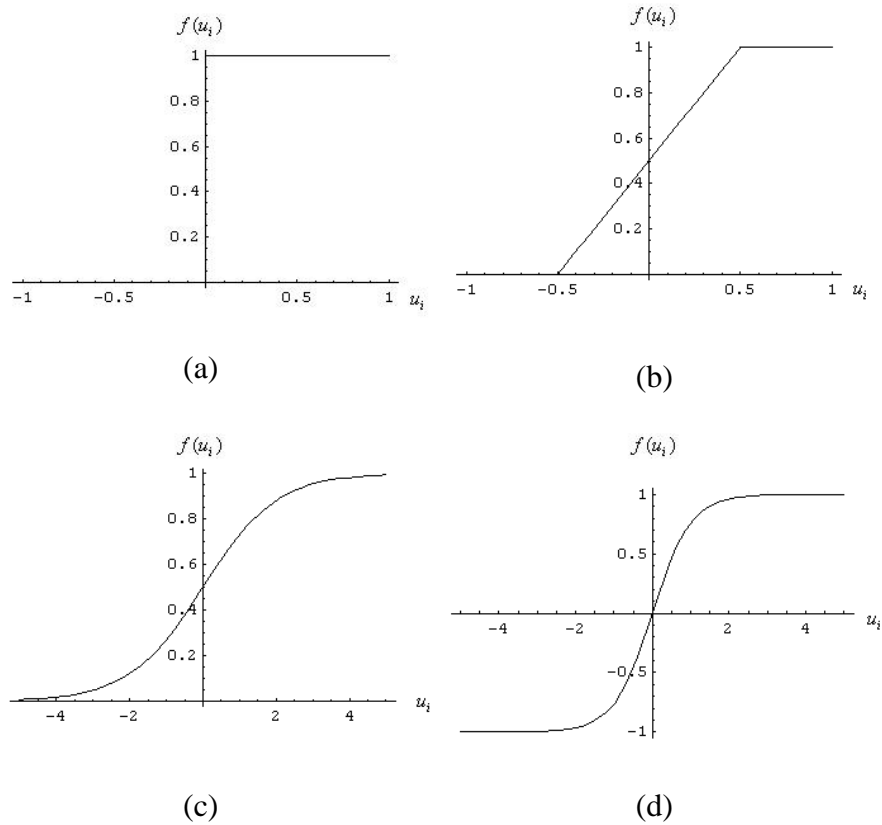


Figure 5.4 Common types of activation functions; (a) Threshold activation function (b) Piecewise-linear function (c) Sigmoid function (d) Hyperbolic tangent function. [87]

NNs, can be implemented three major tasks in SC applications [89],

Pattern association — the NN serves as an associative memory by retrieving an associated output pattern given some input pattern. The association can be *auto-associative* or *hetero-associative*, depending on whether or not the input and output patterns belong to the same set of patterns.

Classification — the network seeks to divide the set of training patterns into a pre-specified number of categories. Binary-valued output values are generally used for classification, although continuous-valued outputs (coupled with a labeling procedure) can do classification just as well.

Function approximation — the network is supposed to compute some mathematical function. The network's output represents the approximated value of the function

given the input pattern as parameters. In certain areas, *regression* may be the more natural term.

NNs not only classified as implementation task but also classified as a lot of different point of view shown in Figure 5.5.

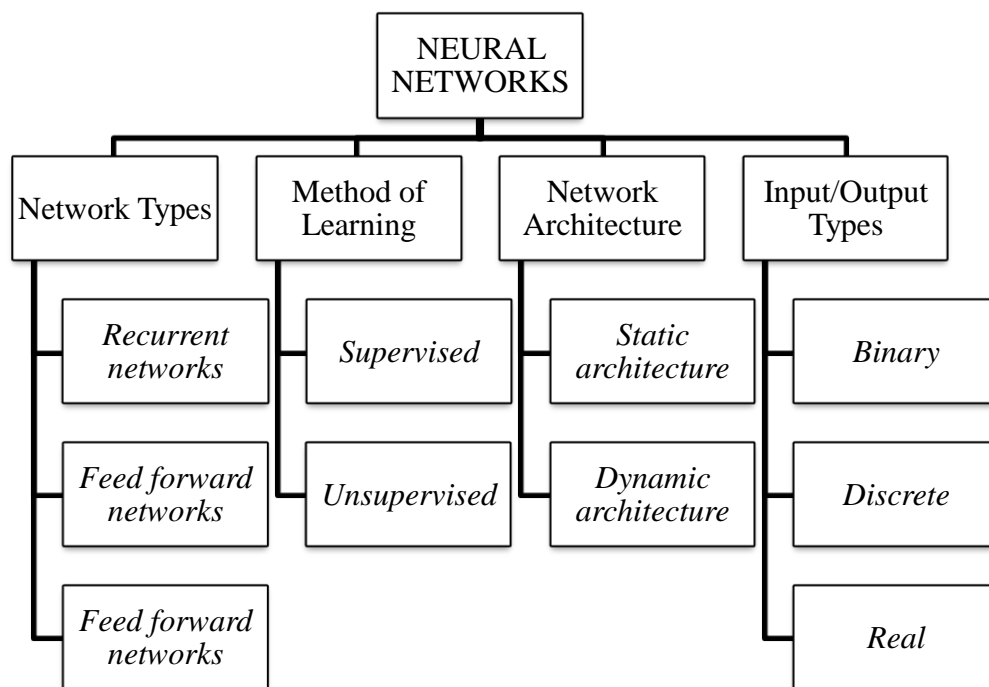


Figure 5.5 Classification of NNs.

5.2.4 Backpropagation Algorithm

Back propagation algorithm is among the most widely applied supervised training methods for training multilayer NNs due to its easiness and applicability. It is supported the generalized delta rule and was highlighted by Rumelhart and his colleagues [90]. As it is a supervised learning algorithm, there is a couple of inputs and matching output. The algorithm is simply supported a weight correction process shown schematically in Fig. 5.6. It lies of two passes: a forward pass and a backward pass. In the forward pass, first, the weights of the network are arbitrarily initialized and an output set is found for a given input set where weights are kept as fixed. The error between the output of the network and the target value is propagated backward during the backward pass and used to update the weights of the previous layers as shown in Figure 5.7 [91].

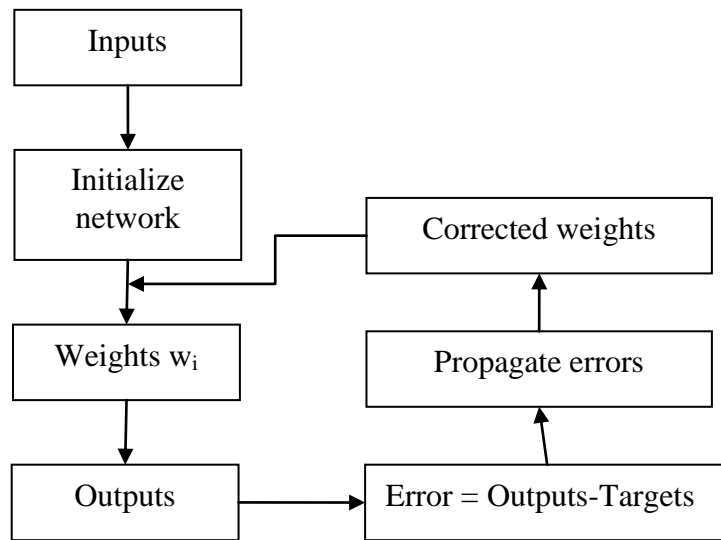


Figure 5.6 Weight correction representation of back propagation NNs.

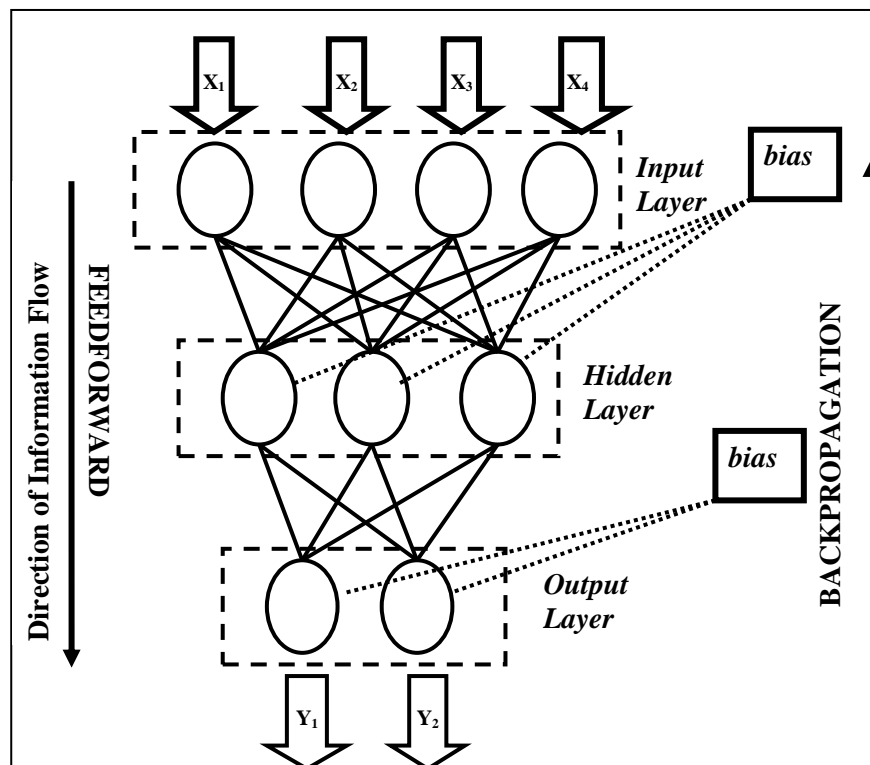


Figure 5.7 Back-propagation algorithm.

The main goal of back-propagation NN is mapping of input vector x_i into output vector y_i : This can be written in short:

$$x_i \xrightarrow{BPNN} y_i \quad (5.3)$$

For the output layer the error δ_j^{last} can be given as the difference between the target value y_i and the network output out_j^{last} :

$$\delta_j^{last} = (y_i - out_j^{last})out_j^{last} (\mathbf{1} - out_j^{last}) \quad (5.4)$$

The weight correction is given as

$$\Delta w_{ji}^l = w_{ji}^{l(new)} - w_{ji}^{l(old)} \quad (5.5)$$

Combining (5.4) and (5.5) the weight correction in a hidden layer can be generalized as follows:

$$\Delta w_{ji}^l = \eta \left(\sum_{k=1}^r \delta_k^{l+1} w_{kj}^{l+1} \right) out_j^l (1 - out_j^l) out_i^{l-1} + \mu \Delta w_{ji}^{l(previous)} \quad (5.6)$$

where η is the learning rate and μ is the momentum constant. (5.5) can be also be expressed in condensed form as:

$$\Delta w_{ji}^l = \eta \delta_j^l out_i^{l-1} + \mu \Delta w_{ji}^{l(previous)} \quad (5.7)$$

5.3 Fuzzy Logic

Fuzzy logic presented by Zadeh [61] in 1965 by has been utilized to a broad range of research areas of engineering, process control, image processing, pattern recognition and classification, management, economics and decision making [92].

Fuzzy systems can be specified as rule-based systems that are constructed from a collection of linguistic rules which can represent any system with accuracy, i.e., they

work as *universal approximators*. The rule-based system of fuzzy logic theory uses linguistic variables as its antecedents and consequents where antecedents express an inference or the inequality, which should be satisfied and consequents are those, which we can infer, and is the result if the antecedent inequality is satisfied. The fuzzy rule-based system is actually an IF-THEN rule-based system, given by, IF antecedent, THEN consequent [93].

Fuzzy logic operations are based on fuzzy sets where the input data may be defined as fuzzy sets or a single element with a membership value of unity. The membership values (μ_1 and μ_2) are found from the intersections of the data sets with the fuzzy sets as shown in Figure 5.8 which illustrates the graphical method of finding membership values in the case of a single input [94].

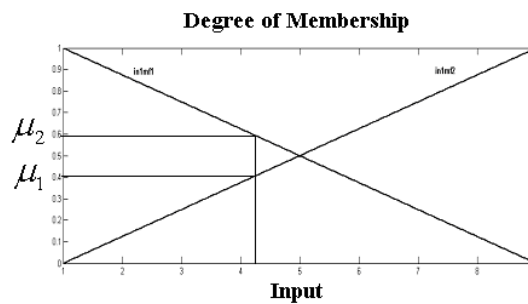


Figure 5.8 Input data membership values [94].

A fuzzy set contains elements which have varying degrees of membership in the set, unlike the classical or crisp sets where a member either belongs to that set or does not (0 or 1). However a fuzzy set allows a member to have a varying degree of membership and this partial degree membership can be mapped into a function or a universe of membership values [95].

The implementation of fuzzy logic to real applications considers the following steps [95]:

1. *Fuzzification* which requires conversion of classical data or crisp data into fuzzy data or membership functions
2. *Fuzzy inference process* which connects membership functions with the fuzzy rules to derive the fuzzy output
3. *Defuzzification* which computes each associated output.

5.3.1 Neuro–Fuzzy Systems

Fuzzy systems can also be connected with NNs to form neuro–fuzzy systems which exhibit advantages of both approaches. Neuro–fuzzy systems combine the natural language description of fuzzy systems and the learning properties of NNs. Various neuro–fuzzy systems have been developed that are known in literature Adaptive Network–based Fuzzy Inference System (ANFIS) developed by Jang et al. [78], ANFIS is one of these Neuro–fuzzy systems which allow the fuzzy systems to learn the parameters using adaptive backpropagation learning algorithm [92]. Mainly three types of fuzzy inference systems have been widely employed in various applications: Mamdani, Sugeno and Tsukamoto fuzzy models. The differences between these three fuzzy inference systems are due to the consequents of their fuzzy rules, and thus their aggregation and defuzzification procedures differ accordingly [78]. Each rule is defined as a linear combination of input variables. In Sugeno FIS: the corresponding final output of the fuzzy model is simply the weighted average of each rule’s output. A Sugeno FIS consisting of two input variables x and y , for example, a one output variable f will lead to two fuzzy rules:

Rule 1: If x is A_1 , y is B_1 then $f_1 = p_1x + q_1y + r_1$

Rule 2: If x is A_2 , y is B_2 then $f_2 = p_2x + q_2y + r_2$

where p_i , q_i , and r_i are the consequent parameters of i^{th} rule. A_i , B_i and C_i are the linguistic labels which are represented by fuzzy sets shown in Figure 5.9.

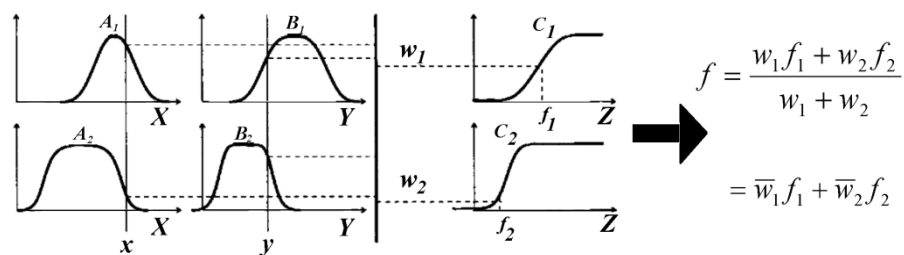


Figure 5.9 The Sugeno fuzzy model [78]

5.3.2 Solving a Simple Problem with ANFIS

To illustrate how ANFIS works for function approximation, let’s suppose one is given a sampling of the numerical values from the simple function below:

$$y_i = a^3 + b^2 \quad (5.8)$$

where a and b are independent variables chosen over randomly points in the real interval $[1, 9]$ and. In this case, a sample of data in the form of 17 set (a, b, y_i) is given where x_i is the value of the independent variable in the given interval $[1, 9]$ and y_i is the output of the function given in (1). The aim is to construct the ANFIS model fitting those values within minimum error for (1) by using the simplest ANFIS model that is available where the numbers of rules are 2 for each variable and the type of output membership function is constant. Initial and final membership values of rules for each input are given in Figures 5.10, and 5.11 respectively. Suppose one will find the output for input values of 1 and 9. The inference diagram of the proposed ANFIS model is given in Figure 5.12 for input values of 1 and 9 with corresponding values of output membership which is chosen as constant. For the first input which is 1 the value of the membership function is observed to be 1 shown on left side of Figure 5.10. For the second input which is 9 the value of the membership function is observed to be 1 again shown on left side of Figure 5.11. Thus the final output will be: $82 \times 1 = 82$.

The exact result for $a=1$ and $b=9$ from (1) will be $y=1^3 + 9^2 = 82$.

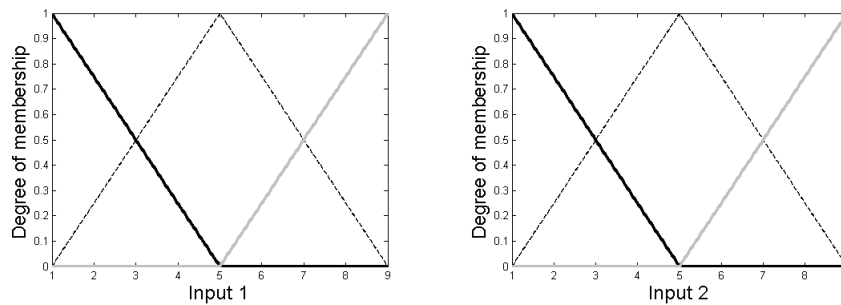


Figure 5.10 Initial membership functions

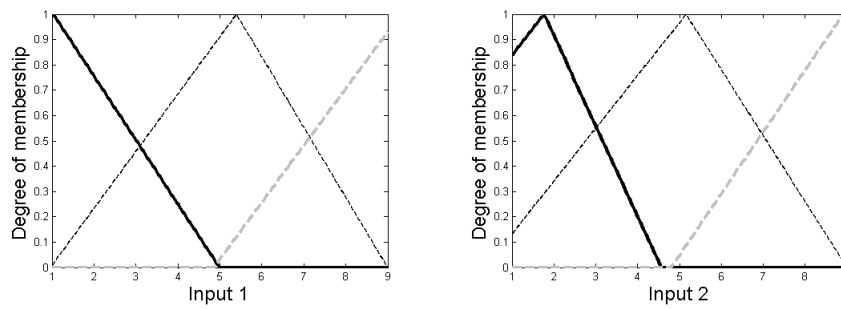


Figure 5.11 Final membership functions.

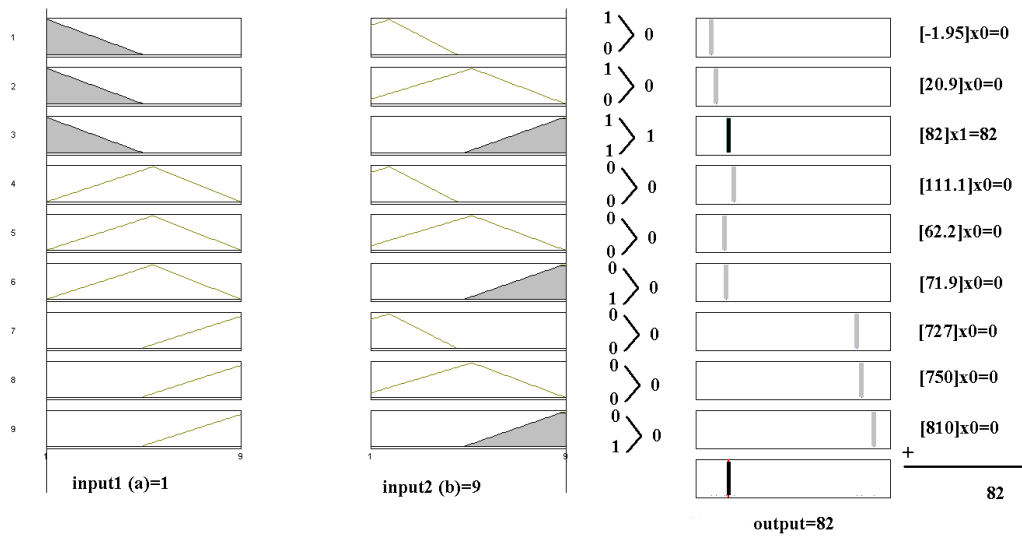


Figure 5.12 Fuzzy inference diagrams

5.4. Evolutionary Computing

Evolutionary computing is a popular research area of various engineering sciences. It is founded on inspiration of process of survival of the fittest in nature. Several different methods have been proposed over the years. From literature, there are generally basic types of evolutionary computing are genetic algorithms, evolutionary programming, evolution strategies, GP and learning classifier systems [96]. In this thesis, applications of genetic algorithms in structural optimization and an extension of GP which is GEP algorithm in function approximation is implemented. Basically, they founded on main idea which behind all these techniques is given population of individuals; the environmental circumstances pressurize natural selection or survival of fittest. As a result of this natural selection, an advance takes place in population.

These operations involved as follows. Given fitness function is to be optimized. Randomly generated set of solution as candidates, are assessed by the fitness function that indicates an abstract of fitness measure. Based on fitness values, fitter candidate solutions have a better chance to be selected to seed next generation through the application crossover and mutation. Offsprings are produced crossover of two or more candidate parent solutions. Mutation operator is applied to one offspring candidate for produce new candidate solution in next generation. The process of selection, crossover and mutation are repeated from one generation to another until termination criteria is accomplished. A general scheme of evolutionary computing is shown in Figure 5.13.

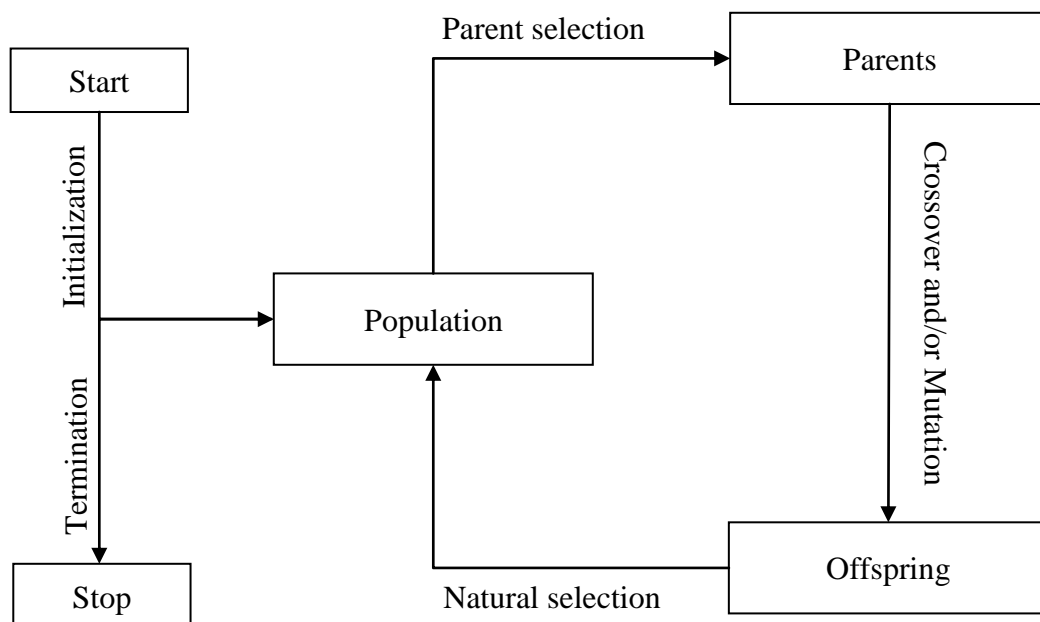


Figure 5.13 General scheme of evolutionary computing.

5.4.1. Genetic Programming

Genetic algorithm (GA) is an optimization and search process founded on the principles of genetics and survival of the fittest. A GA provides a population composed of a lot of individuals to evolve under defined selection rules to a state that maximizes the “fitness” (i.e., minimizes the cost function). The method was proposed by Holland [41] and generalized by among his students, Goldberg [97] who solved a difficult problem involving the control of gas–pipeline transmission for his dissertation. The fitness of each individual in a genetic algorithm is the measure the individual has been adapted to the problem that is solved employing this individual.

It means that fitness is the measure of optimality of the solution offered, as represented by an individual from the genetic algorithm. The basis of genetic algorithms is the selection of individuals in accordance with their fitness; thus, fitness is obviously a critical criterion for optimization [98].

GP is an propagation to Genetic Algorithms suggested by Koza [99]. The former pioneer specifies GP as a domain-independent problem-solving approach in which computer programs are developed to solve, or close to solve, problems grounded on the Darwinian principle of reproduction and natural selection and analogues of naturally occurring genetical operations such as *crossover (sexual recombination)* and *mutation*. GP reproduces computer programs to solve problems by executing the adopting steps which requires:

1. Generate an initial population of random compositions of the functions and terminals of the problem (computer programs).
2. Execute each program in the population and assign it a fitness value according to how well it solves the problem.
 - i) Create a new population of computer programs.
 - ii) Copy the best existing programs (Reproduction).
 - iii) Create new computer programs by mutation.
 - iv) Create new computer programs by crossover (sexual reproduction).
 - v) Select an architecture-altering operation from the programs stored so far.
3. The best computer program that appeared in any generation, the best-so-far solution, is designated as the result of GP [98–100] (see Figure 5.14).

5.4.2. Gene Expression Programming

GEP algorithm which is used in this study is an extension to GP that evolves computer programs of different sizes and shapes encoded in linear chromosomes of fixed length. The chromosomes are composed of multiple genes, each gene encoding a smaller sub-program. Furthermore, the structural and functional organization of the linear chromosomes allows the unconstrained operation of important genetic operators such as mutation, transposition, and recombination. One strength of the GEP approach is that the creation of genetic diversity is extremely simplified as genetic operators work at the chromosome level. Another strength of GEP consists of

its unique, multigenic nature which allows the evolution of more complex programs composed of several sub–programs. As a result GEP surpasses the old GP system in 100–10,000 times [101–103]. A GEP software GeneXpro which invented by Ferreira is used in this study [100].

The fundamental difference between GA, GP and GEP is due to the nature of the individuals: in GAs the individuals are linear strings of fixed length (chromosomes); in GP the individuals are nonlinear entities of different sizes and shapes (parse trees); and in GEP the individuals are encoded as linear strings of fixed length (the genome or chromosomes) which are afterwards expressed as nonlinear entities of different sizes and shapes (i.e., simple diagram representations or expression trees). Thus the two main parameters GEP are the chromosomes and expression trees (ETs). The process of information decoding (from the chromosomes to the ETs) is called translation which is based on a set of rules. The genetic code is very simple where there exist one–to–one relationships between the symbols of the chromosome and the functions or terminals they represent. The rules which are also very simple determine the spatial organization of the functions and terminals in the ETs and the type of interaction between sub–ETs. [101–103]

That’s why two languages are utilized in GEP: the language of the genes and the language of ETs. A significant advantage of GEP is that it enables to infer exactly the phenotype given the sequence of a gene, and *vice versa* which is termed as *Karva* language. Consider, for example, the algebraic expression

$$y = (a^2 + a) \tag{5.9}$$

can be represented by a diagram shown in Figure 5.15 which is the expression tree:

For each problem, the type of linking function, as well as the number of genes and the length of each gene, are *a priori* chosen for each problem. While attempting to solve a problem, one can always start by using a single–gene chromosome and then proceed by increasing the length of the head. If it becomes very large, one can increase the number of genes and obviously choose a function to link the sub–ETs. One can start with addition for algebraic expressions or OR for Boolean expressions,

but in some cases another linking function might be more appropriate (like multiplication or IF, for instance). The idea, of course, is to find a good solution, and GEP provides the means of finding one very efficiently [102].

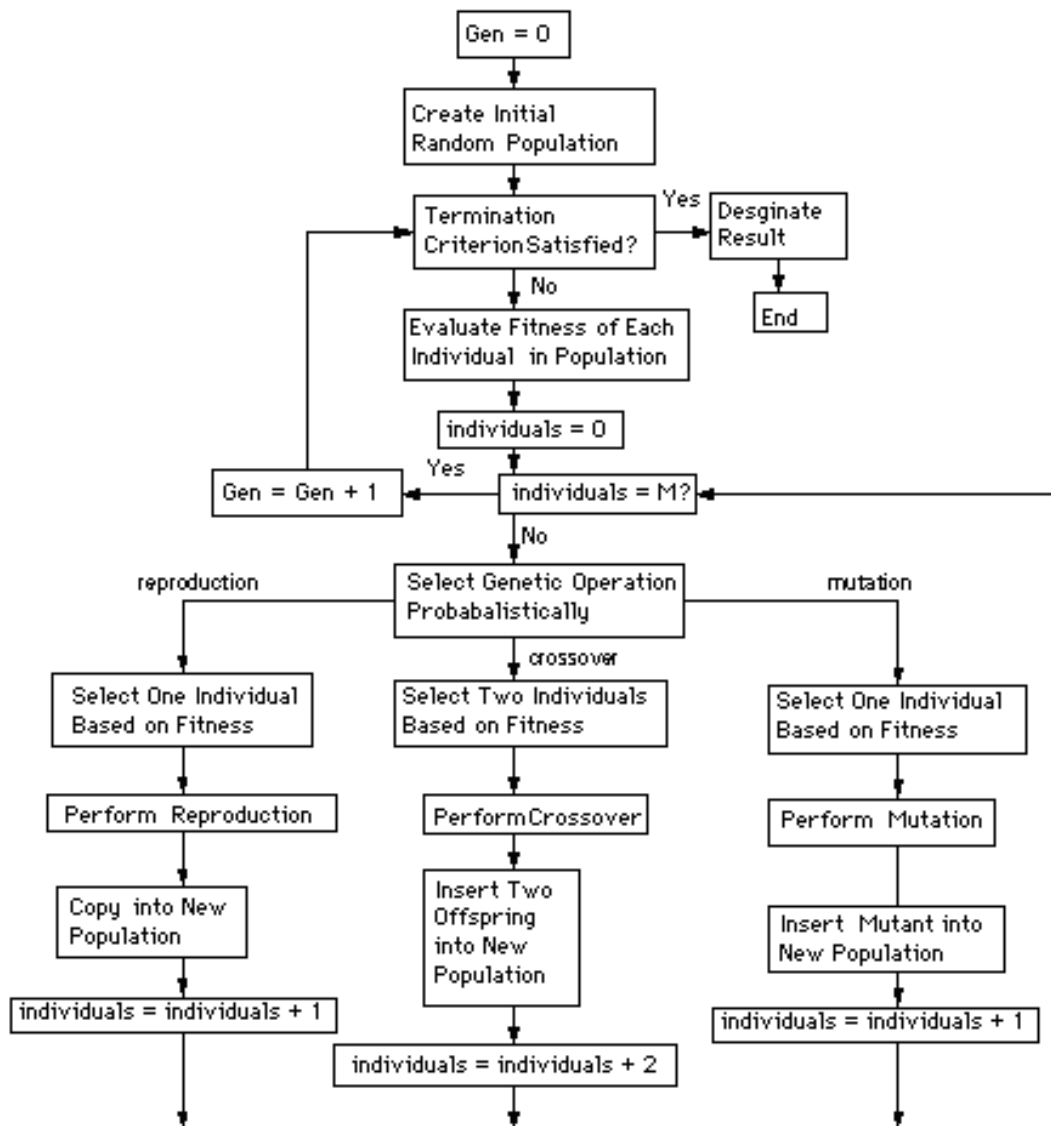


Figure 5.14 GP flowchart [98].

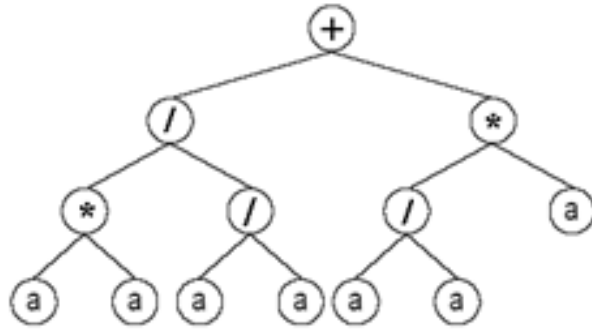


Figure 5.15 Expression tree representation [98].

5.4.3 Implementation of GEP

As an illustrative example consider the following case where the objective is to show how GEP can be used to model complex realities with high accuracy. So, suppose one is given a sampling of the numerical values from the curve (remember, however, that in real-world problems the function is obviously unknown):

$$y = 3a^2 + 2a + 1 \quad (5.10)$$

over 10 randomly chosen points in the real interval $[-10, +10]$ and the aim is to find a function fitting those values within a certain error. In this case, a sample of data in the form of 10 pairs (a_i, y_i) is given where a_i is the value of the independent variable in the given interval and y_i is the respective value of the dependent variable (a_i values: $-4.2605, -2.0437, -9.8317, -8.6491, 0.7328, -3.6101, 2.7429, -1.8999, -4.8852, 7.3998$; the corresponding y_i values can be easily evaluated). These 10 pairs are the fitness cases (the input) that will be used as the adaptation environment. The fitness of a particular program will depend on how well it performs in this environment [102].

There are five major steps in preparing to use GEP. The first is to choose the fitness function. For this problem one could measure the fitness f_i of an individual program i by the following expression:

$$f_i = \sum_{j=1}^{C_i} \left(1 - |C_{(i,j)} - T_j| \right) \quad (5.11)$$

where M is the range of selection, $C_{(i,j)}$ the value returned by the individual chromosome i for fitness case j (out of C_t fitness cases) and T_j is the target value for fitness case j . If, for all j , $|C_{(i,j)} - T_j|$ (the precision) less than or equal to 0.01, then the precision is equal to zero, and $f_i = f_{\max} = C_t * M$. For this problem, use an $M = 100$ and, therefore, $f_{\max} = 1000$. The advantage of this kind of fitness function is that the system can find the optimal solution for itself. However there are other fitness functions available which can be appropriate for different problem types [102].

The second step is choosing the set of terminals T and the set of functions F to create the chromosomes. In this problem, the terminal set consists obviously of the independent variable, i.e., $T = \{a\}$. The choice of the appropriate function set is not so obvious, but a good guess can always be done in order to include all the necessary functions. In this case, to make things simple, use the four basic arithmetic operators. Thus, $F = \{+, -, *, /\}$. It should be noted that there many other functions that can be used.

The third step is to choose the chromosomal architecture, i.e., the length of the head and the number of genes.

The fourth major step in preparing to use GEP is to choose the linking function. In this case we will link the sub-ETs by addition. Other linking functions are also available such as subtraction, multiplication and division.

And finally, the fifth step is to choose the set of genetic operators that cause variation and their rates. In this case one can use a combination of all genetic operators (mutation at $p_m = 0.051$; IS and RIS transposition at rates of 0.1 and three transposons of length 1, 2, and 3; one-point and two-point recombination at rates of 0.3; gene transposition and gene recombination both at rates of 0.1).

To solve this problem, lets choose an evolutionary time of 50 generations and a small population of 20 individuals in order to simplify the analysis of the evolutionary process and not fill this text with pages of encoded individuals. However, one of the

advantages of GEP is that it is capable of solving relatively complex problems using small population sizes and, thanks to the compact Karva notation; it is possible to fully analyze the evolutionary history of a run.

A perfect solution can be found in generation 3 which has the maximum value 1000 of fitness. The sub-ETs codified by each gene are given in Figure 5.16. Note that it corresponds exactly to the same test function given above and its expression tree is shown in Figure 5.16 [98].

$$y = (a^2+a)+(a+1)+(2a^2) = 3a^2+2a+1 \quad (4.12)$$

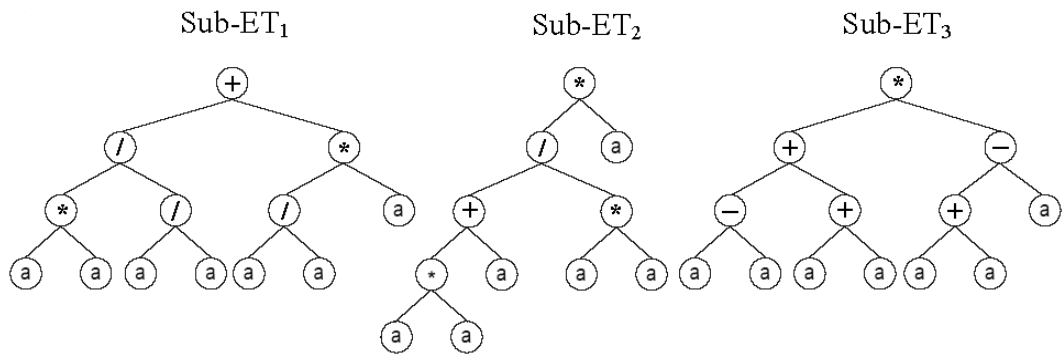


Figure 5.16 Expression tree representation for perfect solution [98].

CHAPTER 6

BUCKLING AND FREE VIBRATION SENSITIVITY ANALYSIS AND SOFT COMPUTING APPLICATIONS

6.1 Introduction

The main purpose of this chapter is to do the sensitivity analysis and SC models of stiffened panels. The elastic buckling and free vibration analyses of stiffened panels are dealt separately. The sensitivity analysis and SC models are done for buckling and free vibration of panel. The database used for model training has been generated by the program developed by Özakça and coworkers [1]. The database is divided into train and test sets where patterns in test set are randomly selected with a ratio 15 % and 85 % respectively.

6.2 Problem Definition of Stiffened Panels

A non-dimensional parametric database has been formed where variables have been given as a ratio of b which is the width of the geometry shown in Figure 6.1. The ranges of variables for the database are given in Table 6.1. Note that L is the length of panel which is taken 1.0 to 2.0 with increment 0.1 and the structures have simply supported end conditions at $y = 0$ and $y = L$, other ends are free. A stiffened panel is typically fabricated from a flat plate with longitudinal stiffeners that span between girders. n_{blade} is number of stiffeners which are taken 2, 3, 4 and 5 respectively. The following material properties are used: $E = 75.0 \times 10^6$ and Poisson's ratio $\nu = 0.33$. Note that all units are consistent.

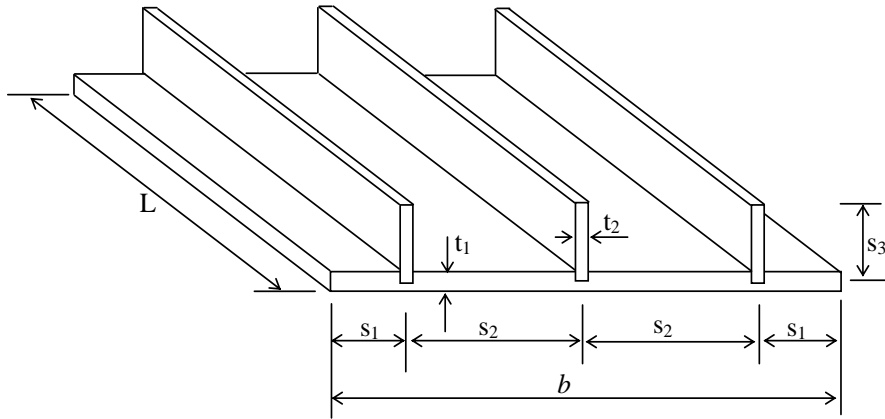


Figure 6.1 Typical section of stiffened panel

Table 6.1 The range of variables used in the database

Variables	Values			
s_1/b	0.100	0.150	0.200	0.250
s_2/b	0.400	0.350	0.300	0.250
s_3/b	0.020	0.040	0.060	0.080
t_1/b	0.004	0.006	0.008	0.010
t_2/b	0.004	0.006	0.008	0.010

The isotropic stiffened panels subjected to longitudinal compression analyzed by FS method is shown in Figure 6.2. Analyses are carried out by using 4-noded strips with reduced integration for avoiding locking phenomena. End of the analysis 14080 data pair is collected for SC models.

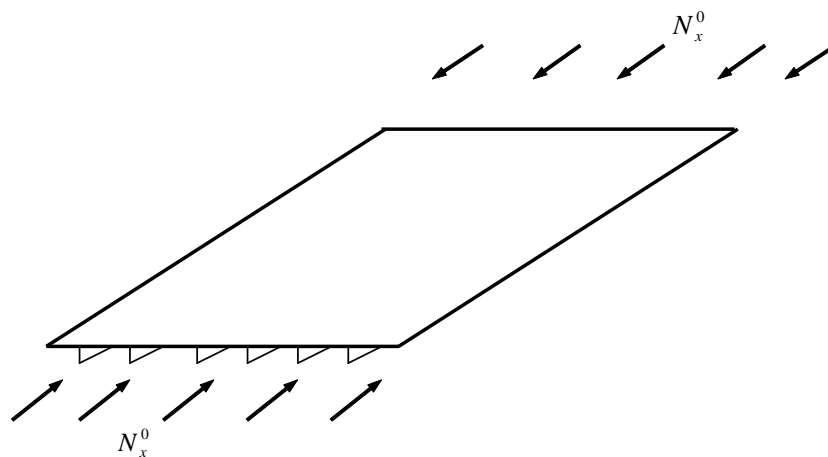


Figure 6.2 Isotropic panels loading for buckling

6.3 Sensitivity Analysis of FS Buckling Results (Main effect plots)

Main effect plots for FS analyses are composed by using 14080 data pairs. Interaction of buckling stresses against all design variables are shown in Figure 6.3. All sampling points shown in figures are mean of the buckling stresses. Effect of the n_{blade} is shown in Figure 6.4–6.6.

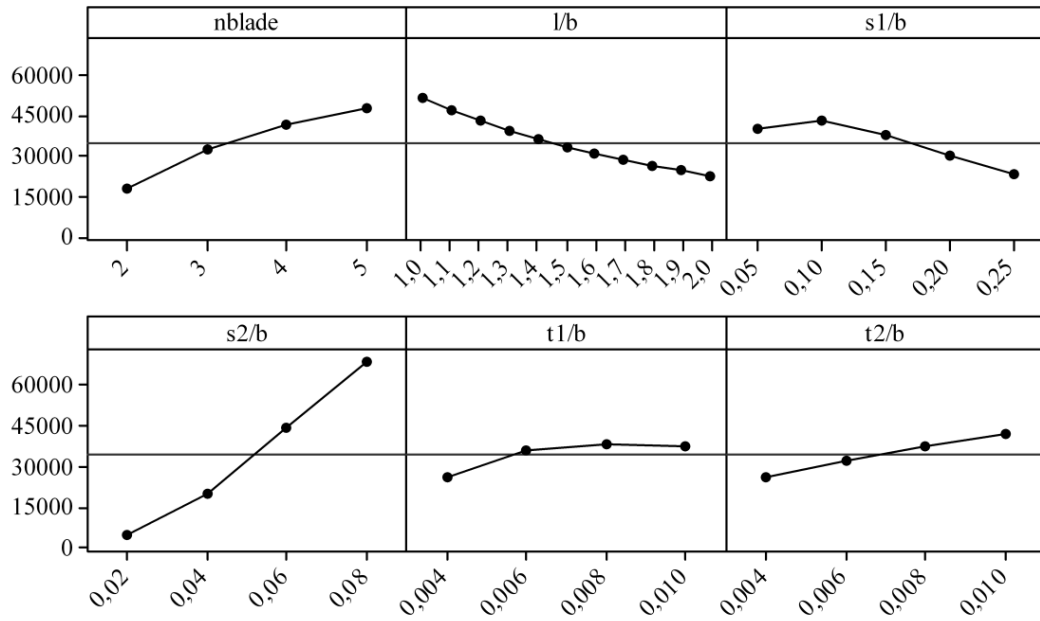


Figure 6.3 Main effect plots of FS for buckling

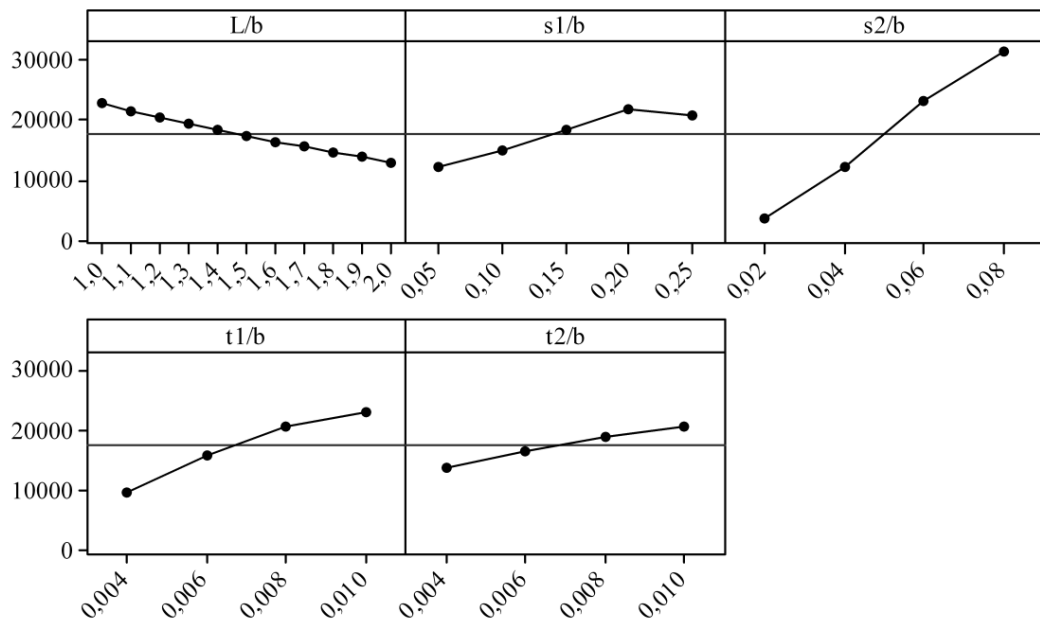


Figure 6.4 Main effect plots of FS for case $n_{blade}=2$ for buckling

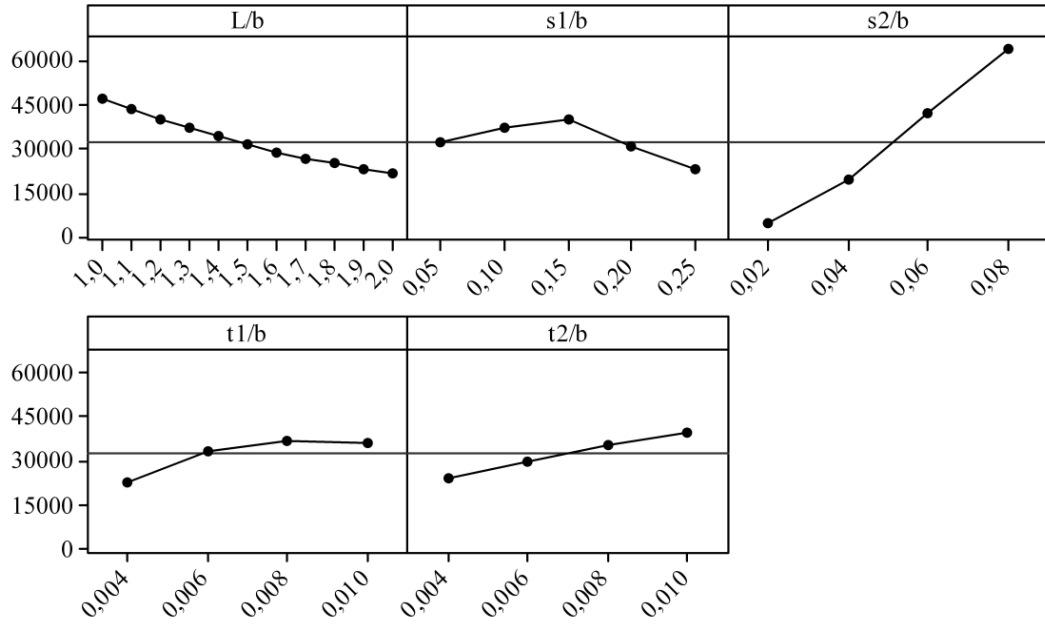


Figure 6.5 Main effect plots of FS for case $n_{blade}=3$ for buckling

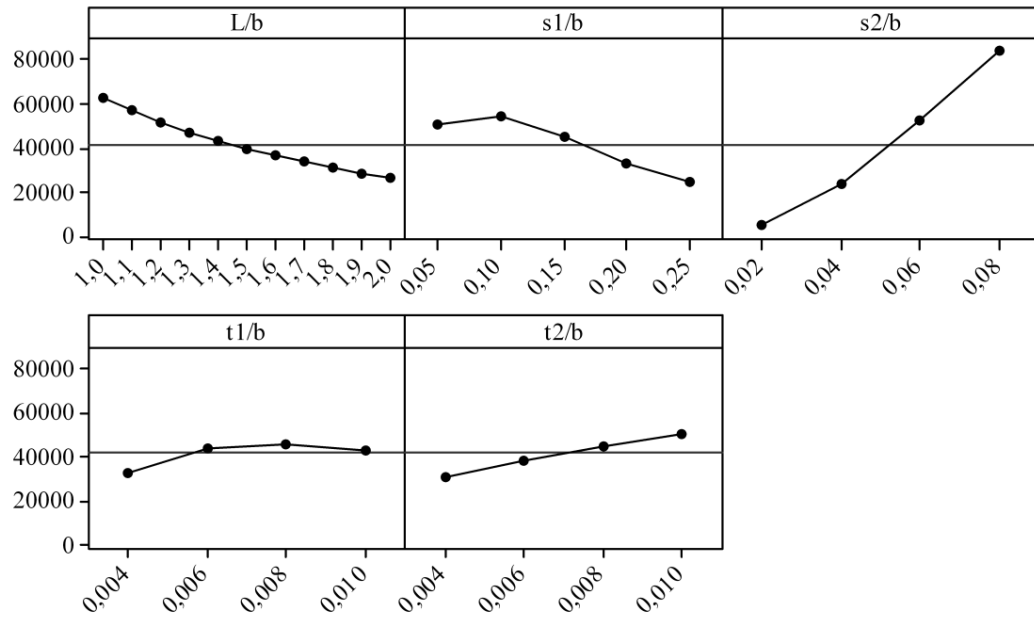


Figure 6.6 Main effect plots of FS for case $n_{blade}=4$ for buckling

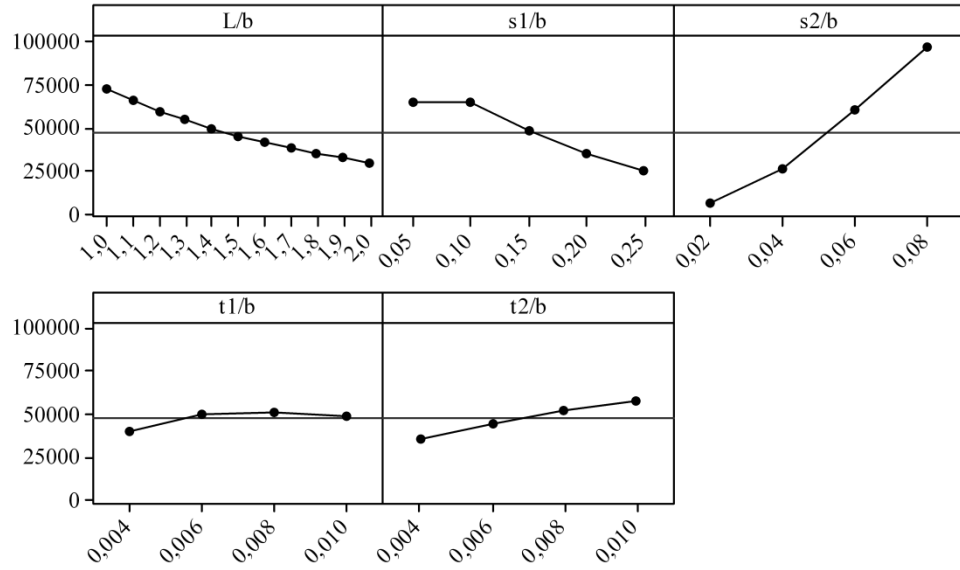


Figure 6.7 Main effect plots of FS for case $n_{blade}=5$ for buckling

6.4 Numerical Applications of Soft Computing Techniques for Buckling

Analysis

Performance and reliability of GEP Model and NN Model are done separately for buckling analysis of stiffened panel.

6.4.1 Performance and Reliability of GEP Model

The main aim is to obtain the explicit formulation of buckling stress of stiffened panels as a function of geometric properties given as follows:

$$F_{\sigma} = (n_{blade}, l/b, s_1/b, s_2/b, t_1/b, t_2/b) \quad (6.1)$$

GEP model training parameters are given in Table 6.2. According to this parameters, obtained expression tree (ET) shown in Figure 6.8. Mathematical representation of ET as follows

$$\sigma_{buck} = \left(\left((d(4) + d(6)) * G1C1 \right) * \left((d(1)/d(2)) - d(4) \right) * \left((d(4) + d(6)) * G3C9 \right) * \left((d(3)/d(5)) - G4C18 \right) \right) \quad (6.2)$$

where the constants are in (6.2) $G1C1=587.5832$, $G3C9=-135.6095$ and $G4C18=74.7249$. The actual parameters are $d(1)=n_{blade}$, $d(2)=l/b$, $d(3)=s_1/b$,

$d(4)=s_2/b$, $d(5)=t_1/b$ and $d(6)=t_2/b$. After putting in the corresponding values and rearrange the (6.2), final equation as follows,

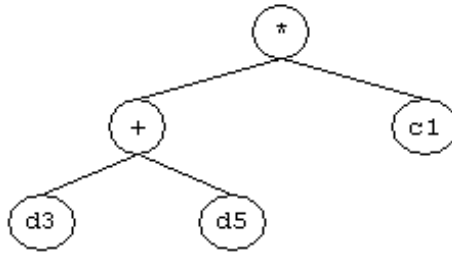
$$\sigma_{buck} = \left(-79681.8640 \times \left(\frac{s_2}{b} + \frac{t_2}{b} \right) \right) \times \left(\frac{nblade}{l/b} - \frac{s_2}{b} \right) \times \left(\frac{s_2/b}{t_1/b} - 74.7249 \right) \quad (6.3)$$

Table 6.2 Parameters of GEP model

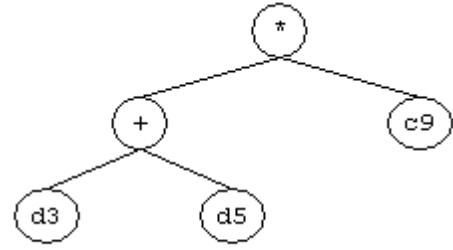
P1	Function set	+, -, *, /
P2	Chromosomes	30
P3	Head Size	2
P4	Number of genes	4
P5	Linking function	Multiplication
P6	Fitness function, error type	Custom, MAE(Mean Abs. Error)
P7	Mutation rate	0.044
P8	Inversion rate	0.1
P9	One-point combination rate	0.3
P10	Two-point combination rate	0.3
P11	Gene recombination rate	0.1
P12	Gene transposition rate	0.1

It should be noted that the proposed GEP formulation is valid for the ranges of the training set given in Table 6.1. Comparison of test, train and total sets of GEP model are given in Table 6.3. The GEP model results versus FS results for test, train and total sets are shown in Figures 6.9–6.11.

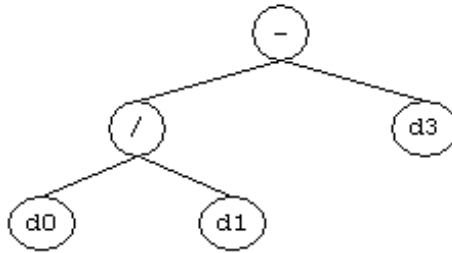
Sub-ET 1



Sub-ET 3



Sub-ET 2



Sub-ET 4

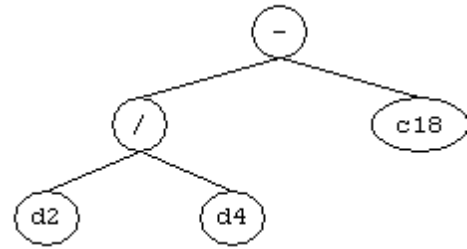


Figure 6.8 Expression tree for proposed GEP model for buckling analyses

Table 6.3 Comparison of test, training and total sets GEP

	Test Set	Training Set	Total set
Mean (GEP/FS)	1.2823	1.2829	1.2822
Standard deviation (GEP/FS)	0.6819	0.6513	0.6781
RMSE	16051.00	15911.10	16033.17
Covariance	0.5318	0.5077	0.5289
Correlation coefficient (R^2)	0.8212	0.8297	0.8219

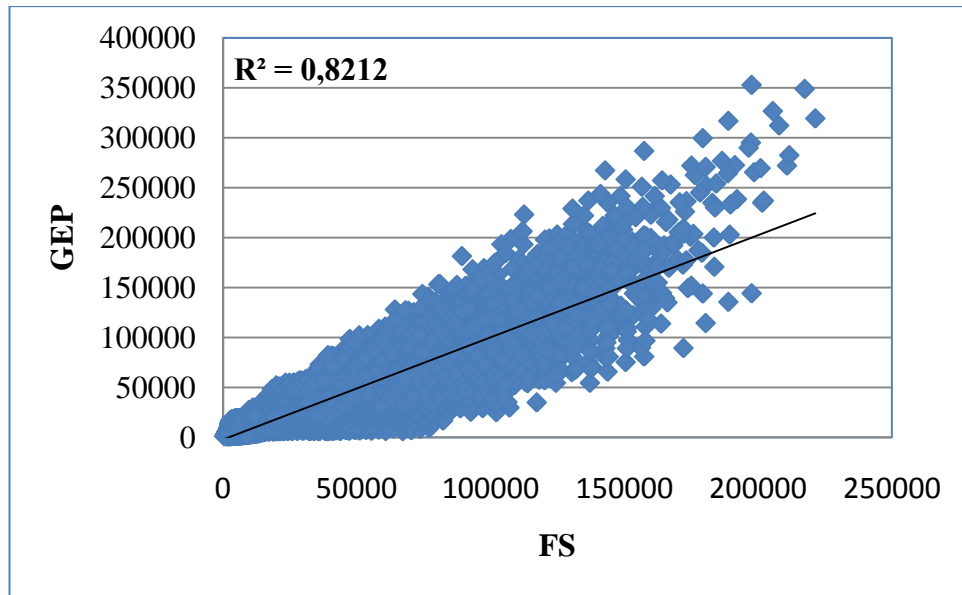


Figure 6.9 GEP Model solutions versus FS solutions and correlations for test set.

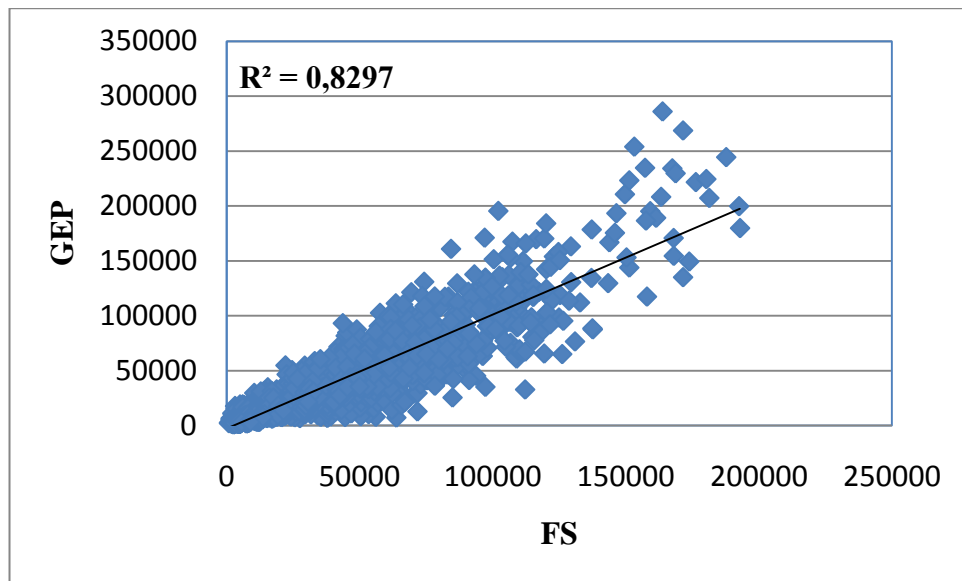


Figure 6.10 GEP Model solutions versus FS solutions and correlations for train set

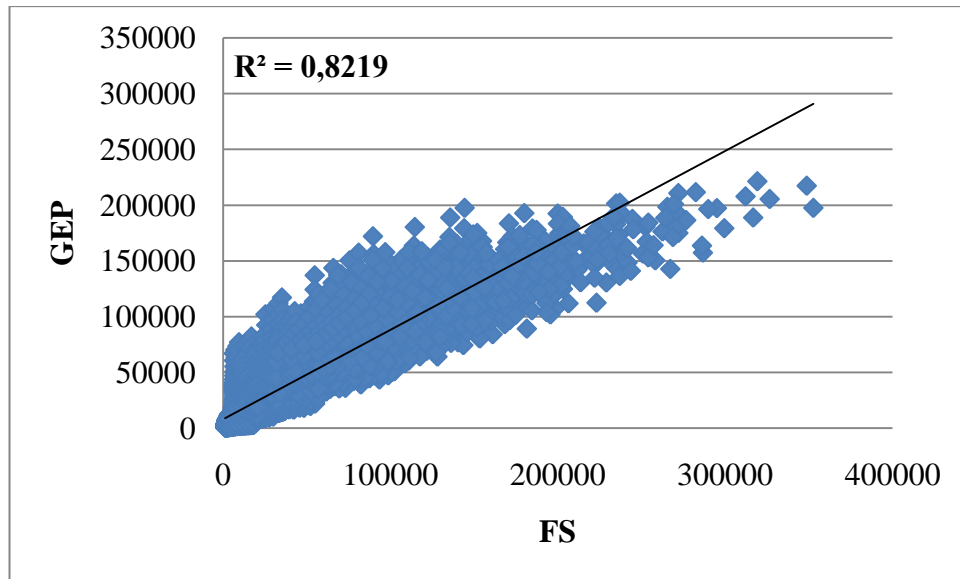


Figure 6.11 GEP Model solutions versus FS solutions and correlations for total set

6.4.2 Performance and Reliability of Neural Network Model

The optimal NN architecture was found to be 6–10–1 NN architecture with tan–sigmoid transfer function (tansig) and log–sigmoid transfer function given in Figure 6.12 with NNBEST program by trial and error approach. The training algorithm was Levenberg–Marquardt back propagation (trainlm). Statistical parameters of test and training sets are presented in Table 6.4. The performance of the proposed NN model versus FS results is shown in Figures 6.13–6.15. As it can be seen from Table 6.4, the performances of the proposed NN model is quite high which indicates the accuracy of the NN model to map the relationship between input and output variables. It should be noted that the proposed NN model is valid for ranges of variables given in Table 6.1.

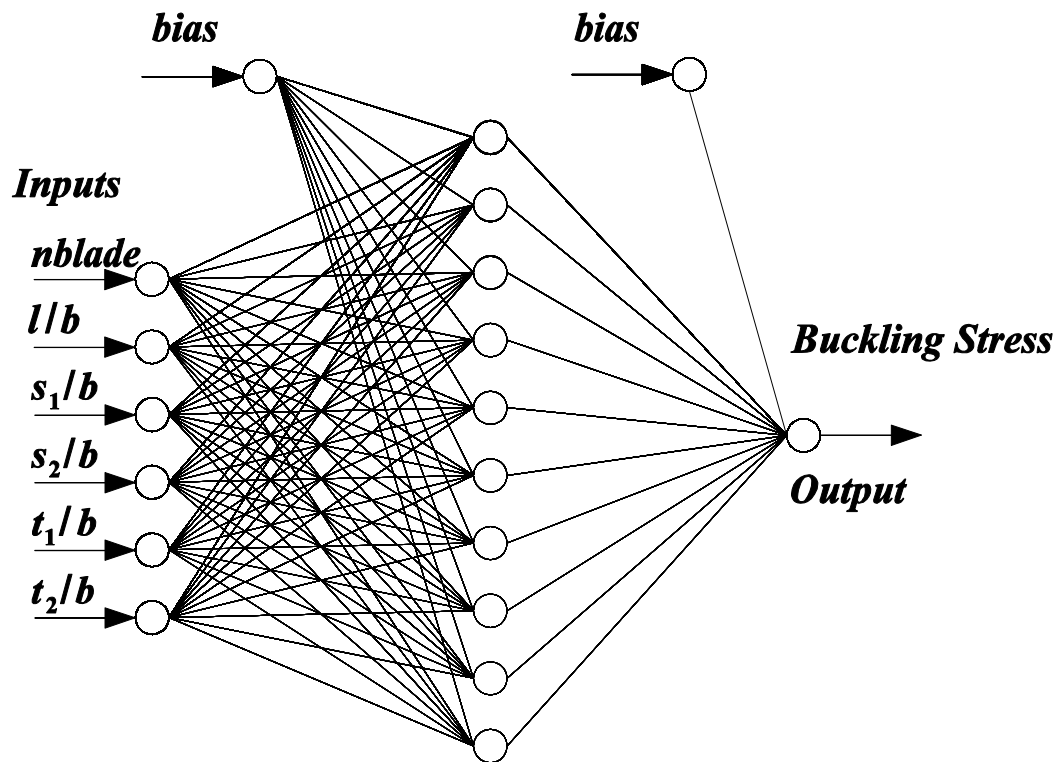


Figure 6.12 Proposed NN architecture for buckling analysis

Table 6.4 Comparison of test, training and total sets for NN for buckling analyses

	Test Set	Training Set	Total set
Mean (NN/FS)	1.0242	1.0251	1.0121
Standard deviation (NN/FS)	0.2092	0.2156	0.2106
RMSE	4049.32	3679.85	3979.18
Covariance	0.2042	0.2103	0.2079
Correlation coefficient (R^2)	0.9880	0.9900	0.9880

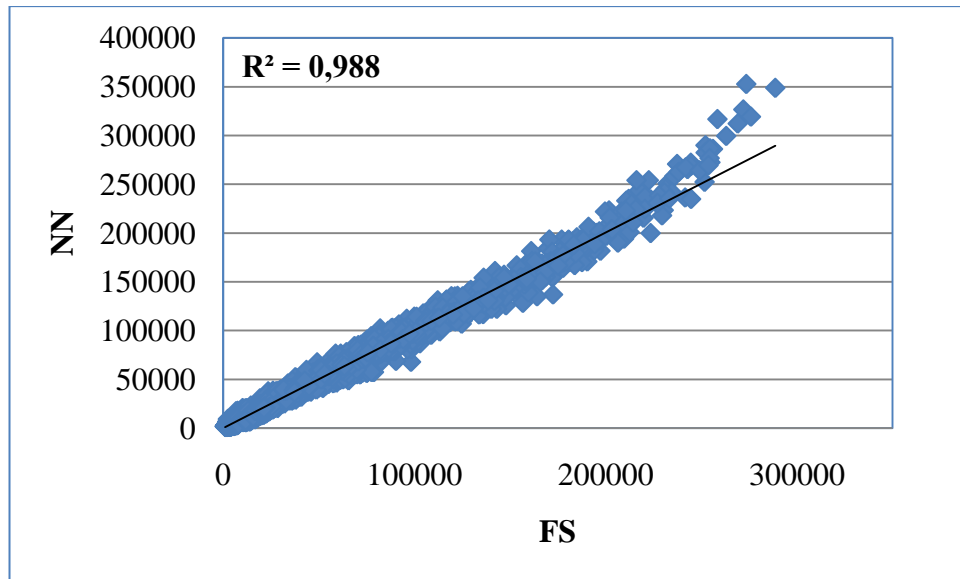


Figure 6.13 NN Model solutions versus FS solutions and correlations for test set.

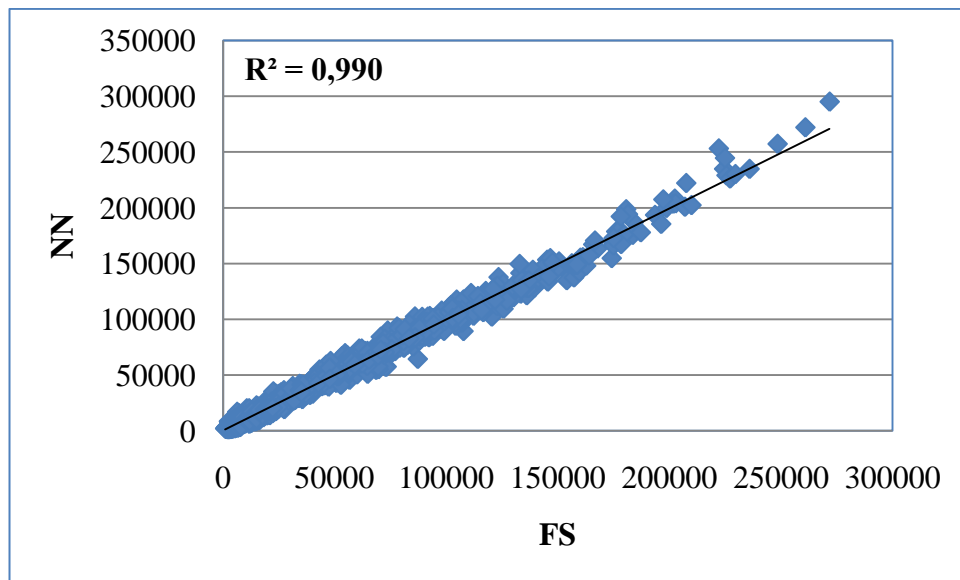


Figure 6.14 NN Model solutions versus FS solutions and correlations for train set

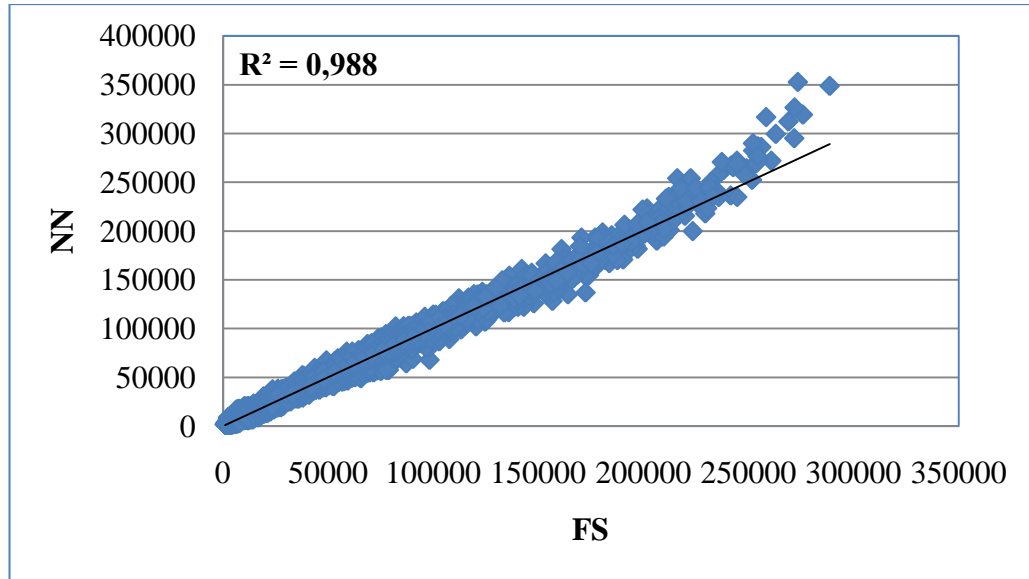


Figure 6.15 NN Model solutions versus FS solutions and correlations for total set

The proposed NN model in this study can also be given in explicit for as a mathematical equation using parameters of the NN model. The NN model can be simply given in a matrix form as follows where the first matrix of (6.4) is the weight matrix for the input layer and the second one added corresponds to the biases for the first hidden layer.

$$\begin{bmatrix} -0.3144 & -1.869 & 4.2033 & 52.5591 & -491.8541 & 39.7125 \\ -0.4136 & -0.263 & 0.2334 & 7.2173 & -16.9382 & 14.6314 \\ -0.3463 & -0.1725 & -5.0872 & 3.9451 & -53.7731 & 8.0766 \\ 0.2545 & -1.2006 & 8.3593 & 21.7969 & -77.0355 & 53.1702 \\ -0.073 & 0.0265 & -9.0083 & 0.2895 & -26.3989 & -4.0512 \\ -0.0133 & -0.2597 & 3.0985 & 1.1375 & -124.9477 & 505.436 \\ -0.2405 & -0.013 & -5.6963 & -0.4866 & -35.403 & -0.8994 \\ -0.021 & 0.6433 & -0.0219 & -273.1465 & 40.0307 & -28.0294 \\ -0,2610 & 1,2201 & -9,5637 & -21,4957 & 90,0044 & -51,9011 \\ -0,4400 & -2,2318 & 5,9429 & 62,2485 & -581,3790 & 38,5513 \end{bmatrix} \begin{bmatrix} n_b \\ L \\ b \\ s_1 \\ b \\ s_2 \\ b \\ t_1 \\ b \\ t_2 \\ b \end{bmatrix} + \begin{bmatrix} 0.6795 \\ -0.6397 \\ 2.0928 \\ -2.6714 \\ 1.3569 \\ -1.1002 \\ 1.6379 \\ 9.4438 \\ 2.7954 \\ 0.9322 \end{bmatrix} = \begin{bmatrix} U_1 \\ U_2 \\ U_3 \\ U_4 \\ U_5 \\ U_6 \\ U_7 \\ U_8 \\ U_9 \\ U_{10} \end{bmatrix} \quad (6.4)$$

The calculation for the second hidden layer can be shown as:

$$W = \begin{bmatrix} -4.9274 \\ -10.0449 \\ 8.9473 \\ 10.7818 \\ 3.8275 \\ 0.2168 \\ -13.5502 \\ -0.5783 \\ 10.0795 \\ 3.4914 \end{bmatrix}^T \begin{bmatrix} \tanh U_1 \\ \tanh U_2 \\ \tanh U_3 \\ \tanh U_4 \\ \tanh U_5 \\ \tanh U_6 \\ \tanh U_7 \\ \tanh U_8 \\ \tanh U_9 \\ \tanh U_{10} \end{bmatrix} - 14.3845 \quad (6.5)$$

Finally the output σ_{buck} can be computed as follows,

$$\sigma_{buck} = 352742 \left(\frac{1}{1+e^{-W}} \right) \quad (6.6)$$

6.5 Free Vibration Sensitivity Analysis of FS Results (Main effect plots)

Main effect plots for FS analyses are composed by using 14080 data pairs. Interaction of eigenvalues against all design variables are shown in Figure 6.16. All sampling points shown in figures are mean of the eigenvalues. Effect of the n_b is shown in Figures 6.17–6.20.

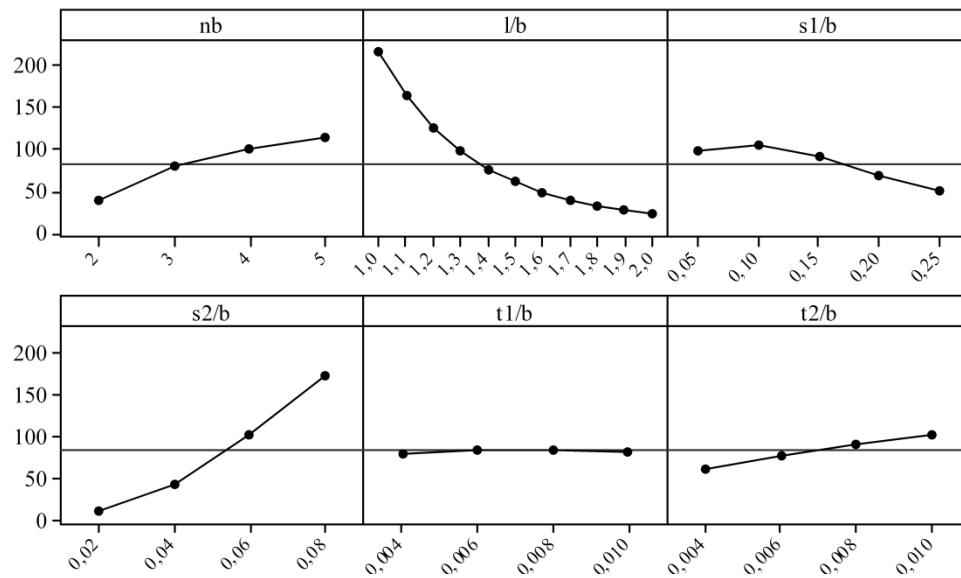


Figure 6.16 Main effect plots of FS.

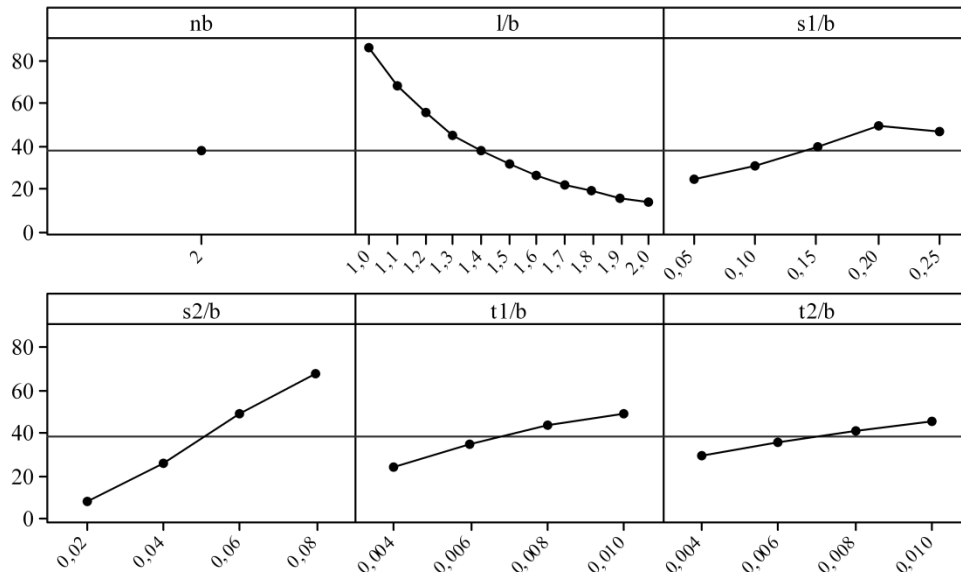


Figure 6.17 Main effect plots of FS for case $n_{blade}=2$

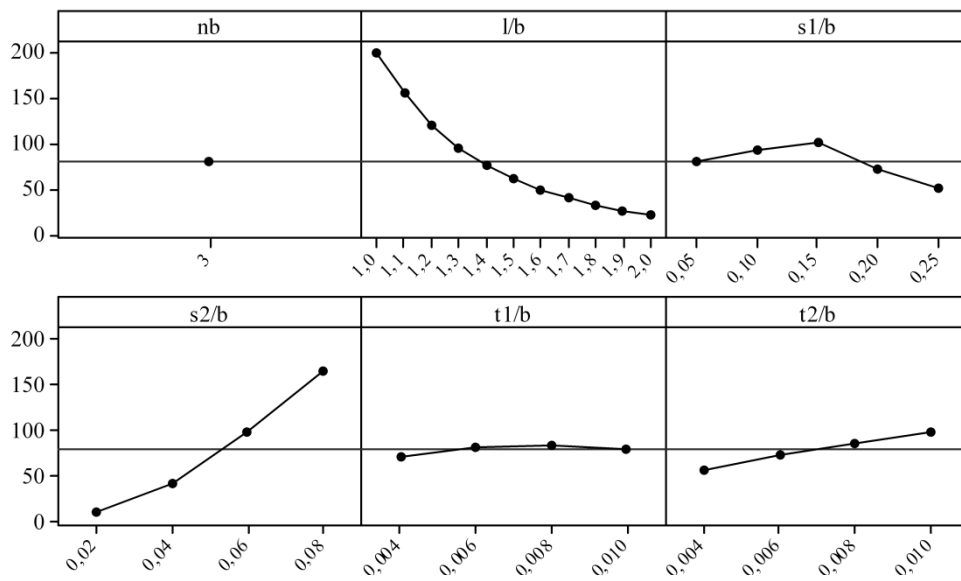


Figure 6.18 Main effect plots of FS for case $n_{blade}=3$

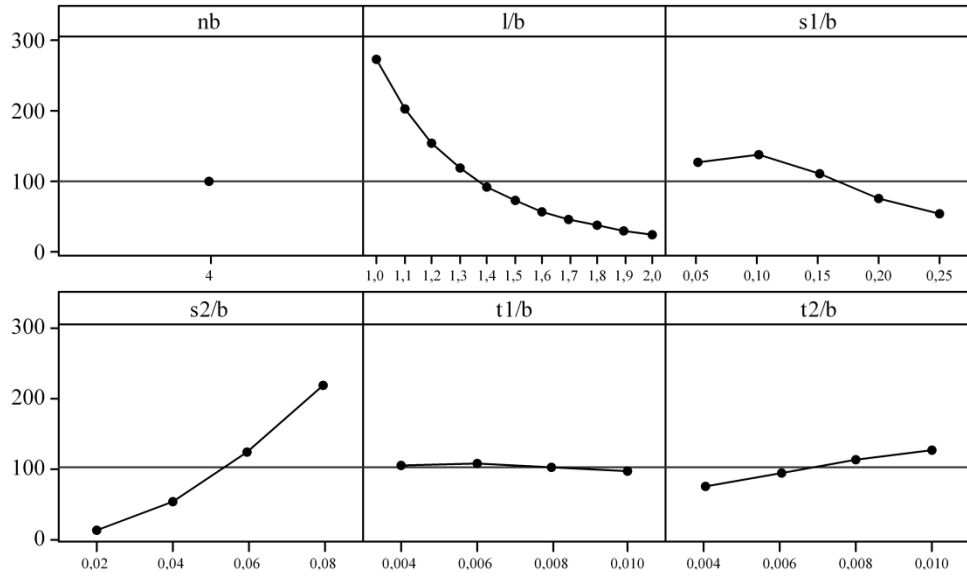


Figure 6.19 Main effect plots of FS for case $n_{blade}=4$

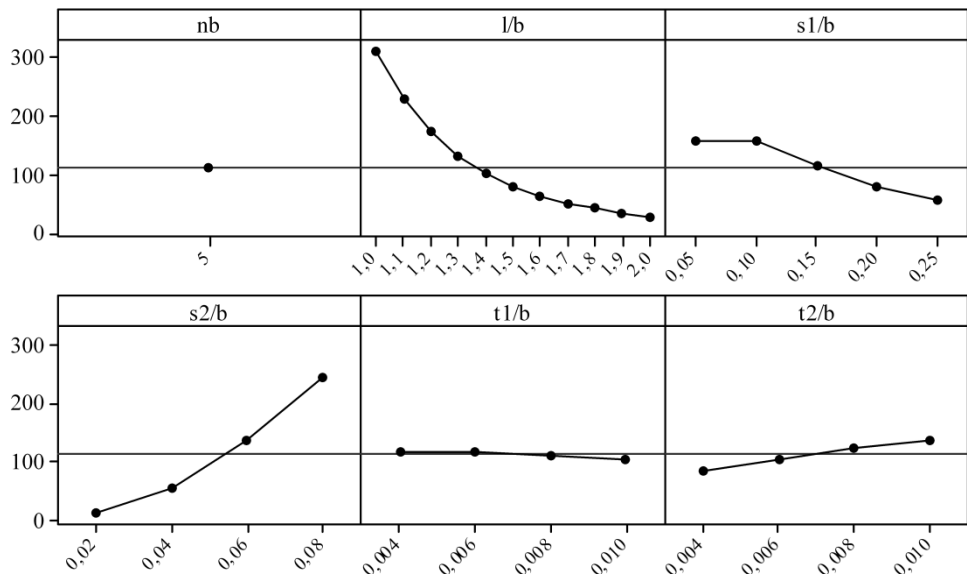


Figure 6.20 Main effect plots of FS for case $n_{blade}=5$

6.6 Free Vibration Numerical Applications of Soft Computing Techniques

Performance and reliability of GEP Model and NN Model are done separately for free vibration analysis of stiffened panel.

6.6.1 Performance and Reliability of GEP Model

The main aim in this method is to obtain the explicit formulation of dynamic analysis of stiffened panels as a function of geometric properties given as follows:

$$F_{\omega^2} = (n_b, l/b, s_1/b, s_2/b, t_1/b, t_2/b) \quad (6.7)$$

GEP model training parameters are given in Table 6.5. According to this parameters obtained ET shown in Figure 6.21. Mathematical representation of ET as follows,

$$\omega^2 = \left(\left(\frac{d(4) * d(1)}{d(2)} \right) * (d(5) + d(1)) \right) * \left(\frac{d(4)}{d(1)} + \frac{d(6)}{d(2)} \right) * \left((G3C0^3) - G3C1 \right) * \left(G3C0 + d(4) \right) * \left((G4C1 - d(3)) - (d(2) + d(3)) \right)^3 \quad (6.8)$$

where the constants are in formulation $G3C0=5.9023$, $G3C1=-8.1304$ and $G4C1=3.5483$. The actual parameters are $d(1)=n_b$, $d(2)=l/b$, $d(3)=s_1/b$, $d(4)=s_2/b$, $d(5)=t_1/b$ and $d(6)=t_2/b$. After putting in the corresponding values and rearranges the (6.8), final equation becomes,

$$\omega^2 = \frac{1}{\frac{l}{b}} \times \left(213.7480 \times n_b \left(3.5483 - \frac{l}{b} - \left(2 \times \frac{s_1}{b} \right) \right)^3 \times \frac{s_2}{b} \times \left(5.9023 \times \frac{s_2}{b} \right) \times \left(\frac{l}{b} + \frac{t_1}{b} \right) \times \left(\frac{\frac{s_2}{b}}{n_b} + \frac{\frac{t_2}{b}}{l/b} \right) \right) \quad (6.9)$$

It should be noted that the proposed GEP formulation is valid for the ranges of the training set given in Table 6.1. Comparison of test, train and total sets of GEP model are presented in Table 6.6. The GEP model results versus FS results for test, train and total sets are shown in Figures 6.22–6.24.

Table 6.5 Parameters of GEP model

P1	Function set	+, -, *, /
P2	Chromosomes	30
P3	Head Size	4
P4	Number of genes	4
P5	Linking function	Multiplication
P6	Fitness function, error type	Custom, MAE(Mean Abs. Error)
P7	Mutation rate	0.044
P8	Inversion rate	0.1
P9	One-point combination rate	0.3
P10	Two-point combination rate	0.3
P11	Gene recombination rate	0.1
P12	Gene transposition rate	0.1

Table 6.6 Comparison of test, training and total sets GEP

	Test Set	Training Set	Total set
Mean (GEP/FS)	1.5000	1.0086	1.1126
Standard deviation (GEP/FS)	0.6168	0.4836	0.6931
RMSE	63.4930	49.6701	50.4947
Covariance	0.4111	0.4795	0.6229
Correlation coefficient (R^2)	0.8413	0.8422	0.8414

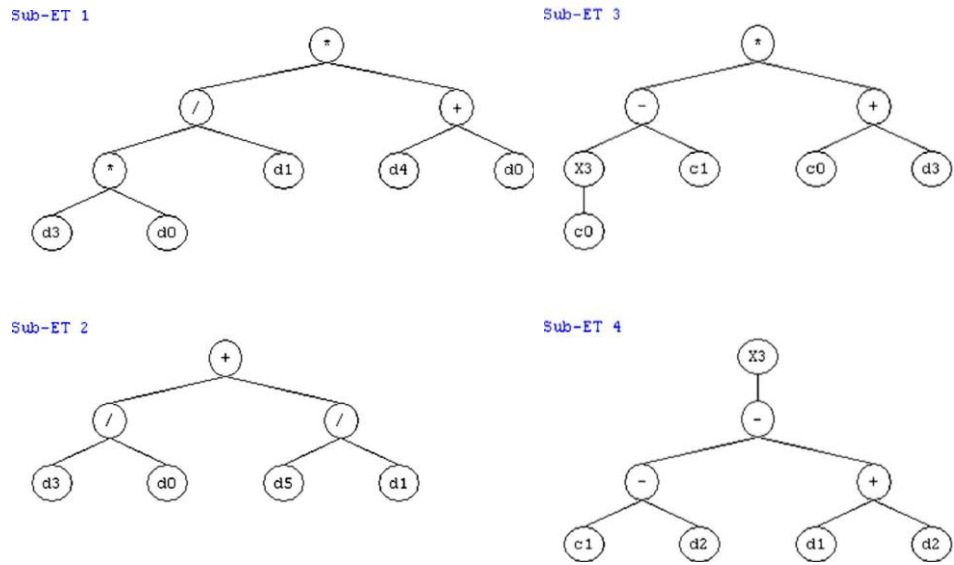


Figure 6.21 Expression tree for proposed GEP model

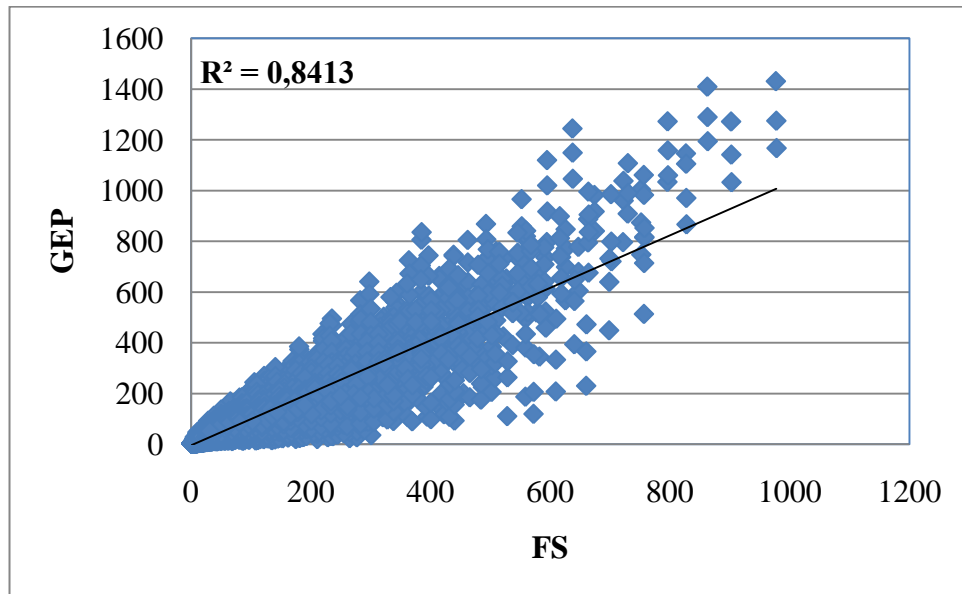


Figure 6.22 GEP Model solutions versus FS solutions and correlations for test set.

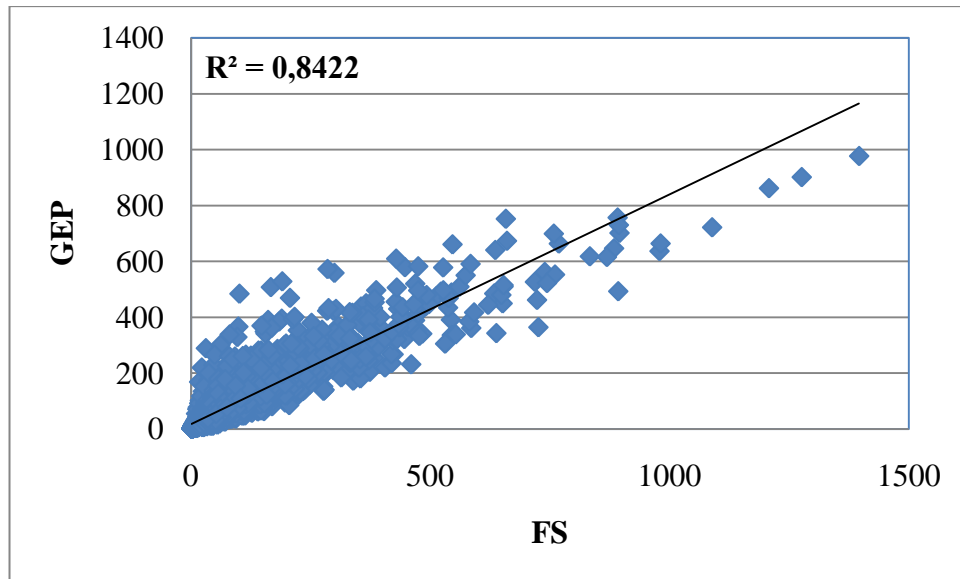


Figure 6.23 GEP Model solutions versus FS solutions and correlations for train set

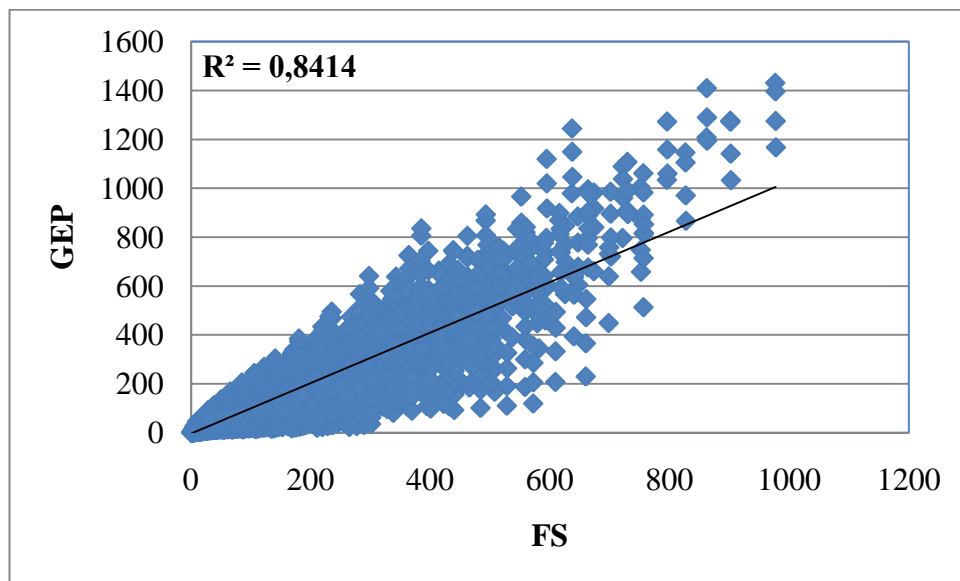


Figure 6.24 GEP Model solutions versus FS solutions and correlations for total set

6.6.2 Performance and Reliability of Neural Network Model

The optimal NN architecture was found to be 6–6–1 NN architecture with tan–sigmoid transfer function (tansig) and log–sigmoid transfer function given in Figure 6.25 with NNBEST program by trial and error approach. The training algorithm was Levenberg–Marquardt back propagation (trainlm). Statistical parameters of test and training sets are presented in Table 6.7. The performance of the proposed NN model

versus FS results is shown in Figures 6.26–6.28. As it can be seen from Tables 6.7, the performances of the proposed NN model is quite high which indicates the accuracy of the NN model to map the relationship between input and output variables. It should be noted that the proposed NN model is valid for ranges of variables given in Table 6.1.

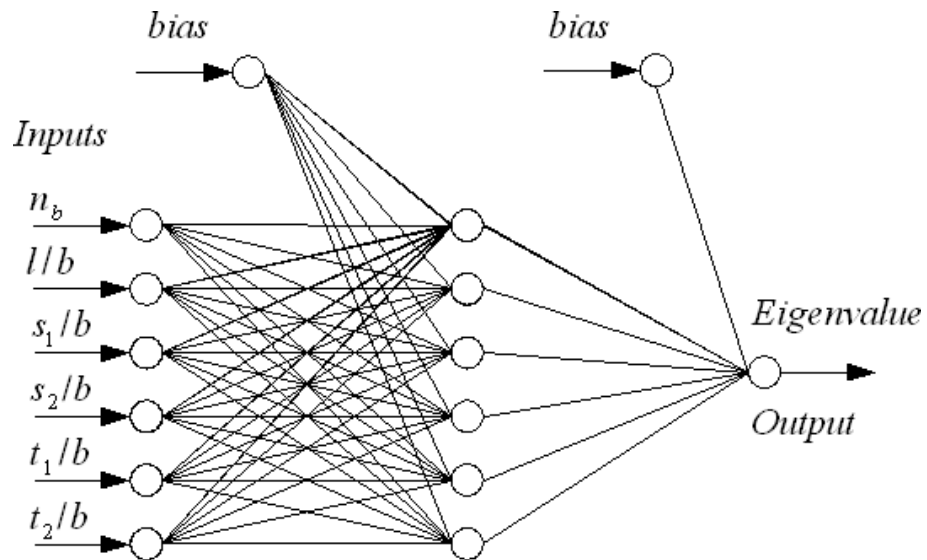


Figure 6.25 Proposed NN architecture for free vibration analysis

Table 6.7 Statistical parameters of test, training and total sets for NN for free vibration analysis

	Test Set	Training Set	Total set
Mean (NN/FS)	1.0043	1.0042	1.0042
Standard deviation (NN/FS)	0.1761	0.1735	0.1741
RMSE	30.5187	30.2620	30.3133
Covariance	0.1754	0.1728	0.1733
Correlation coefficient (R^2)	0.9868	0.9870	0.9868

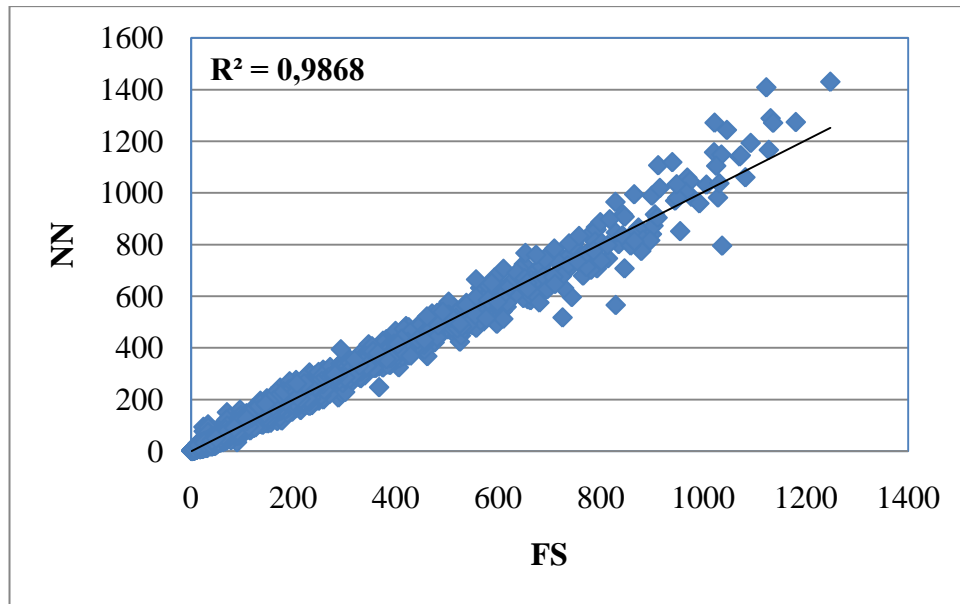


Figure 6.26 NN Model solutions versus FS solutions and correlations for test set

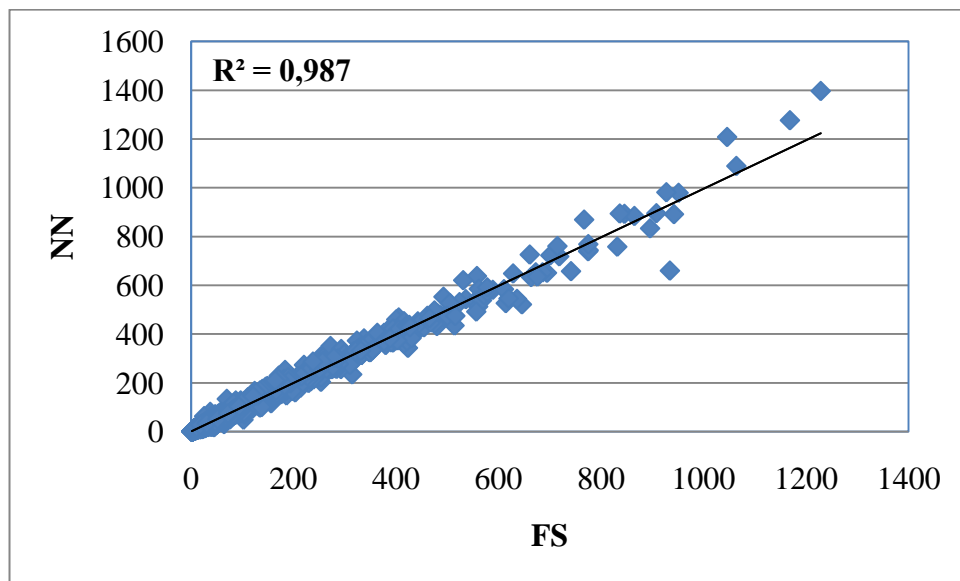


Figure 6.27 NN Model solutions versus FS solutions and correlations for train set

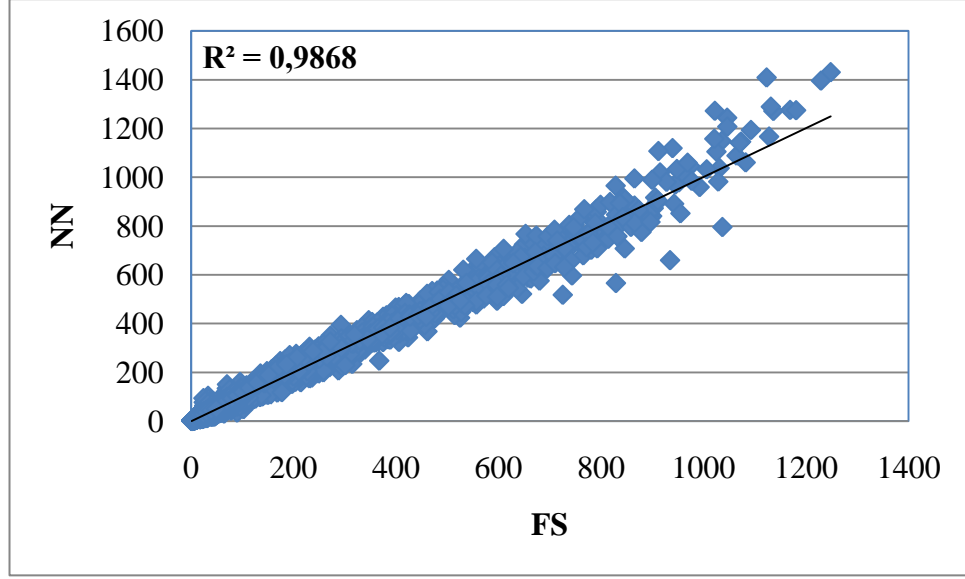


Figure 6.28 NN Model solutions versus FS solutions and correlations for total set

The proposed NN model in this study can also be given in explicit form as a mathematical equation using parameters of the NN model. The NN model can be simply given in a matrix form as follows where the first matrix of (6.10) is the weight matrix for the input layer and the second one added corresponds to the biases for the first hidden layer.

$$\begin{bmatrix} -1.1772 & 0.0589 & -0.1712 & -0.0527 & -1.1031 & 0.1661 \\ -1.9345 & -0.6475 & 0.7697 & 1.5947 & 5.4300 & -0.4586 \\ -7.2468 & 1.3742 & -9.1635 & 2.3311 & -0.0454 & 9.3354 \\ 30.7648 & 28.8815 & -13.2412 & -10.9098 & -22.9642 & 9.3698 \\ -224.4984 & -7.0292 & 137.0303 & -16.8929 & 130.6543 & -117.1694 \\ 40.8026 & 16.2645 & -18.2667 & -36.5506 & -361.3202 & 6.6624 \end{bmatrix} \begin{bmatrix} \frac{L}{b} \\ \frac{s_1}{b} \\ \frac{s_2}{b} \\ \frac{t_1}{b} \\ \frac{t_2}{b} \end{bmatrix} + \begin{bmatrix} 4.3248 \\ -0.0791 \\ 1.1104 \\ 0.7537 \\ -2.2970 \\ -1.4900 \end{bmatrix} = \begin{bmatrix} U_1 \\ U_2 \\ U_3 \\ U_4 \\ U_5 \\ U_6 \end{bmatrix} \quad (6.10)$$

The calculation for the second hidden layer can be shown as:

$$W = \begin{bmatrix} -1.8398 \\ 2.4152 \\ -5.2747 \\ -9.1423 \\ -0.2235 \\ -5.6979 \end{bmatrix}^T \begin{bmatrix} \tanh U_1 \\ \tanh U_2 \\ \tanh U_3 \\ \tanh U_4 \\ \tanh U_5 \\ \tanh U_6 \end{bmatrix} + 1.7765 \quad (6.11)$$

Finally the output σ_{buck} can be computed as follows,

$$\omega^2 = 1430.8 \left(\frac{1}{1+e^{-W}} \right) \quad (6.12)$$

CHAPTER 7

CONCLUSION

7.1 Summary of Achievements

In this work, computational tools have been developed for reliable, accurate and efficient SC tools for the analysis and design of structures. Five main computer programs have been developed and verified for analysis and optimization. BUCKFS deals with the buckling FS analysis and shape optimization of shells. VIBFS deals with the free vibration analysis and shape optimization of shells. These programs are modified in Fortran90 using double precision based on Özakça and co workers program [1]. SCGEN deals with SC generation of data sets for models. It was also written in FORTRAN90. It is an interface of BUCKFS and VIBFS programs to NNBEST and GeneXpro which is produced by Gepsoft. NNBEST deals with determination of best NN architecture by trial and error approach and genetic algorithms. SCOPT deals with optimization of SC models by mathematical programming and genetic algorithms. NNBEST and SCOPT were written on MATLAB computing environment.

7.2 General Conclusions

Throughout this thesis, detailed conclusions were given after each example; therefore the main conclusions are drawn from various aspects and summarized in the following sections.

7.2.1 Structural analysis

An existing FS code for the linear elastic analysis of stiffened panel structures was upgraded to FORTRAN 90 and automatic geometry modelling was implemented by adding new subroutines for buckling and free vibration analysis. Most of the results obtained using FSs was compared well with the results of other researchers based on different formulations. The results illustrate that the FS method presented here can be used with confidence for buckling or the free vibration analysis of prismatic structures.

7.2.2 Structural shape optimization

A general methodology for SSO of stiffened panel structures has been presented by integrating the tools developed for shape definition, automatic mesh generation and FS analysis with SQP (mathematical programming technique).

Various optimization examples were presented, maximizing critical buckling load, maximizing fundamental frequency and minimizing the weight of the structures. Thickness, widths and shape design variables were used. The influence of the number of design variable employed was also investigated. Some of the optimal shapes obtained are not practical and are included to illustrate the optimization method. However, introducing certain constraints can lead to practical solutions.

If the optimization of all stiffened plates results is glanced, it is obviously seen that in all plate types the maximum buckling load is obtained from shape optimization (type two) of eight stiffeners case. Due to this result, it can be mentioned that lengths of elements are important for buckling fails as much as element thicknesses.

In optimized plates maximum critical buckling load is obtained from straight stiffened plate with substiffeners and pads under stiffeners. The most crucial result that obtained from optimizations is the effect of the pad elements. Plates with pads and without pads have remarkable difference of buckling loads. From this consequence, it is unquestionable that pad elements are the most effective ones against buckling.

The obtained maximum load difference between straight and L shaped stiffened plates is also originated from the difference of effect of flanges and pads. In L shaped stiffened plates, flanges use somewhat volume from pads and plate skin. Therefore, the effective elements, against buckling failure become thinner. So the L shaped stiffened plates' maximum buckling load cannot reach the straights'.

Nevertheless, in plate types without pads, L shaped stiffened plates have larger critical buckling load values. This result emphasizes the effect of the flange elements.

It is necessary to mention about effect of substiffener elements finally. Plates with substiffeners have a little difference of buckling load when compared only straight stiffener case. Thus, it is understood that flange elements are more effective than substiffener elements so that substiffeners use volume from flanges and skin then critical buckling load decreases. In straight stiffened plate because of absence of flanges, substiffeners become effective and strengthen stability of plates slightly.

7.2.3 Soft computing

The efficiency of SC techniques in structural design, particular algorithms based on NN, GEP, solving large-scale, continuous or discrete structural design problems was studied.

The algorithms were studied both in deterministic and reliability based structural design problems. An effort to increase the computational efficiency is as well as the robustness of the design procedure. The use of SC techniques is motivated by the time-consuming repeated FS analysis required during the optimization process. Trained SC techniques were used to perform either the deterministic constraints check or, in the case of reliability based design, both the deterministic and the probabilistic constraints checks. The suitability of the SC techniques predictions was investigated in a number of structural design problems in order to demonstrate the computational advantages of the proposed methodologies.

In this work, some conclusions related with SC can be summarized:

- SC methods such as NNs, GP were effectively used for computation of buckling strength and dynamic characteristics of stiffened panels.
- The testing set is taken as 85% and the training set as 15% of the total set. In general the procedure accepted in SC modeling is the reverse case where the test set is about 20–30% and the training set is about 70–80% of the total set. By choosing a large testing set, for showing the high generalization capability of the models.
- All SC models used in this study are presented in explicit form NN and GEP models. The most accurate results are obtained by NN model rather than GEP.
- SC methods such as NNs, GP can be effectively used for dynamic analyses of stiffened panels.
- NN model in this study is quite complex models that cannot be used for daily pre-modeling calculations. Most suitable model for pre-modeling calculations is GEP model but it is quite accuracy loss between other models.
- NNs are treated as black box in general. This thesis does not only verify NNs as alternative robust tools for stiffened panel analyses but gives the solution in an explicit form of the proposed NN models as well. It aims to open the black box and to present the NN models in its implicit form. It should be noted that explicit formulation of NN models is of significant importance as it will serve for important advantages in the analysis and design of structures. This will also enable to open a new era in optimization analysis of structures.
- One of the major tasks in NN studies which are quite difficult is the selection of optimum NN architecture which is based on trial and error approaches or GA. However, this thesis proposes an alternative algorithm for the selection of optimum NN architecture that automatically selects the best architecture.
- The optimum learning algorithm for modeling of stiffened panels was found to trainlm (Marquardt–Levenberg). Another learning algorithm trainlm also gave satisfactory results where as trainlm algorithm should be used with a definite reserve. The optimum error learning algorithm was found to be SSE. It is impossible to define an optimum NN architecture but it can be concluded

that single hidden layer architecture with less than 20 nodes is enough in general for the optimum NN architecture.

Suggestion for Further Work

Some suggestions for further work are listed as follows:

- By integrating a standard CAD system to the programs developed, a wider range of optimization problems could be solved.
- In FS method two opposite edges are simply supported and other two sides can be defined in any boundary condition. Some modifications can be made to apply any boundary conditions.
- In this thesis straight and L shaped stiffened plates are investigated. Nevertheless, some other types of stiffeners exist in practice. Some of them are T shaped, U shaped tube, Y shaped stiffeners and etc..
- Although currently computer processing power is growing exponentially, the option of parallel progressing during GA optimization should be used when considering large three dimensional problems.
- The use of multi-objective functions should be investigated.
- The use of different discrete optimization methods such as the evolution method would be useful to check the optimum results obtained with the GAs.
- It is obvious that artificial intelligence techniques or specifically SC approaches such as fuzzy logic, Neuro Fuzzy, and step wise regression Programming will have much more profound application areas in the future for structural mechanics and structural analysis problems.
- The proposed models in this work can also be used in inverse engineering analysis as well.
- For elastoplastic analysis of structures to an extent, no general study has been carried out covering a wide range of elastoplastic behavior of structures by SC techniques.
- A new approach so called neuro-optimization can offer many advantages and open a new era in optimization studies.
- The SC techniques could be applied to the optimization of composite structures.

REFERENCES

- [1] Hinton, E., Sienz, J. and Özakça, M. (2003). Analysis and optimization of prismatic and axisymmetric shell structures — theory, practice and software. London: Springer–Verlag.
- [2] Tayşi, N., Göğüş, M.T. and Ekmekyapar, T. (2009). Takviyeli Panellerin Burkulmaya Karşı Optimum Tasarımı. TÜBİTAK, Project Grand No:107M648.
- [3] Cheung, Y. K., (1968). The finite strip method in the analysis of elastic plates with two opposite simply supported ends, *Proc. Inst. Civ. Eng.*
- [4] Dawe, D. J. (1977). Finite strip buckling analysis of curved plate assemblies under biaxial loading, *Solids Structures*, **13**, 1141–1155.
- [5] Dawe, D. J. and Roufaeil, O. L. (1982). Buckling of rectangular Mindlin plates, *Computers and Structures*, **15**, 1249–1266.
- [6] Dawe, D. J. and Craig, T. J. (1988). Buckling and vibration of shear deformable prismatic plate structures by complex finite strip methods, *International Journal of Mechanical. Science*, **30 (2)**, 77–99.
- [7] Peshkam, V. and Dawe, D. J. (1989). Buckling and vibration of finite–length composite prismatic plate structures with diaphragm ends, Part I: Finite strip formulation, *Computer Methods for Applied Mechanic and Engineering*, **77**, 1–30.
- [8] Peshkam, V. and Dawe, D. J. (1989). Buckling and vibration of finite–length composite prismatic plate structures with diaphragm ends, Part II: Computer programs and buckling applications, *Computer Methods for Applied Mechanic and Engineering.*, **77**, 227–252.
- [9] Dawe, D. J. and Peshkam, V. (1990). Buckling and vibration of long plate structures by complex finite strip methods, *International Journal of Mechanical Science*, **32(9)**, 743–766.
- [10] Dawe, D. J., Lam S. S. E. and Azizian, Z. G., (1993). Finite strip post–local buckling analysis of composite prismatic plate structures, *Computers and Structures*, **48(6)**, 1011–1023.

- [11] Wang, S. and Dawe, D. J. (1996). Finite strip large deflection and post–overall–buckling analysis of diaphragm–supported plate structures, *Computers and Structures*, **61(1)**, 155–170.
- [12] Benson, P. and Hinton, E. (1976). A thick finite strip solution for static, free vibration and stability problems, *Journal of Numerical Methods in Engineering*. **10**, 665–678.
- [13] Hinton, E., Özakça, M. and Rao, N. V. R., (1995). Free vibration analysis and shape optimization of variable thickness prismatic folded plates and curved shells–Part I : Finite strip formulation, *Journal of Sound and Vibration*, **181(4)**, 553–566.
- [14] Özakça, M., Hinton, E. and Rao, N. V. R. (1994). Free vibration analysis and shape optimization of variable thickness prismatic folded plates and shells with curved planform, *Journal of Numerical Methods in Engineering*, **37**, 1713–1739.
- [15] Hinton, E. and Rao, N. V. R. (1994). Structural shape optimization of shells and folded plates using two noded finite strips, *Computers and Structures*, **46**, 1055–1071.
- [16] Hinton, E. and Rao, N. V. R. (1993). Analysis and shape optimization of variable thickness prismatic folded plates and curved shells. Part II: Shape optimization, *Thin Walled Structures*, **17**, 161–183.
- [17] Hinton, E., Petrinic, N. and Özakça, M. (1993). Buckling analysis and shape optimization of variable thickness prismatic folded plates. Part I: Finite strip formulation, *Engineering Computations*, **10**, 483–498.
- [18] Özakca, M., Tayşi, N. and Kolcu, F. (2003). Buckling optimization of variable thickness prismatic folded plates *Thin–Walled Structures*, **41(8)**, 711–730.
- [19] Xie, W.C. and Ibrahim, A. (2000). Buckling mode localization in rib–stiffened plates with misplaced stiffeners – a finite strip approach. *Chaos, Solitons and Fractals* **11** 1543–1558.
- [20] Bui, H.C. (2009). Buckling analysis of thin–walled sections under general loading conditions. *Thin–Walled Structures*, **47**, 730–739.
- [21] Bradford, M. A. and Azhari, M. (1995). Buckling of plates with different end conditions using the finite strip method. *Computers and Structures*, **56(1)**, 75–83.
- [22] Lilloco, M., Butler, R., Hunt, G.W. Watson, A. and Kennedy, D., (2003). Postbuckling of Stiffened Panels Using Strut, Strip and Finite Element Methods, *AIAA Journal*, **41(6)**, 1172–1180.

- [23] Riks, E. (2000). Buckling and post-buckling analysis of stiffened panels in wing box structures. *Int. Journal of Solids and Structures*, **20**, 6795–6824.
- [24] Kwon, Y. B. and Hancock, G. J. (1991). A non-linear elastic spline finite strip analysis for thin walled sections, *Thin Walled Structures*, **12**, 295–319.
- [25] Azhari, M., Hoshdar, S. and Bradford, MA. (2000). On the use of bubble functions in the local buckling analysis of plate structures by the spline finite strip method. *Computers and Structures* **48(4)**, 583–593.
- [26] Guo, YL., and Lindner, J. (1993). Analysis of elastic-plastic interaction buckling of stiffened panels by spline finite strip method. *Computers and Structures*, **46(3)**, 529–536.
- [27] Gabor, MV., (2009). Buckling and free vibration analysis of stiffened panels, *Thin-Walled Structures*, **47(4)**, 382–390.
- [28] Bisagni, C. and Vesconi, R. (2009). Analytical formulation for local buckling and post-buckling analysis of stiffened laminated panels. *Thin-Walled Structures*, **47(3)**, 348–334.
- [29] Barik, M. and Mukhopadhyay, M. (2002). A new stiffened plate element for the analysis of arbitrary plates. *Thin-Walled Structures*, **40**, 625–639.
- [30] Patel, S.N., Datta, P.K. and Seikh, A.H. (2006), Buckling and dynamic instability analysis of stiffened shell panels, *Thin-Walled Structures*, **44**, 321–333.
- [31] Liew, K. M., Zou, G. P. and Rajendran, S. (2003). A spline strip kernel particle method and its application to two-dimensional elasticity problems. *Int. J. Numer. Meth. Engng*; **57**, 599–616.
- [32] Xie, W.C. and Chen, R.Z.H. (2002). Vibration mode localization in rib-stiffened plates with misplaced stiffeners in one direction. *Chaos, Solitons and Fractals* **14** 311–333.
- [33] Yuan, W.X. and Dawe, D.J. (2004). Free vibration and stability analysis of stiffened sandwich plates. *Composite Structures*, **63**, 123–137.
- [34] Sheikh, A.H. and Mukhopadhyay, M. (1992). Analysis of stiffened plate with arbitrary planform by the general spline finite strip method. *Computers and Structures*, **42(1)**, 53–67.
- [35] Sheikh, A.H. and Mukhopadhyay, M. (2002). Linear and nonlinear transient vibration analysis of stiffened plate structures. *Finite Elements in Analysis and Design*, **38**, 477–502.

- [36] Arora, J.S. (1989). *Introduction to Optimum Design*, McGraw–Hill, Singapore,.
- [37] Vanderplaats, G.N. (1984). *Numerical Optimization Techniques for Engineering Design*, McGraw–Hill Inc., London.
- [38] Rao, S.S. (1996). *Engineering Optimization*, John Wiley and Sons, New York.
- [39] Zienkiewicz, O.C., and Campbell, J.S. (1973). *Shape Optimization and Sequential Linear Programming*, John Wiley, New York.
- [40] Svanberg, K. (1987). The Method of Moving Asymptotes—A New Method for Structural Optimization, *Int. J. Num. Meth. Engng.*, 23, 359–373,
- [41] Holland, J.H. (1975). *Adaptation in Natural and Artificial Systems*. The University of Michigan Press, Michigan.
- [42] Murphy A., Quinn D., Mawhinney P., Özakça M. and Veen S., (2006). Tailoring static strength performance of metallic stiffened panels by selective local sub–stiffening, *47th AIAA/ASME/ASCE/AHS/ASC Structures, Structural Dynamics and Material Conference, Newport–Rhode Island*.
- [43] Özakça M., Murphy A., and Veen A., (2006). Buckling and postbuckling of sub–stiffened or locally tailored aluminium panels, *25th International Congress of the Aeronautical Sciences*.
- [44] Kim, S.H. and Kim, G.H. (2008). Optimal design of composite stiffened panel with cohesive elements using micro–genetic algorithm. *Journal of Composite Materials*, 42; 2259–2273.
- [45] Bedair, O. and Troitsky, M.S. (1997). A study of the fundamental frequency characteristics of eccentrically and concentrically simply supported stiffened plates. *Int. J. Mech. Sci.*, 39, 1257– 1272.
- [46] Topping, B.H.V. and Bahreininejad, A. (1997). *Neural Computing For Structural Mechanics*, Saxe–Coburg Publications.
- [47] Yagawa C. and Okuda H. (1996), Neural networks in computational mechanics, *Arch.Comp. Meth. Eng.*, 4, 435–512
- [48] Zeng, P.(1998). Neural Computing in mechanics, *Appl. Mech. Rev.*,51(2) ,173–197
- [49] Waszczyszyn, Z. (1999). *Neural networks in the analysis and design of structures*. CISM Courses and Lectures no. 404. New York: Springer

- [50] Hajela, P., and Berke, L. (1991). Neurobiological computational modes in structural analysis and design, *Computers and Struct.*, **41(4)**, 657–667.
- [51] Ghaboussi, J., Garrett, J.H. and Wu, X. (1991). Knowledge-Based Modelling of Material Behaviour with Neural Networks. *Journal of Engineering Mechanics*, **117(1)**,132–153.
- [52] Masri, S. F., Chassiakos, A.G., and Caughey, T. K. (1993). Identification of nonlinear dynamics system using neural networks. *Appl.Mech.*, **60(1)**,123–133
- [53] Kang, H.–T. and Yoon, C.J. (1994). Neural network approaches to aid simple truss design problems. *Microcomputers in Civ. Engrg.*, **9(3)**, 211–218.
- [54] Adeli, H. and Park,H.S. (1995). Counterpropagation neural networks in structural engineering, *Journal of Structural Engineering*, **121(8)**, 1205–1212
- [55] Lu J.G., Zhou J and Wang H. (1994). Approach to structural approximation analysis by ANN, *Sci in China*, **37(8)**, 990–997
- [56] Bisagni, C. and Lanzi, L. (2002). Post-buckling optimisation of composite stiffened panels using neural Networks. *Composite Structures*, **58**, 237–247.
- [57] Lanzi, L. and Giavotto, V. (2006). Post-buckling optimization of composite stiffened panels: computations and experiments. *Composite Structures* **73**, 208–220.
- [58] Kicinger, R., Arciszewski, T. and De Jong, K. (2005). Evolutionary computation and structural design: A survey of the state-of-the-art. *Computers and Structures*, **83**, 1943–1978.
- [59] Iuspa, L. and Ruocco, E. (2008). Optimum topological design of simply supported composite stiffened panels via genetic algorithms. *Computers and Structures*, **86**, 1718–1737.
- [60] Wang, W., Guo, S., Chang, N. and Yang, W. (2010). Optimum buckling design of composite stiffened panels using ant colony algorithm. *Composite Structures*, **92**, 712–719
- [61] Zadeh LA., 1965. Fuzzy sets, *Information and Control*, vol. 8, no. 3, pp.338–353.
- [62] Gazdik, I. (1996). Zadeh extension principle in design reliability, *Fuzzy Sets and Systems*,**83**, 169–178.
- [63] Noor, A.K., Starnes Jr.,J.H. and Peters J.M. (2001). Uncertainty analysis of stiffened composite panels. *Composite Structures*, **51**, 139–158.

- [64] Ji, L., Mace, B.R. and Pinnington, R.J. (2004). A hybrid mode/Fourier–transform approach for estimating the vibrations of beam–stiffened plate systems. *Journal of Sound and Vibration*, **274** 547–565.
- [65] Ji, L., Mace, B.R. and Pinnington, R.J. (2005). A mode–based approach for the mid–frequency vibration analysis of coupled long– and short–wavelength structures. *Journal of Sound and Vibration*, **289(1–2)** 148–170.
- [66] Hinton, E. (1987). Numerical methods and software for dynamic analysis of plates and shells, Pineridge Press, Swansea, U.K.
- [67] Timoshenko, S. P. and Gere, J. M., (1961). *Theory of Elastic Stability 2/e*, McGraw–Hill.
- [68] Cheung, Y.K. and Tham, L.G. (1997). *The finite strip method*. CRC Press.
- [69] Brush, Don O. and Almroth, Bo O. (1975). *Buckling Analysis of Shells and Plate*, McGraw–Hill.
- [70] Bathe, K.J. (2000). *Finite Element Procedures*. New Jersey: Prentice Hall.
- [71] Stroud, W.J., Greene, W.H. and Anderson, M. S. (1984). Buckling loads of stiffened panels subject to longitudinal compression and shear: results obtained with PASCO, EAL, and STAGS computer programs, NASA, TP 2215.
- [72] Cheung, Y. K. and Cheung, M. S. (1972). Free vibration of curved and straight beam slab or boxgirder bridges. Publications, *J. IABSE*, **324**, 41–52.
- [73] Bushnell D. and Rankin C. (2005). Optimum Design of Stiffened Panels with Sub–Stiffeners, *46th AIAA Conference*, Austin–Texas.
- [74] Jadhav P. and Mantena P.R. (2007). Parametric Optimization of Grid–Stiffened Composite Panels for Maximizing Their Performance Under Transverse Loading, *Composite Structures*, **77**, 353–363.
- [75] Jarmai, K., Snyman, J.A. and Farkas, J. (2006). Minimum Cost Design of Welded Orthogonally Stiffened Cylindrical Shell, *Computers and Structures*, **84**, 787–797.
- [76] Kang J.H and Kim C.G. (2005). Minimum–Weight Design of Compressively Loaded Composite Plates and Stiffened Panels for Postbuckling Strength by Genetic Algorithm, *Composite Structures*, **69**, 239–246.
- [77] Chaturvedi, D.K. (2008). Soft computing techniques and its applications in electrical engineering. Springer–Verlag, Berlin, Heidelberg.

- [78] Jang, J–S.R., Sun, C–T.E. and Mizutani, E. (1997). *Neuro–fuzzy and soft computing: A computational approach to learning and machine intelligence*. Prentice–Hall, NJ.
- [79] Beale, R. and Jackson, T. (1990). *Neural computing: an introduction*. Taylor & Francis, New York.
- [80] Kasabov, K.N. (1996). *Foundations of Neural Networks, Fuzzy Systems, and Knowledge Engineering*, A Bradford Book The MIT Press Cambridge.
- [81] Tarassenko, L. (1998). *A guide to neural computing applications*. John Wiley & Sons Inc., New York.
- [82] Hecht–Nielsen, R. (1990). *Neurocomputing*, Addison–Wesley, Reading, MA.
- [83] Haykin, S. (1999). *Neural Networks: A Comprehensive Foundation*, 2nd ed. Englewood Cliffs, NJ: Prentice–Hall
- [84] Nigrin, A. (1993). *Neural Networks for Pattern Recognition*, Cambridge, The MIT Press.
- [85] Zurada, J.M. (1992), *Introduction to Artificial Neural Systems*, Boston:PWS Publishing Company.
- [86] Çevik, A. (2006). *A new approach for elastoplastic analysis of structures: neural networks*, PhD Thesis, University of Gaziantep, Turkey.
- [87] Guzelbey, İ.H., Çevik, A. and Göğüş, M.T. (2006). Prediction of rotation capacity of wide flange beams using neural networks. *Journal of Constructional Steel Research*, **62**, 950–961.
- [88] Howard Demuth, H., Beale, M. and Hagan, M. (2009). *Neural Network Toolbox User’s Guide*. Mathworks. Inc., Natick, MA.
- [89] www.comp.nus.edu.sg/~pris/ArtificialNeuralNetworks/BasicConcepts.htm
- [90] Rumelhart, D.E., Hinton, G.E. and Williams, R.J. (1986). Learning internal representation by error propagation parallel distributed processing: exploration in the microstructure of cognition, vol. 1. MIT Press, Cambridge, MA, C 8.
- [91] Zupan, J., Gasteiger, J. (1993). *Neural Networks for Chemists – An Introduction*; VCH: Weinheim,
- [92] Rutkowski L., (2004). *Flexible neuro–fuzzy systems: structures, learning and performance evaluation*, Kluwer Academic Publishers.

- [93] Sivanandam, S.N., Sumathi, S. and Deepa S.N., (2007) Introduction to Fuzzy Logic using MATLAB. Springer–Verlag, Berlin, Heidelberg.
- [94] Haris, J., (2006). *Fuzzy logic applications in engineering science*, Springer–Verlag, Berlin, Heidelberg.
- [95] Ying Bai, Y., Zhuang, H. and Wang, D., (2006). *Advanced fuzzy logic technologies in industrial applications*, Springer–Verlag, Berlin, Heidelberg.
- [96] Jain, L.C., Palade, V. and Srinivasan, D. (2007). *Advances in evolutionary computing for system design*. Springer–Verlag, Berlin, Heidelberg.
- [97] Goldberg, D.E. (1989). Genetic Algorithms in Search, Optimization and Machine Learning, Addison–Wesley, (1989).
- [98] Çevik, A (2007). A new formulation for web crippling strength of cold–formed steel sheeting using genetic programming. *Journal of Constructional Steel Research*, 63(7), 887–883.
- [99] Koza, J. R., (1992). Genetic programming: on the programming of computers by means of natural selection. MIT Press, Cambridge, MA.
- [100] Ferreira, C., (2006). Gene expression programming: mathematical modeling by an artificial intelligence. Springer–Verlag, Berlin, Heidelberg.
- [101] Ferreira, C., (2001). Gene Expression Programming in Problem Solving. Invited tutorial of the 6th Online World Conference on Soft Computing in Industrial Applications, September 10–24.
- [102] Ferreira C., (2001). Gene Expression Programming: A New Adaptive Algorithm for Solving Problems. *Complex Systems*, **13(2)**, 87–129.
- [103] www.gepsoft.com

APPENDIX A

INTERACTION PLOT FOR BUCKLING ANALYSIS OF STIFFENED PANELS

A.1 Introduction

Interaction plot for FS analysis results are scored by using 14080 data pairs. Interactions of parameters of buckling analysis against two design variables are shown in Figure A.1-15. Importance of interaction plots for design engineers is all parameters effects on buckling behavior panel can be investigated. All sampling points shown in figures are mean of the eigenvalues.

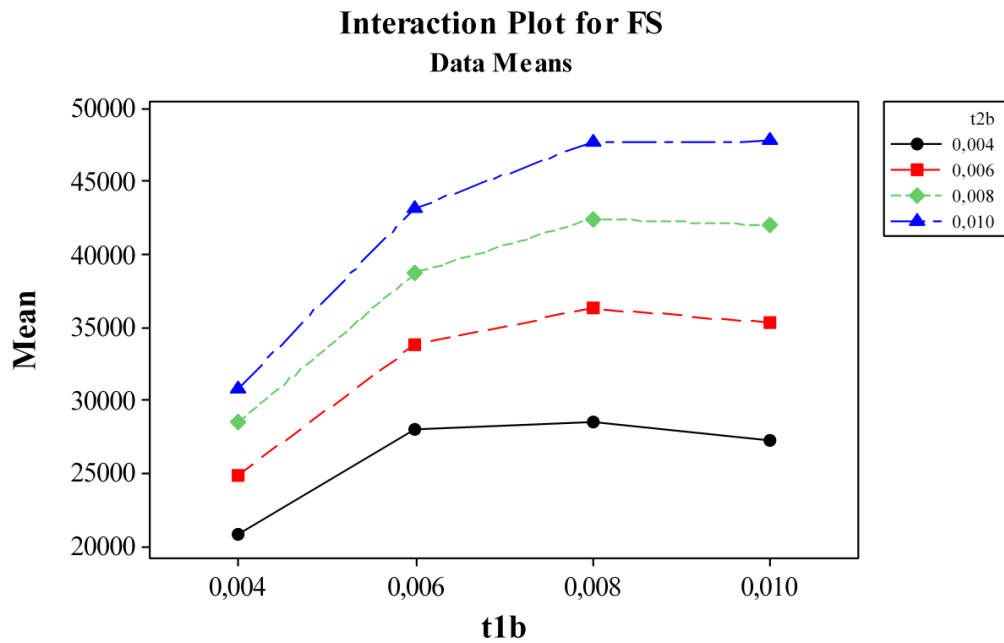


Figure A.1. Interaction plot for FS for t_1/b versus t_2/b

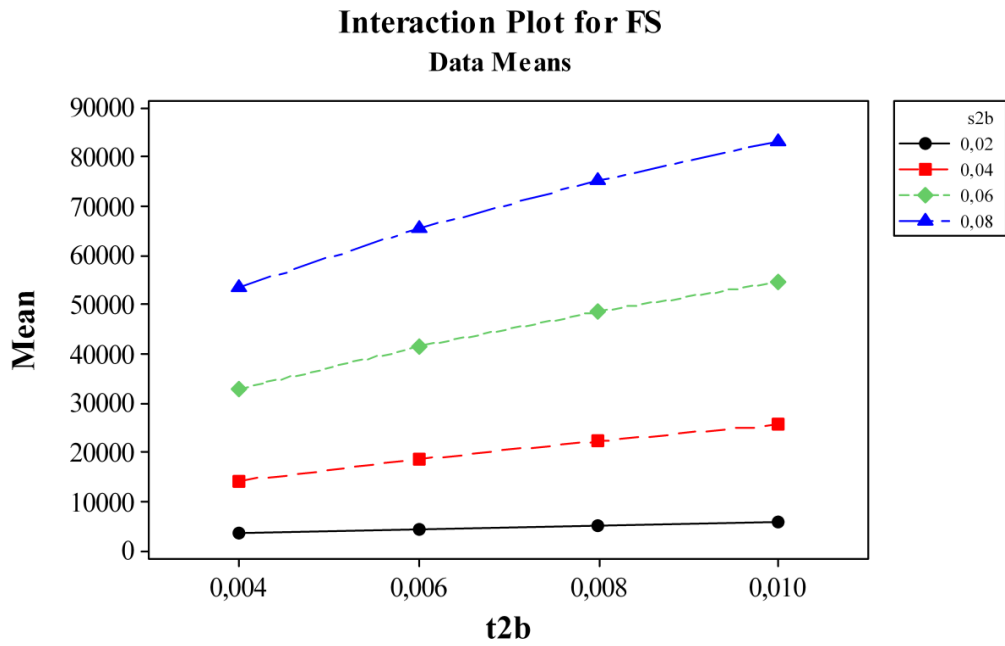


Figure A.2. Interaction plot for FS for t_2/b versus s_2/b

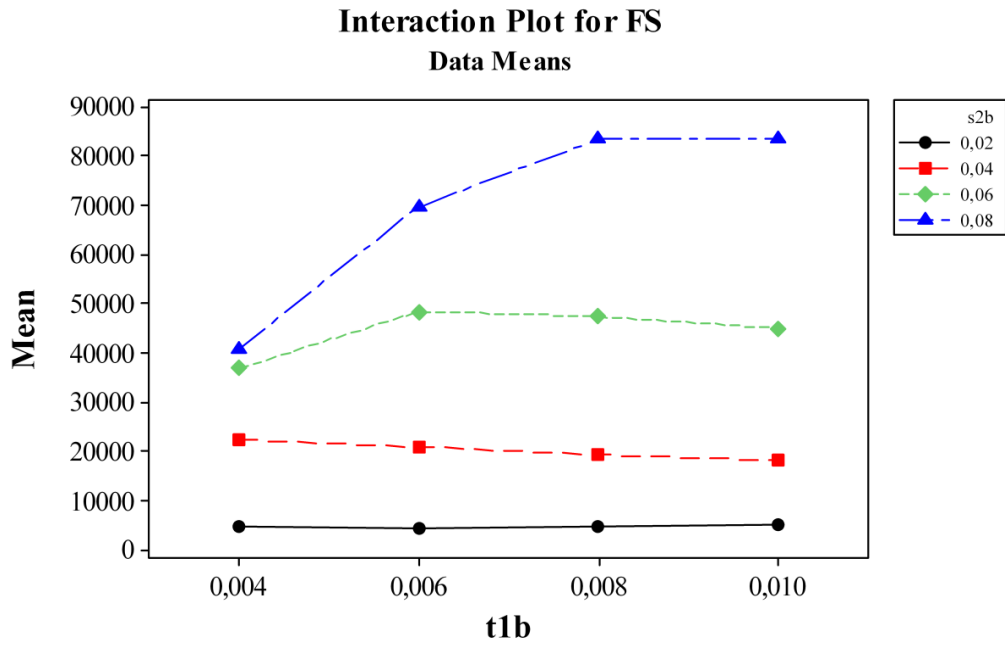


Figure A.3. Interaction plot for FS for t_1/b versus s_2/b

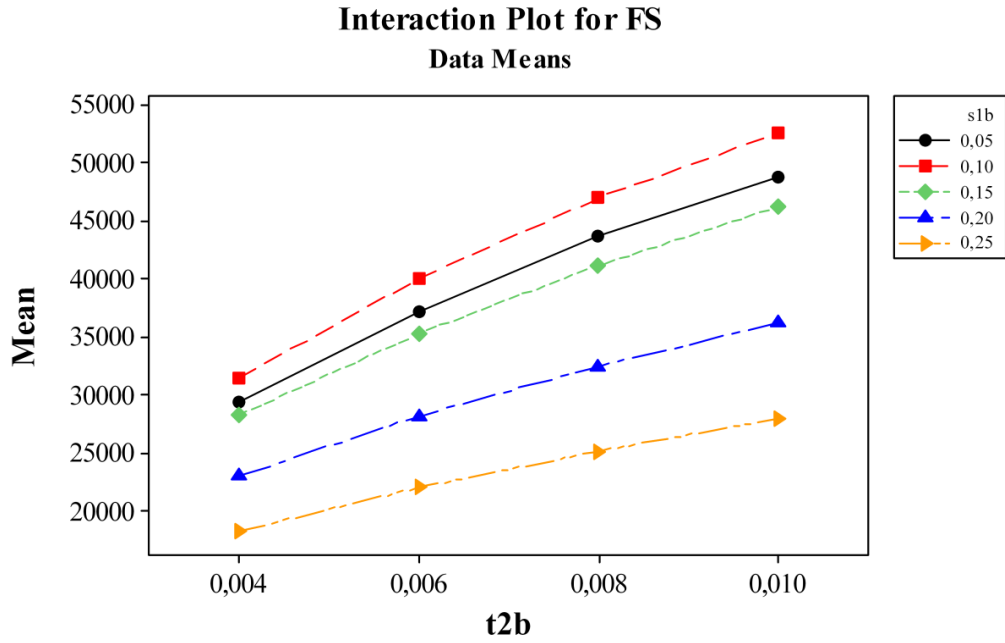


Figure A.4. Interaction plot for FS for t_2/b versus s_1/b

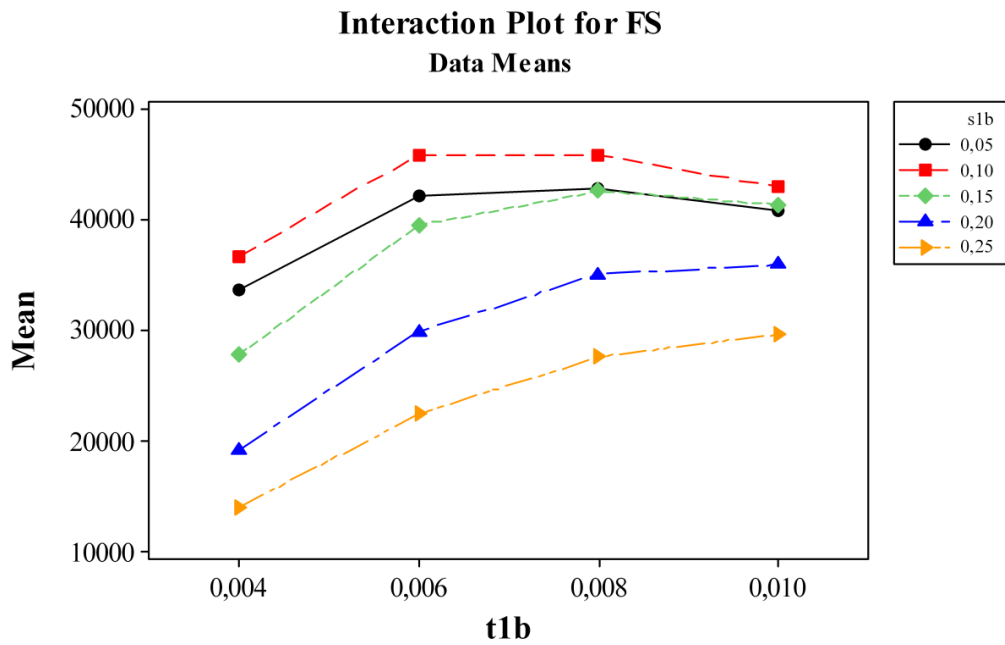


Figure A.5 Interaction plot for FS for t_1/b versus s_1/b

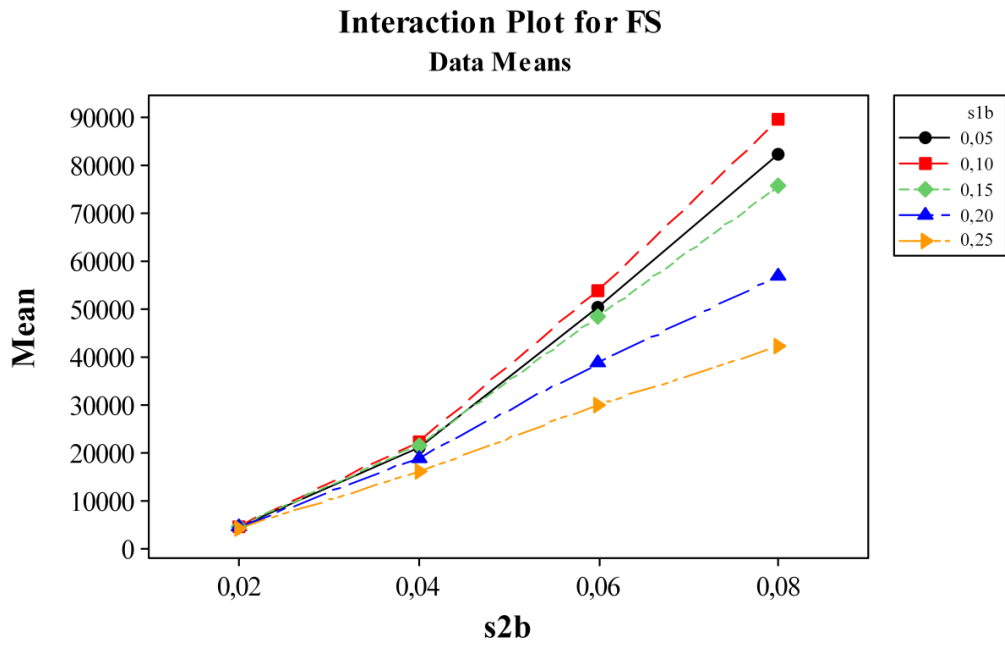


Figure A.6. Interaction plot for FS for s_2/b versus s_1/b

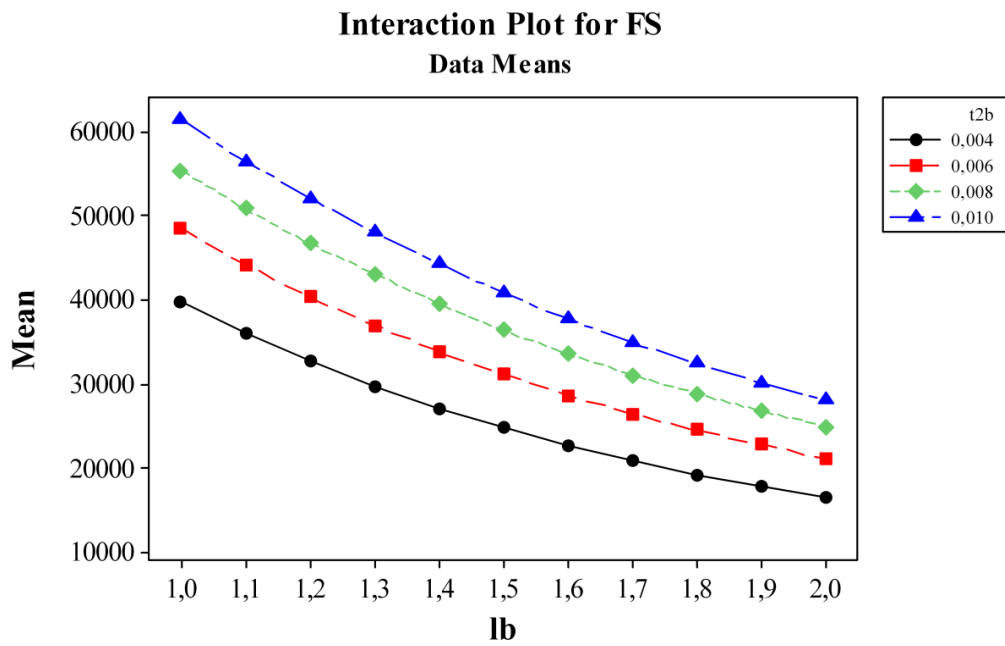


Figure A.7. Interaction plot for FS for t_2/b versus l/b

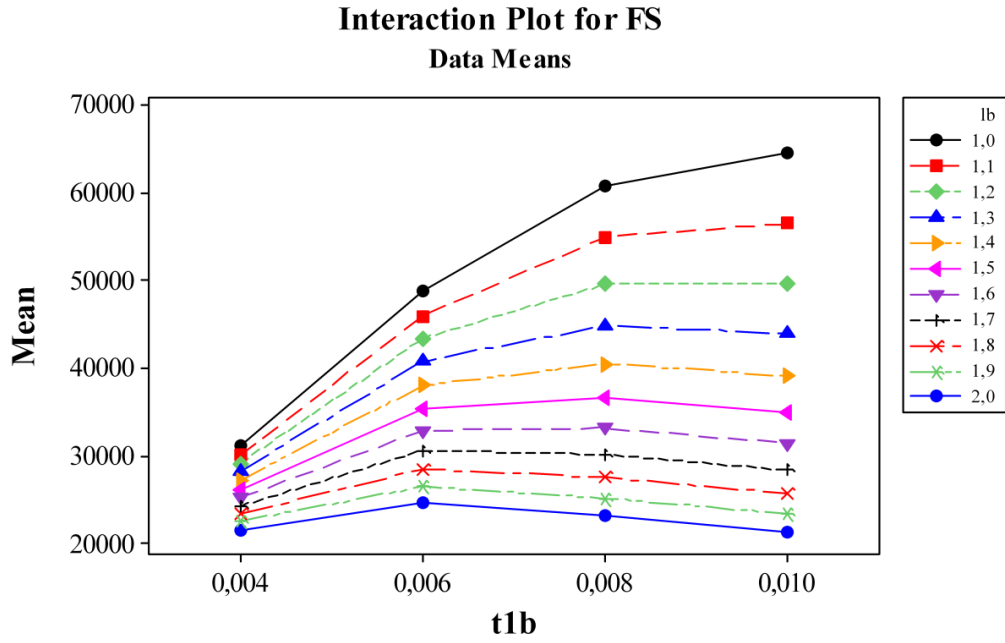


Figure A.8. Interaction plot for FS for t_1/b versus l/b

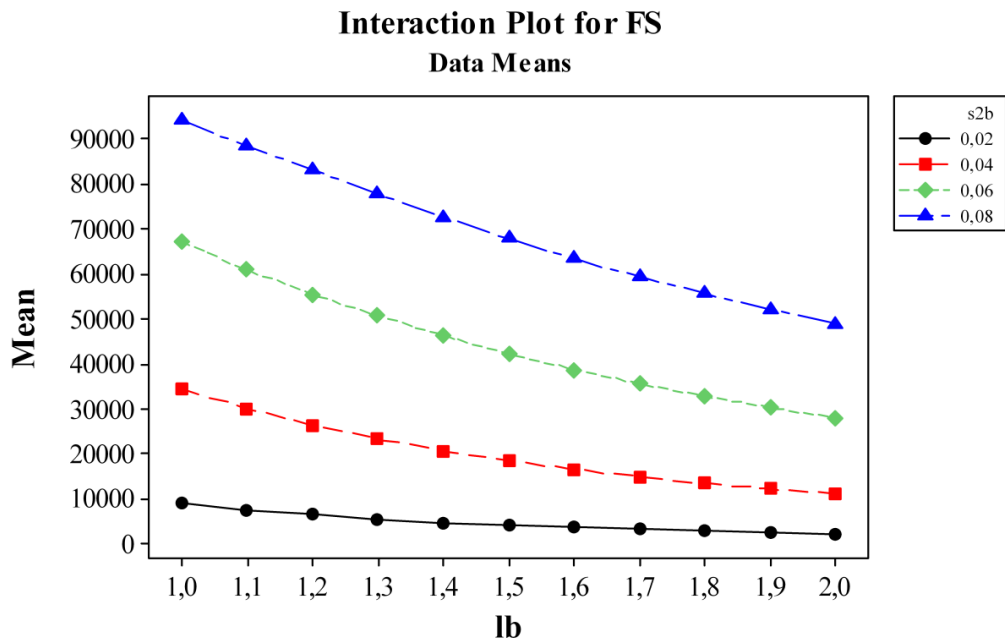


Figure A.9. Interaction plot for FS for l/b versus s_2/b

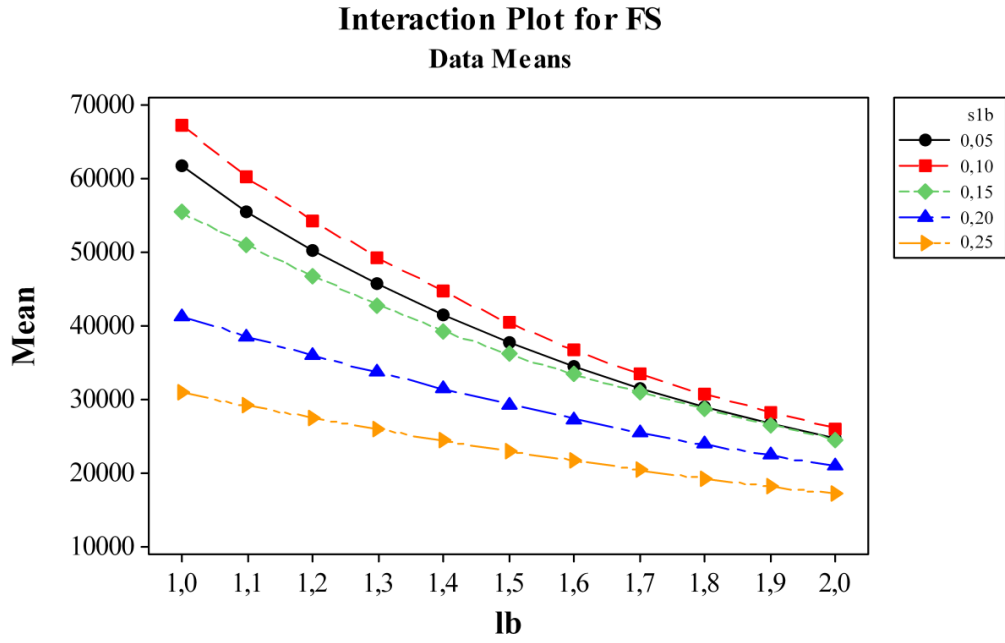


Figure A.10. Interaction plot for FS for l/b versus s_1/b

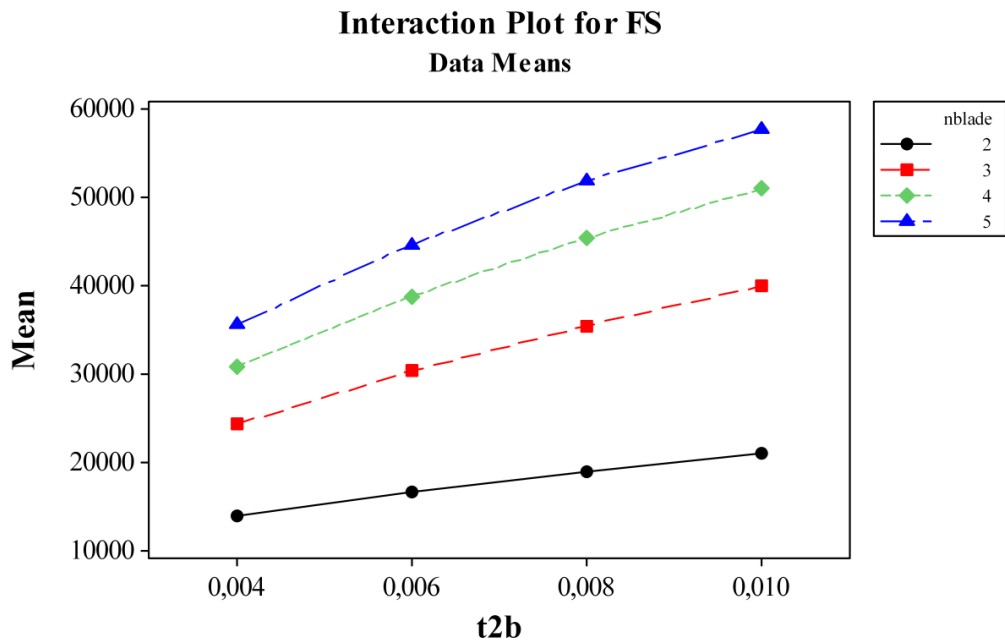


Figure A.11. Interaction plot for FS for t_2/b versus n_{blade}

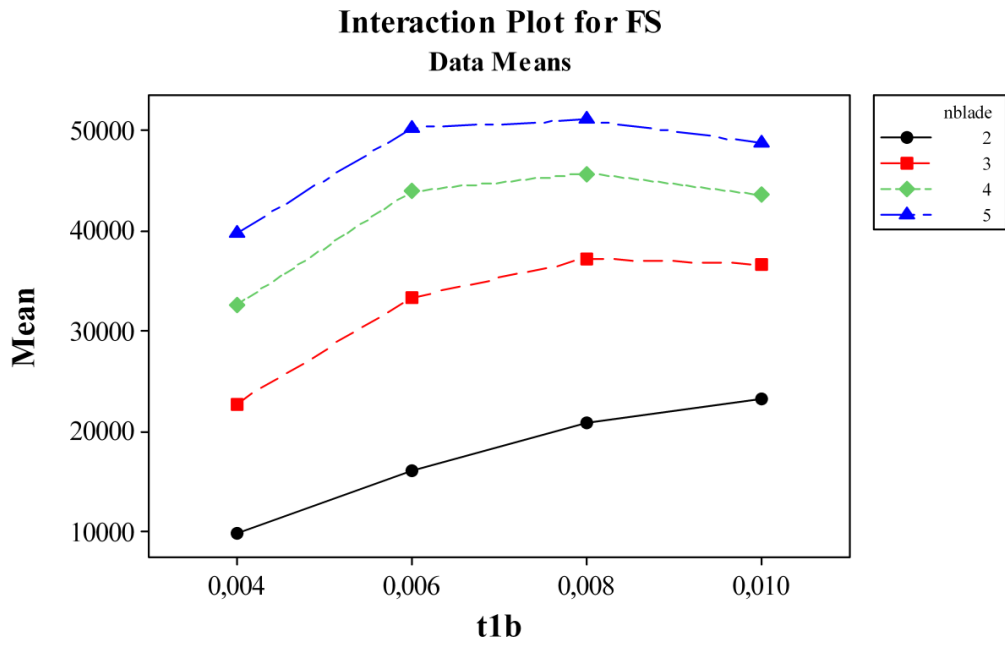


Figure A.12 Interaction plot for FS for t_1/b versus n_{blade}

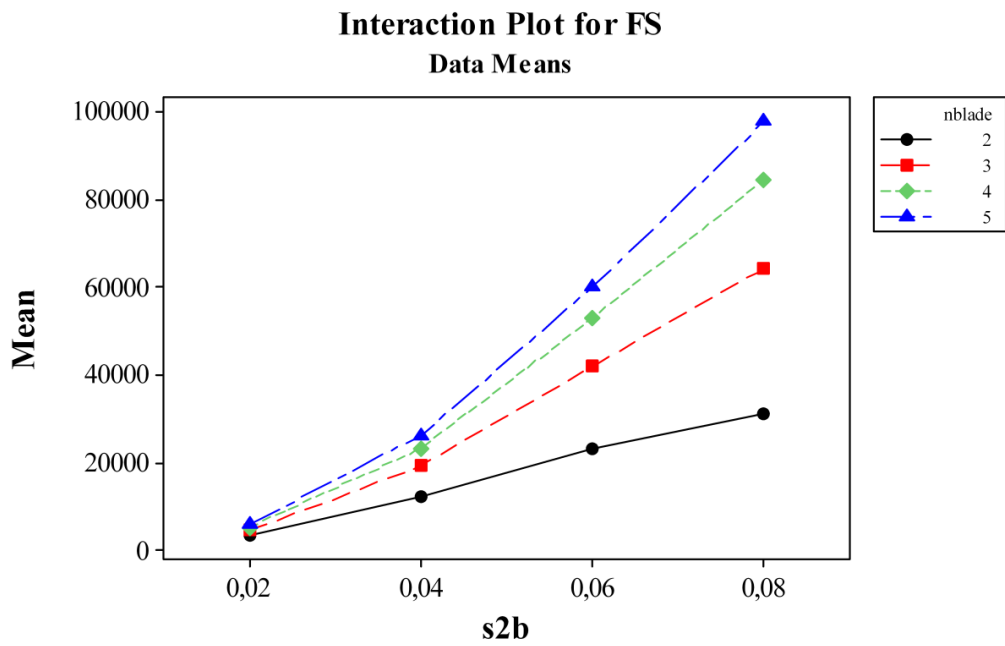


Figure A.13. Interaction plot for FS for n_{blade} versus s_2/b

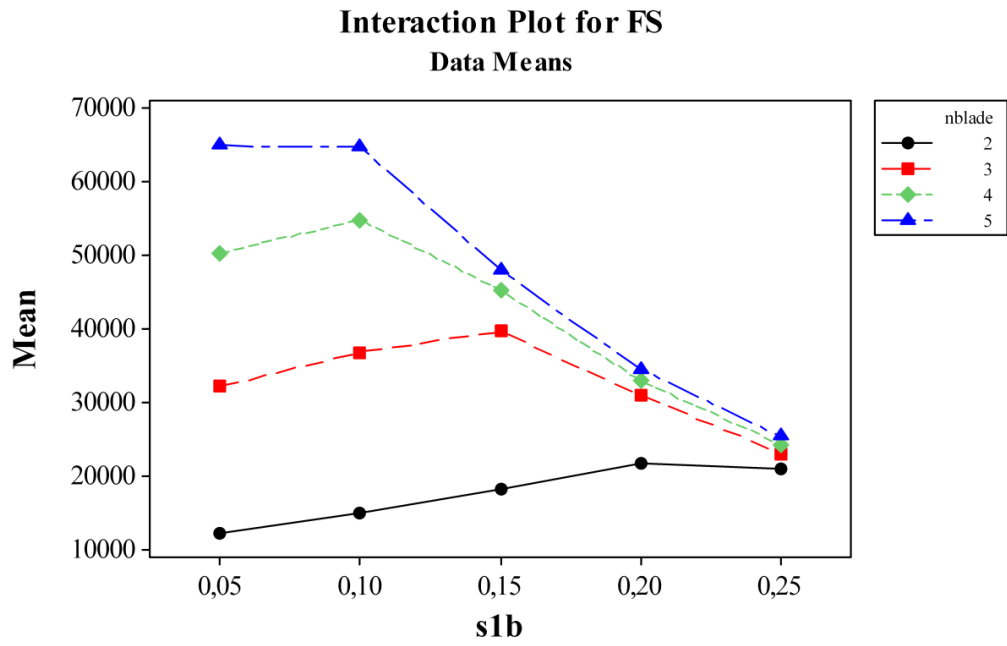


Figure A.14. Interaction plot for FS for s_1/b versus n_{blade}

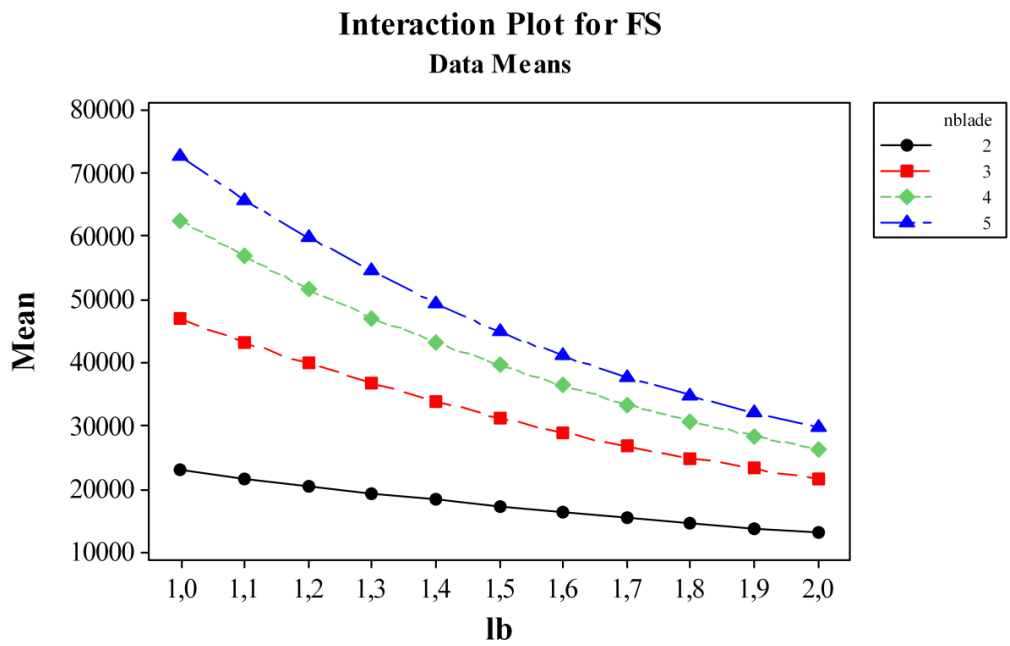


Figure A.15. Interaction plot for FS for l/b versus n_{blade}

APPENDIX B

CONTOUR PLOT FOR FREE VIBRATION ANALYSIS OF STIFFENED PANELS

B.1 Introduction

Interaction plot for FS analysis results are scored by using 14080 data pairs. Interactions of parameters of free vibration analysis against two design variables are shown in Figure B.1-15. Importance of interaction plots for design engineers is all parameters effects on dynamic characteristics of panel can be investigated. All sampling points shown in figures are mean of the eigenvalues.

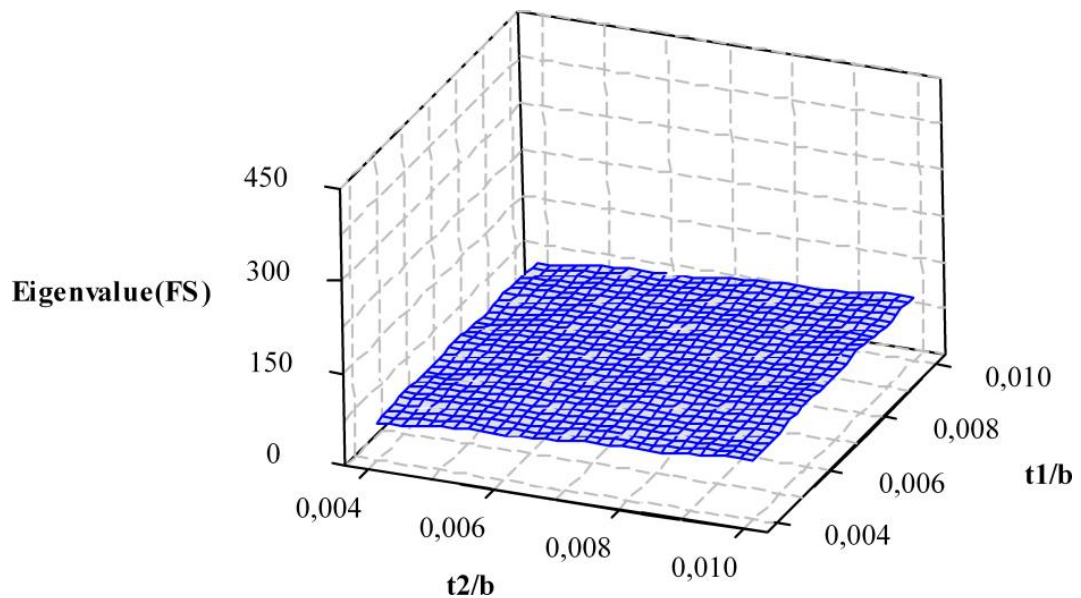


Figure B.1. Contour plot for FS for t_1/b versus t_2/b

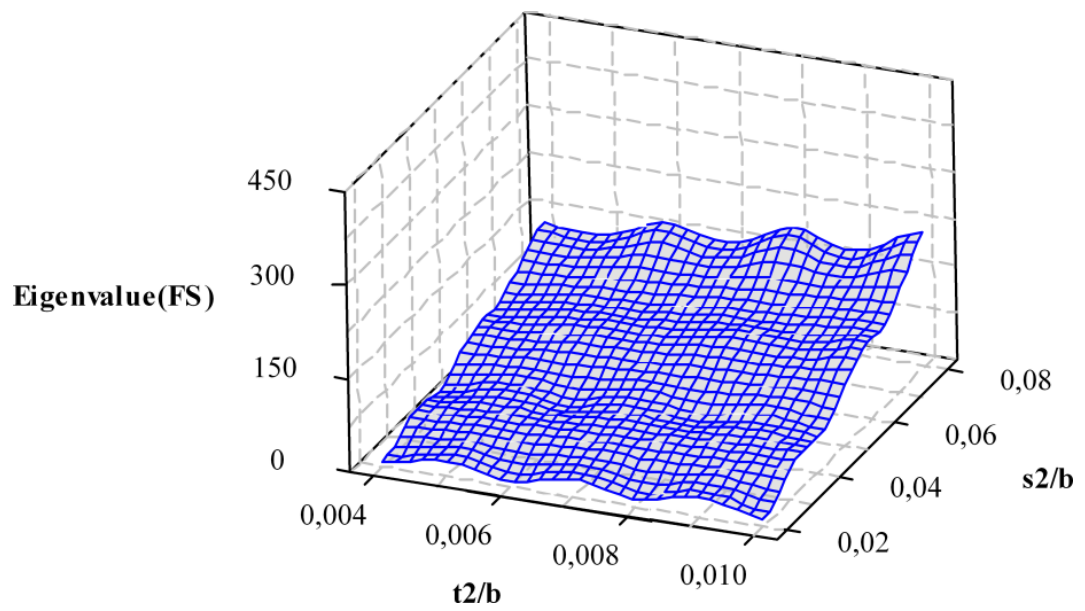


Figure B.2. Contour plot for FS for t_2/b versus s_2/b

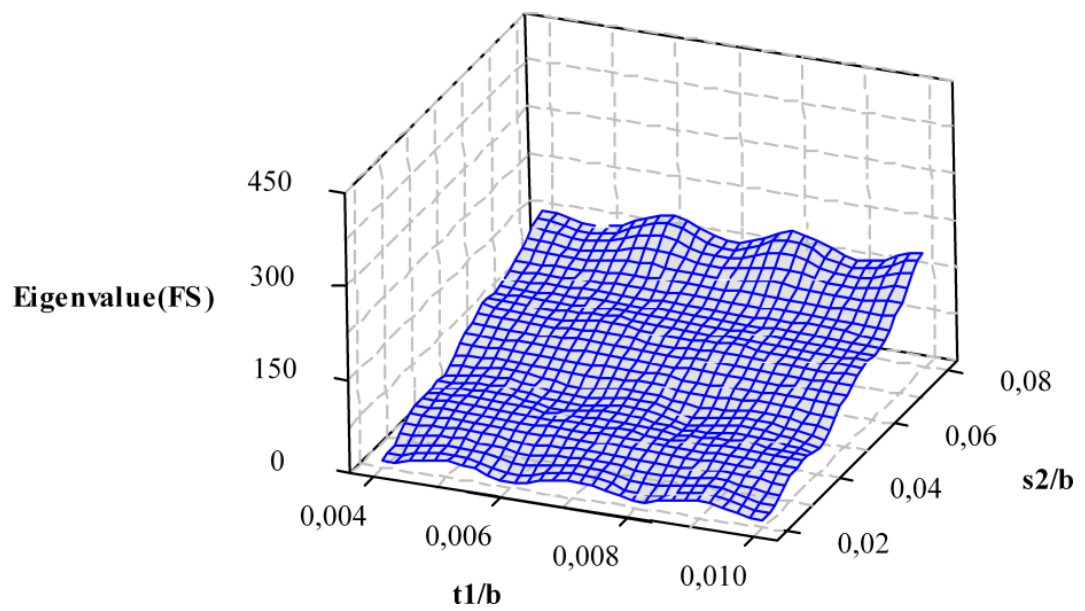


Figure B.3. Contour plot for FS for t_1/b versus s_2/b

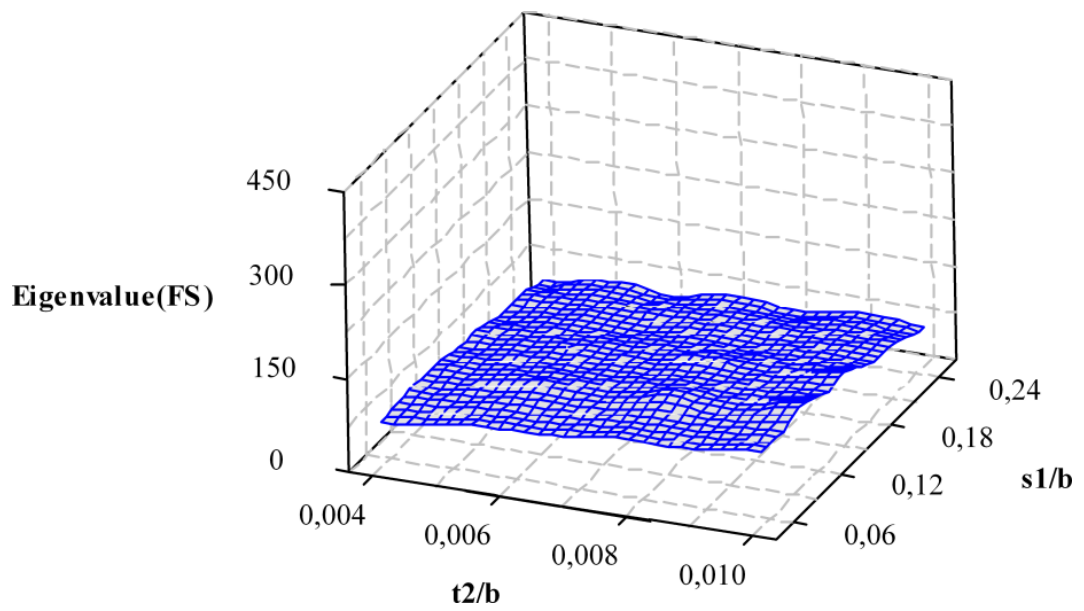


Figure B.4. Contour plot for FS for t_2/b versus s_1/b

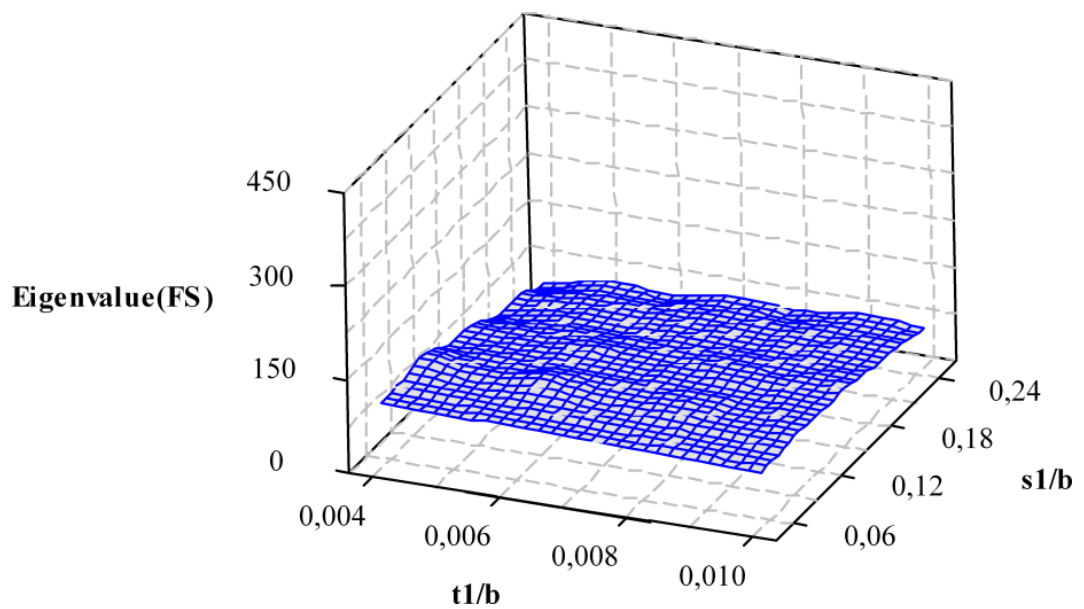


Figure B.5. Contour plot for FS for t_1/b versus s_1/b

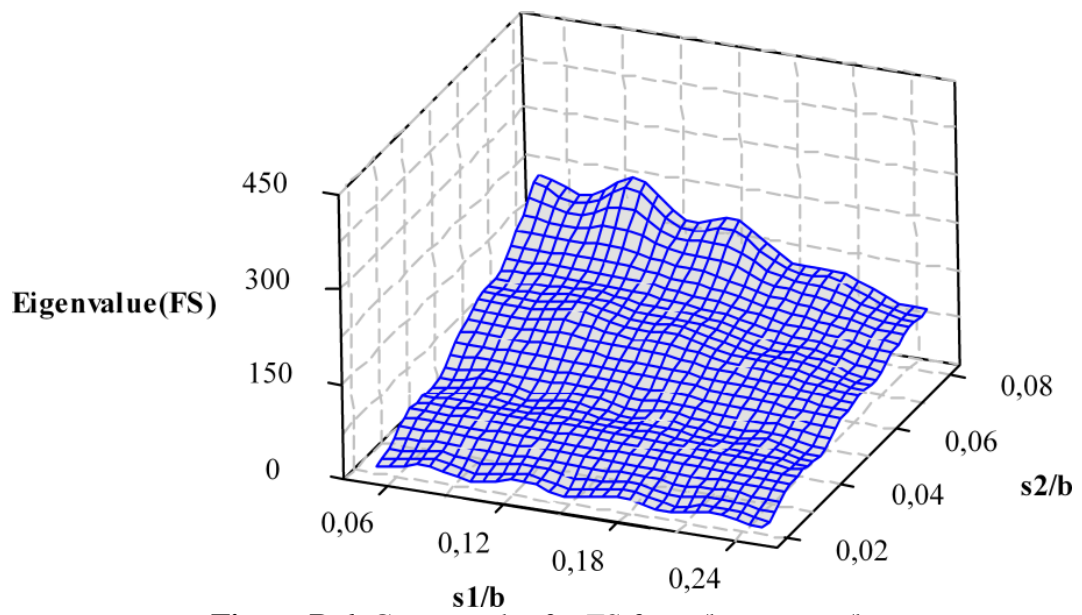


Figure B.6. Contour plot for FS for s_2/b versus s_1/b

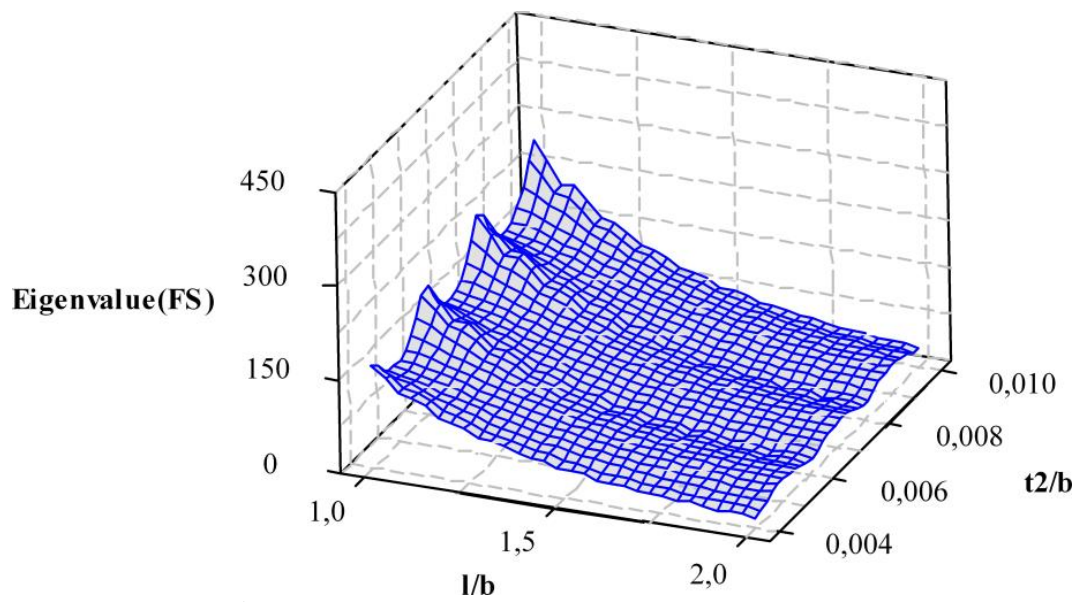


Figure B.7. Contour plot for FS for t_2/b versus l/b

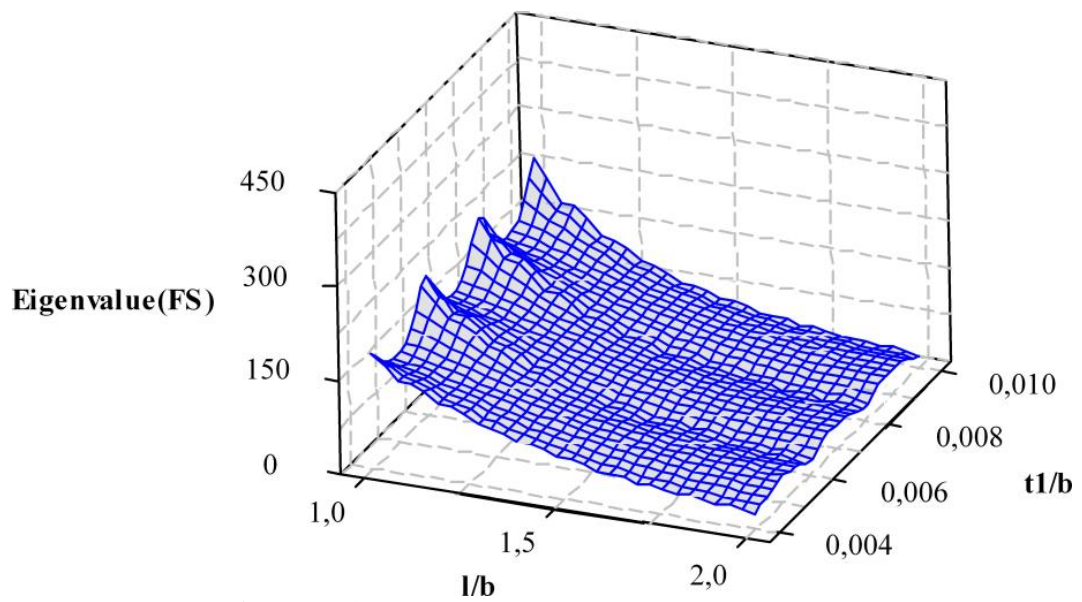


Figure B.8. Contour plot for FS for t_1/b versus l/b

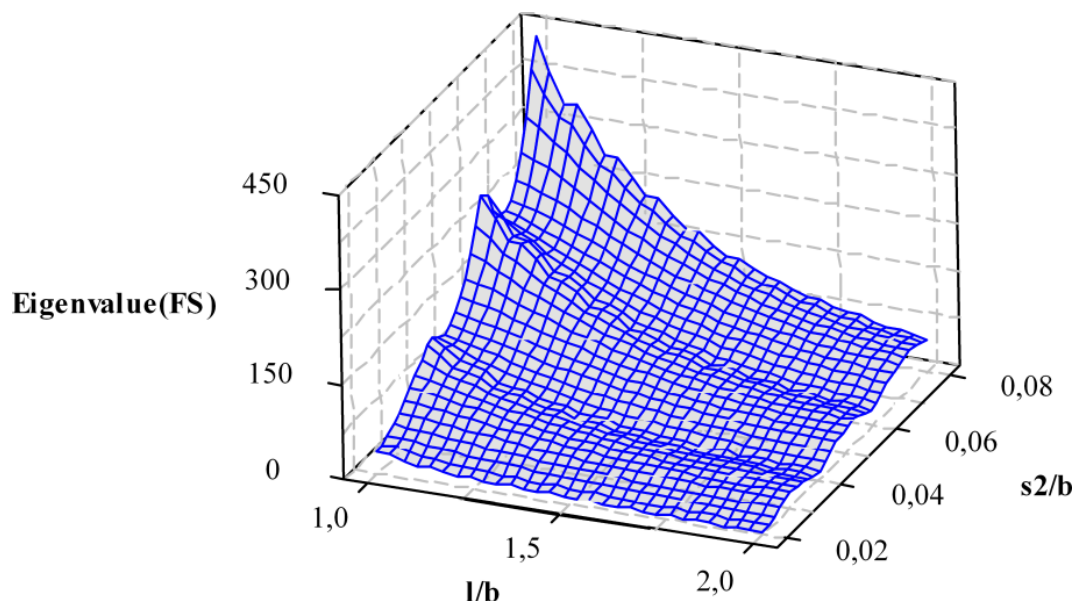


Figure B.9. Contour plot for FS for l/b versus s_2/b

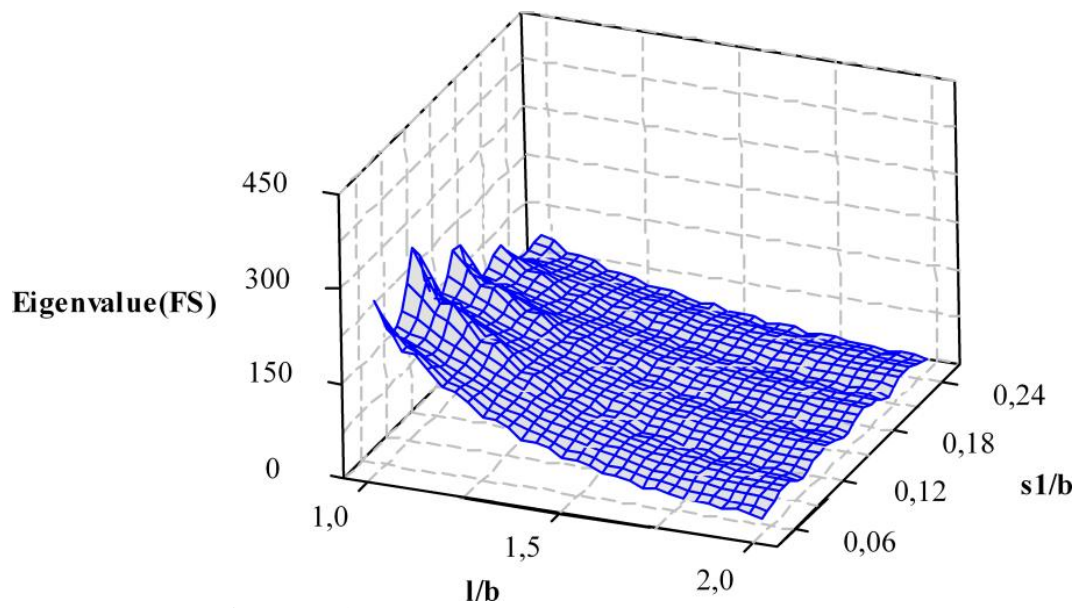


Figure B.10. Contour plot for FS for l/b versus s_1/b

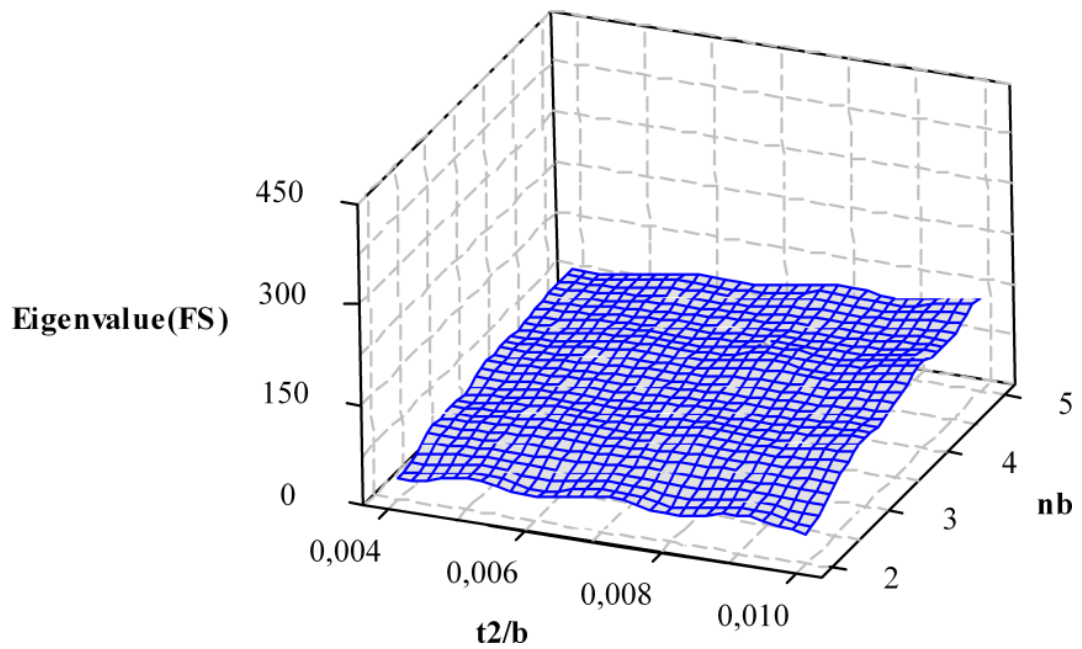


Figure B.11. Contour plot for FS for t_2/b versus n_{blade}

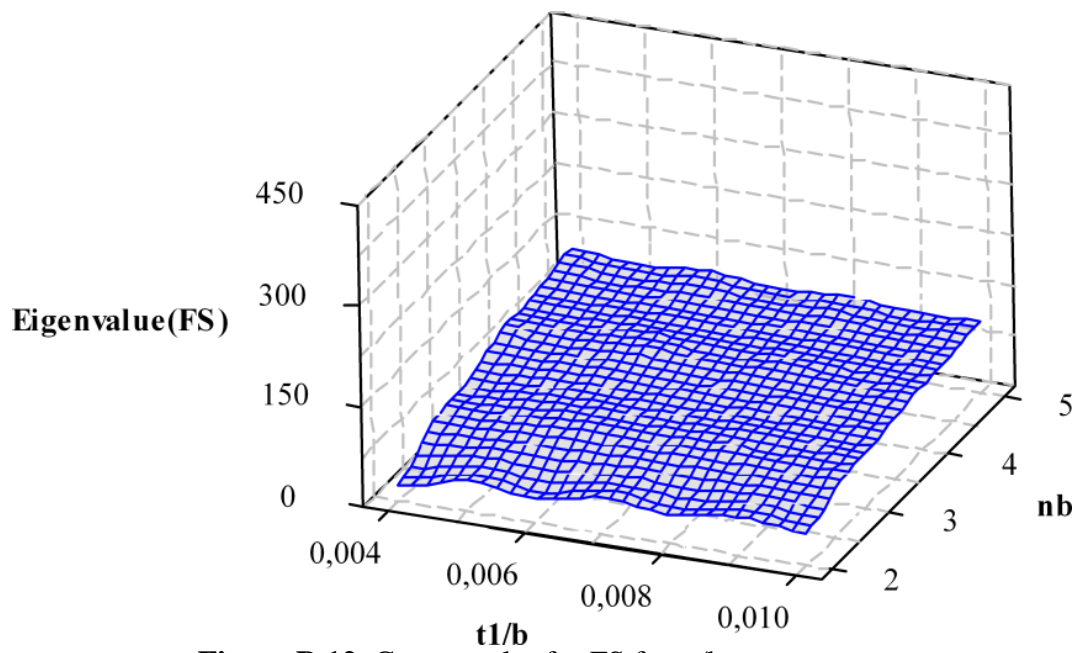


Figure B.12. Contour plot for FS for t_1/b versus n_{blade}

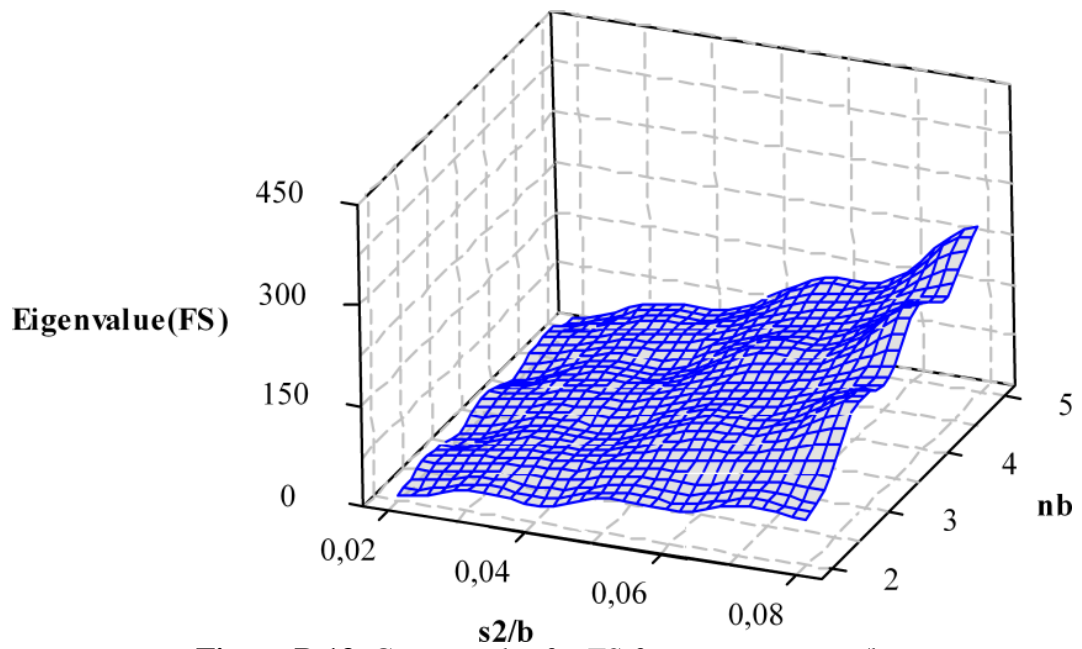


Figure B.13. Contour plot for FS for n_{blade} versus s_2/b

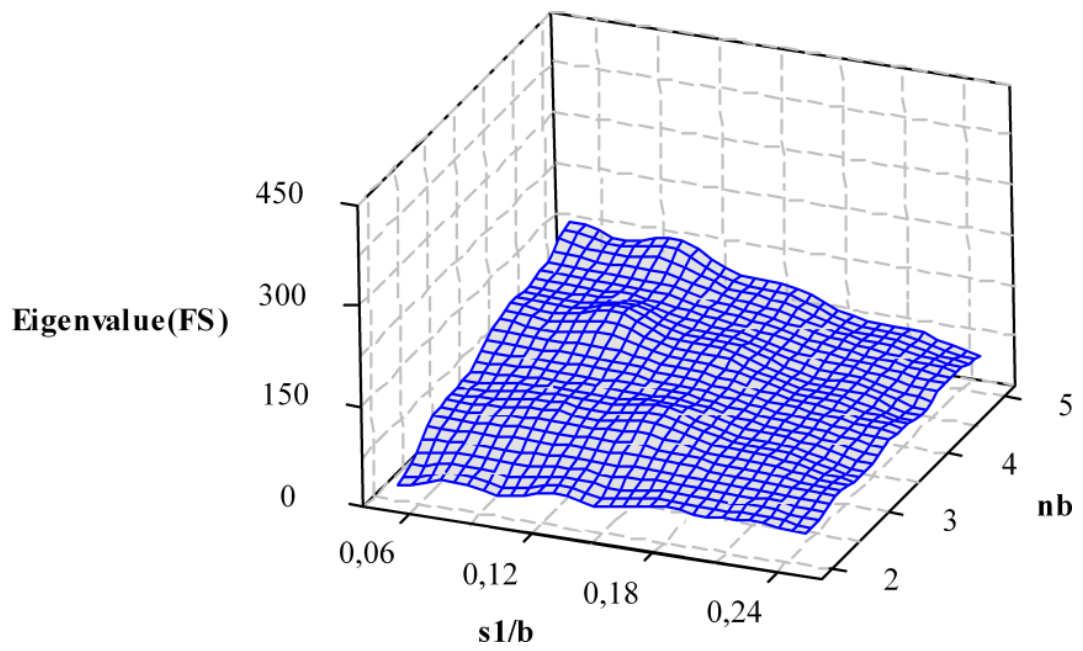


Figure B.14. Contour plot for FS for s_1/b versus n_{blade}

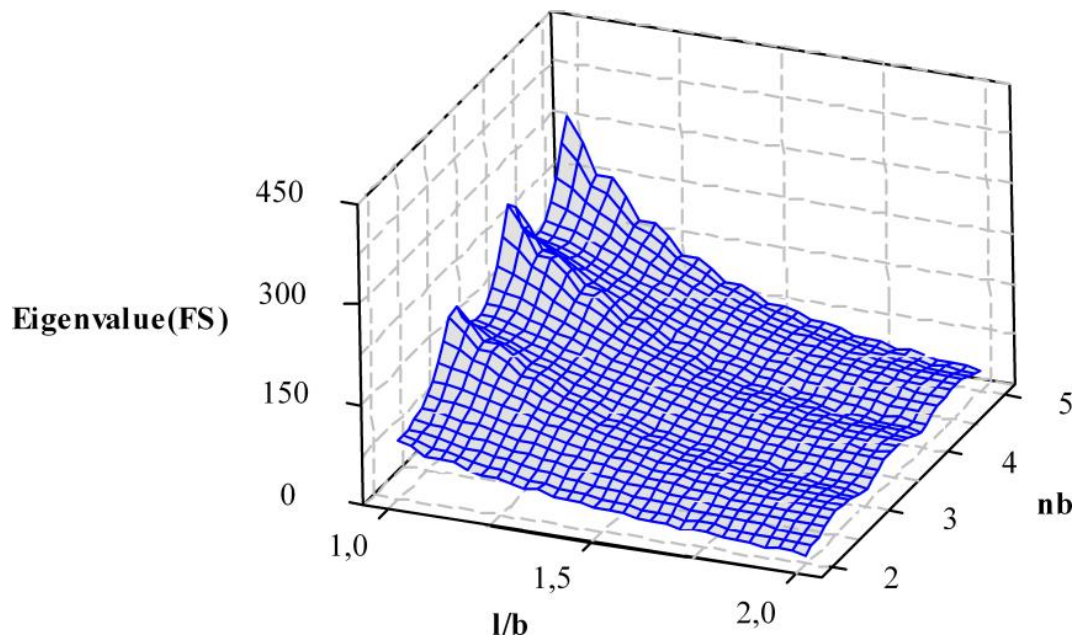


Figure B.15. Contour plot for FS for l/b versus n_{blade}

CURRICULUM VITAE

PERSONAL INFORMATION

Surname, Name: GÖĞÜŞ, Mehmet Tolga
Nationality: Turkish (TC)
Date and Place of Birth: 14 October 1977, Gaziantep
Marital Status: Single
Phone: +90 342 317 24 25
Fax: +90 342 360 11 07
email: mtgogus@gantep.edu.tr, mtgogus@yahoo.com

EDUCATION

Degree	Institution	Year of Graduation
MS	University of Gaziantep	2003
BS	Yıldız Technical University	1999
High School	Gaziantep Anatolian High School	1995

WORK EXPERIENCE

Year	Place	Enrollment
2000– Present	University of Gaziantep	Research assistant

FOREIGN LANGUAGES

English (Reading, writing)

PUBLICATIONS

Özakça, M. and Göğüş, M.T., (2004). Structural analysis and optimization of bells using finite elements. *Journal of New Music Research*, **33(1)**, 61–69.

Guzelbey, İ.H., Çevik, A and Göğüş, M.T. (2006). Prediction of rotation capacity of wide flange beams using neural networks. *Journal of Constructional Steel Research*, **62**, 950–961.

Tayşi, N., Göğüş, M.T. and Özakça, M., (2008). Optimization of arches using genetic algorithm. *Computational Optimization and Applications*, **41(3)**, 377–394.

Tayşı, N., Göğüş, M.T. and Ekmekyapar, T. (2009). Takviyeli Panellerin Burkulmaya Karşı Optimum Tasarımı. TÜBİTAK, Project Grand No:107M648

Çevik, A., Göğüş, M.T., Guzelbey, İ.H., and Filiz, H. (Article in Press). Soft computing based formulation for strength enhancement of CFRP confined concrete cylinders. *Advances in Engineering Software*, doi:10.1016/j.advengsoft.2009.10.015.

Çevik, A., Göğüş, M.T., Guzelbey, İ.H., and Filiz, H. (Article in Press). A new formulation for longitudinally stiffened webs subjected to patch loading using stepwise regression method . *Advances in Engineering Software*, doi:10.1016/j.advengsoft.2009.12.001.

HOBBIES

Reading, traveling, computer technology

